# Developmentally-regulated localization and possible functions of HRP-3 in the murine nervous tissue

**Dissertation**

**zur**

**Erlangung des Doktorgrades (Dr. rer. Nat.)**

**der**

**Mathematische Naturwissenschaftlichen Fakultät**

**der**

**Rheinischen Friedrich-Wilhelms Universität Bonn**

vorgelegt von

Heba Mahmoud Ahmed Eltahir

Aus

Kena, Egypt

Bonn, Oktober 2009

Angefertigt mit Genehmigung der Mathematisch-Naturwissenschaftlichen Fakultät
der Rheinischen Friedrich-Wilhelms-Universität Bonn

1. Gutachter: Prof. Dr. med. Volkmar Gieselmann
2. Gutachter: Prof. Dr. Klaus Mohr

Tag der Promotion: 10. März 2010
Erscheinungsjahr: 2010

For

My small family,

& for the soul of my

parents.

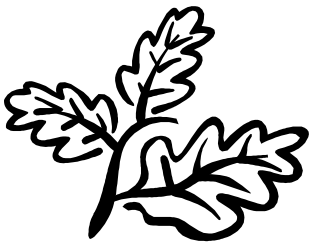

## Acknowledgement

First, I would thank God for helping me to finish this work in the best I can way then the people who helped me in every step of this work.

I would like to thank

Prof. Dr. med. Volkmar Gieselmann for giving me the generous chance to do my doctoral thesis in his lab. His interesting ideas and constructive discussion have been of major importance for this work.

Prof. Dr. Klaus Mohr for taking the responsibility of being my second referee

I would also like to deeply thank my co-supervisor Dr. Sebastian Franken for his excellent supervision of my work. He was always able to invent new ideas that gave my work much better dimensions. His constructive criticism, great support, help and cooperation were of great importance for my work and always gave me a push forward. He was always there answering my questions and had made a great effort correcting and revising until this work had come out in its final shape.

The group of Dr. Franken; Rainer Gallitzendörffer, Katharina Klein, Stephanie Bremer, Robert and specially Angela sedlmeier for the precise reading of the last manuscript of this work.

The members of the anatomy department for their great help and instructions in preparing the Vibratome sections. And also I would like to thank them for the facilities they provided in using the confocal laser microscope.

The group of Prof. Dr. Magin for the microscope facilities they provided.

Dr. Kappler, Dr. Eckhardt and Dr. Matzner for their help and cooperation.

All co-workers for their cooperation and for providing a friendly work atmosphere.

Mrs. Simonis for her great help in general DNA techniques, Mrs. Buttkau and Mr. Rösel for their great help in technical work.

Mr. Pflüger for his great and brilliant help in the use of computer programs.

My husband, Mekky, for his incredible help and endless support. He sacrificed many important things to provide me with the suitable atmosphere to do my work. Without his help, love and patience, I would never be able to do this work.

My children, Ahmed and Radwa who pushed me forward with their love and smiles.

My brother and sister and my big family in Egypt, they provided me with support and encouragement and they have done too much for me especially my mother.

Finally, I wanted to thank my mother for all what she had done for me, for being always behind me and for all her words, advices and love even when she is not there any more to read these words.

# Table of content

# List of figures

# List of tables

# Abbreviations

| | |
|---|---|
| µg | microgram |
| µl | microliter |
| β | Beta |
| B-gal | Beta gal |
| A | Aorta |
| ABTS | 2,2'-azino-di-[3-ethylbenzthiazoline sulfonate] |
| ANR | Anterior nerve root |
| BDNF | Brain derived neurotrophic factor |
| Bp | Base pair |
| BSA | Bovine serum albumin |
| CA | Cornu ammonis |
| CNS | Central nervous system |
| CNTF | Ciliary neurotrophic factor |
| $CO_2$ | Carbon dioxide |
| CR cells | Cajal-Retzius |
| ctrl | control |
| $Cu^{2+}$ | Cupric ion |
| CV | Column volume |
| Cy3 | Cyanine -3 |
| DAB | Diaminobenzidine |
| DABCO | 1,4-diazabicyclo(2,2,2)octan |
| DAPI | 4,6-diamidino-2-phenylindole |
| dBcAMP | Dibutyryl cyclic adinosine monophosphate |
| DG | Dentate gyrus |
| DIV | Days in vitro |
| DMEM | Dulbecco's modified eagle medium |
| DMSO | Dimethyl sulfoxide |
| DNA | Deoxyribonucleic acid |
| Dpc | Days post conception |
| DPX | Distyrene-Plasticizer-Xylene |
| DRG | Dorsal root ganglia |
| DsRNA | Double-stranded ribonucleic acid |
| E | Embryonic day |
| ECM | Extracellular matrix |
| EDTA | Ethylene diamine tetra acetic acid |
| EGL | External granular cell layer |
| ELISA | Enzyme-linked immunosorbent assay |
| EST | Expression sequence tag |
| FCS | Foetal calf serum |
| FGF | Fibroblast growth factor |
| g | gram |
| GABA | Gamma amino butyric acid |
| GFAP | Glial fibrillary acidic protein |
| GFP | Green fluorescent protein |
| GST | Glutathion-S-transferase |
| HATH | Homologue to amino terminus of HDGF |
| HB-GAM | heparin-binding growth-associated molecule |
| HBSS | Hank´s balanced salt solution |
| HDGF | Hebatoma-derived growth factor |

| | |
|---|---|
| HRP-1 to 4 | Hebatoma-derived growth factor related protein 1 to 4 |
| HEPES | 4-(2-hydroxyethyl)-1-piperazineethanesulfonic acid |
| HIV | Human immunodeficiency virus |
| HPLC | High performance liquid chromatography |
| Hrs | hours |
| IGL | Internal granular cell layer |
| KDa | Kilo dalton |
| LEDGF | Lense epithelium derived growth factor |
| Lys | Lysine |
| Map-2 | Microtubules associated protein -2 |
| MATra | Magnet Assisted Transfection |
| MCL | Molecular cell layer |
| Min | Minutes |
| MN | Motor neurons |
| MOPS | 3-(N-morpholino) propanesulfonic acid |
| mRNA | Messenger ribonucleic acid |
| miRNA | Micro ribonucleic acid |
| MTS | 3-(4,5-dimethylthiazol-2-yl)-5-(3-carboxymethoxyphenyl)-2-(4-sulfophenyl)-2H-tetrazolium |
| MWCO | Molecular weight cut-off |
| MZ | Marginal zone |
| NBM | Neurobasal medium |
| N-CAM | neural cell adhesion molecule |
| ng | nanogram |
| NGF | Nerve growth factor |
| $Ni^{2+}$ | Nickel ion |
| NLS | Nuclear localizing signal |
| nM | Nano mole |
| NMR | Nuclear magnetic resonance |
| OB | oval bundle |
| PBS | Phosphate-buffered saline |
| PCL | Purkinje cell layer |
| PCR | polymerase chain reaction |
| PDL | Poly-D-lysine |
| PFA | paraformaldehyde |
| PM | Pia mater |
| Pmol | Pico mole |
| PMS | Phenazine methosulfate |
| PNS | Peripheral nervous system |
| PNR | Posterior nerve root |
| PP | Preplate |
| RAGE | Receptor of advanced glycation end product |
| REDOX | Reduction-oxidation reaction |
| RISC | RNA-induced silencing complex |
| RNAi | Ribonucleic acid interference |
| Sds-page | Sodium dodecylsulfate poly acrylamide gel electrophoresis |
| SG | Sympathetic ganglia |
| siRNA | Small interfering ribonucleic acid |
| SN | Spinal nerve |
| SNC | Sensory neurons cell bodies |
| SP | Subplate |

| | |
|---|---|
| Ssc | Sodium saline citrate |
| Sub | Subiculum |
| TBS | Tris-buffered saline |
| trkA | Tyrosin kinase A |
| UV | Ultra violet |
| VB | Visceral branch |
| VSM | Vascular smooth muscles |
| VZ | Ventricular zone |
| WM | White matter |
| Wt | Wild type |

# 1. Introduction

## 1.1 Development of the murine nervous system

Early during the embryonic life of the mouse, the neural plate starts to form at about 7.25 to 8 days post conception (dpc) from the embryonic ectoderm layer. Within a few days, the neural plate starts to fold and the neural groove deepens as seen in figure 1A. The two neural folds become elevated until gradually meeting each other at the middle point of the embryo back (figure 1B & C). By the time, it continues to close in both directions, cranially and caudally, to form the neural tube (figure 1D & E).

.

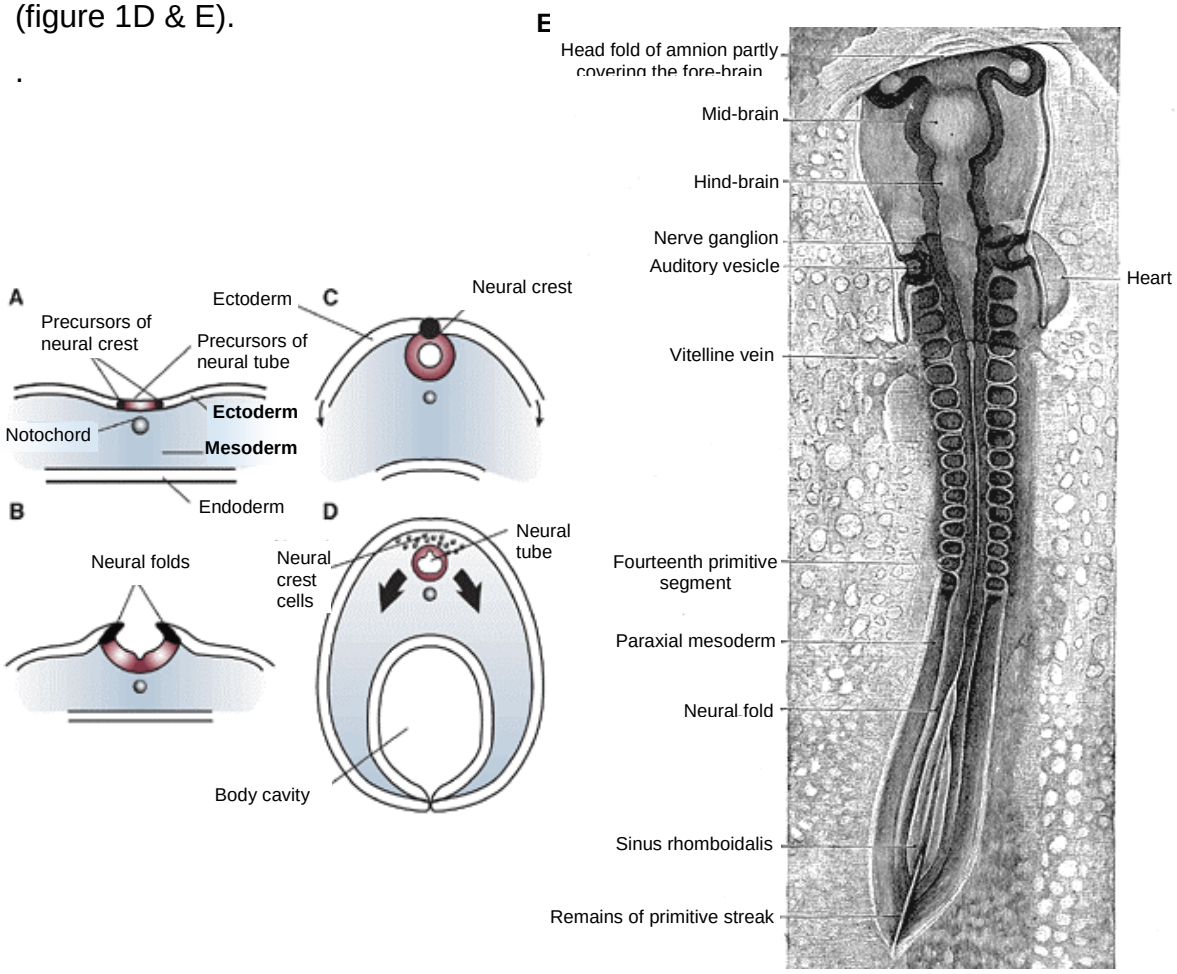


**Figure 1: Formation of the neural tube**. A-D neural tube in cross view. Early in the development, the notochord (A) induces the ectoderm cells to become the primitive nervous system (i.e., neuroepithelium). The neuroepithelium wrinkles and folds over (B). The tips of the folds fuse together and a hollow tube (the neural tube) forms (C). The ectoderm and endoderm continue to curve around and fuse to create the body cavity transforming the embryo from a flattened disk to a three-dimensional body. Cells originating from the fused tips of the neuroectoderm (neural crest cells) migrate to various locations throughout the embryo to initiate the diverse body structures (D, Goodlett and Horn, 2001). (E) Chick embryo of thirty-three hours incubation, viewed from the dorsal aspect (Grey's anatomy).

The formed neural tube is the embryo's precursor of the central nervous system (CNS) which consists of the brain and the spinal cord. CNS can be divided into four subdivisions; prosencephalon (fore-brain precursor), mesencephalon (midbrain precursor), rhombencephalon (hindbrain precursor) and the spinal cord. As soon as the cranial part of the neural tube folds to form the brain, neurogenesis begins in the different parts with slight differences in the onset, peak and end. Neurogenesis is a process that includes cell division, migration and differentiation. These three steps are critical and universal steps in the formation of the complex structure of the nervous system.

Neurogenesis in the neocortex commences when some progenitor cells divide asymmetrically generating postmitotic neurons that migrate away from the ventricular zone (*VZ*) towards the outer edge of the cortical wall along the basal fiber of the radial glial cells (Rakic, 1978; Goffinet, 1984). Neocortical development begins with the appearance of the preplate (*PP*) above the ventricular zone (Figure 2). The preplate is the earliest cortical layer generated by postmitotic cells migrating from the *VZ* (Luskin and Shatz, 1985; Marin-Padilla, 1998; Rickmann, et al., 1977; Uylings, et al., 1990; Bayer and Altman, 1991) and is composed of subcortical afferents and two populations of postmitotic neurons, the Cajal-Retzius (*CR*) cells and the subplate (*SP)* neurons (Marin-Padilla 1998; Super, et al., 1998). The PP becomes soon divided into the superficial, cell-sparse, marginal zone (*MZ*) and the deeper *SP* by the invasion of successive waves of neurons produced from the VZ (Marin-Padilla, 1971, Luskin and shatz, 1985, Caviness, 1982; Caviness, et al., 1995; Sheppard and Pearlman, 1997). *CR* cells are among the earliest neurons to be generated in the mammalian neocortex, where they occupy positions near the pial surface on the superficial aspect of the brain (Meyer & Goffinet 1998, König, et al 1977). The next phase of development occurs when the cortical plate (*CP*) neurons exit the cell cycle near the ventricular surface and invade the *PP*. Migrating neurons move past the *SP*, displacing this layer away from the *CR* cells, which remain adjacent to the pial surface in the *MZ*. As new cortical plate neurons arrive travelling along the radial glia, they migrate past the older *SP* and cortical plate neurons before inserting directly beneath *CR* cells. The systematic migration of younger neurons past their predecessors results in the "inside-out" pattern of development, in which the cortical plate (future Layers II-VI) develops between the *MZ* (future Layer I) and the *SP*.

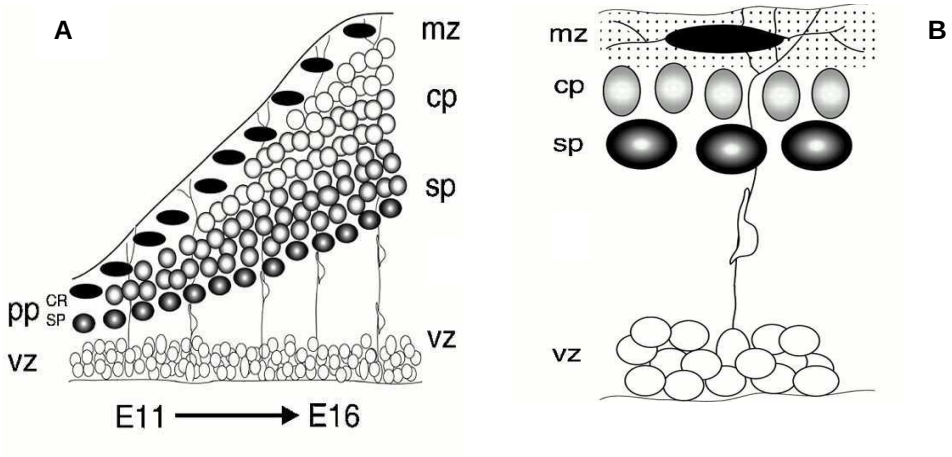


**Figure 2: A simplified view of corticogenesis of the developing cerebral wall in mammals**. (**A**) Corticogenesis in mammals begins with the appearance of the preplate (pp), which is located directly above the proliferating cells in the ventricular zone (vz) and contains Cajal-Retzius neurons (CR) and subplate (SP) neurons, among others. Cells destined for the cortical plate are generated near the ventricular zone and the first wave of cortical plate (CP) cells (gray) migrates past the subplate and stops beneath the Cajal-Retzius cells in the marginal zone (mz). Successively generated waves (gray to white) of cells migrate past their predecessors and stop beneath the Cajal-Retzius cells. (**B**) By E16.5 in the mouse, young cortical plate neurons are positioned above the older neurons except Cajal-Retzius cells.

Migrating neurons are arranged in six distinct layers as they migrate towards the pial surface and occupy their final positions. These young migrating neurons are guided through the *SP* mainly by a glycoprotein named reelin which is produced by *CR* cells in the *MZ*. Reelin is also responsible for the formation of the characteristic “inside first, outside last” cortical laminar structure of layers II-VI (D'Arcangelo, et al., 1995; Rice and Curran, 2001). These layers were identified in the developed cortex by Karbinian Brodmann and they can be described as follows:

1. The molecular layer (I), the outermost layer which contains few neurons and consists mainly of extensions of apical dendrites and horizontally-oriented axons.
2. The external granular layer (II), which contains small pyramidal neurons and numerous stellate neurons
3. The external pyramidal layer (III), which contains predominantly small and medium-size pyramidal neurons as well as non-pyramidal neurons with vertically-oriented intracortical axons.

4. The internal granular layer (IV), which contains different types of pyramidal and stellate neurons.
5. The internal pyramidal layer (V), which contains large pyramidal neurons.
6. The multiform layer (VI), which contains few large pyramidal neurons and many small spindle-like pyramidal and multiform neurons (Brodmann, 1909).

The different cortical layers start neurogensis at consequent -mostly overlapping- days starting from the older deeper layer (layer VI) reaching the more superficial, younger layers (layer II/III) as shown in the table below.

***Table 1: Timing of neurogenesis stages of the different cortical layers.*** A timetable that shows the approximate embryonic days on which neurogenesis starts, peaks and ends in the different cortical layers of mouse embryo (Ashwell, et al., 1996; Dunlop, et al., 1997; Finlay and Darlington, 1995; Robinson and Dreher, 1990).

| Neurogenesis stage | Cortical layer VI | Cortical layer V | Cortical layer IV | Cortical layer II/III |
|---|---|---|---|---|
| Start (in dpc) | 11.4 | 12.8 | 14.4 | 15.2 |
| Peak (in dpc) | 13 | 14.2 | 15.5 | 16.9 |
| End (in dpc) | 14.3 | 15.3 | 17.1 | 18.3 |

Shortly after neurogenesis reaches its end, differentiation starts to take first place in the deeper layers (about 18.5 to 19 dpc in layer V, Finlay and Darlington, 1995) and continues for some time after birth. It was believed earlier that neurogenesis and differentiation of neurons totally ceases in adulthood and no more mitotic or differentiating cells could be found in mature nervous system. Interestingly, recent researches have shown that this hypothesis does not apply for all brain structures. It could be observed that some brain structures continue to undergo neurogenesis in the adult mammalian brain. This phenomenon known as adult neurogenesis has been shown to take place in many mammalian species like rat, rabbit, cow and mouse (Wyss and Sripanidkulchai, 1985; Gueneau, et al., 1982; Kempermann, et al., 1997). Examples for brain structures showing adult neurogenesis and/or differentiation are the lateral subventricular and subgranular zones of the dentate gyrus which produce stem cells that migrate and differentiate in the olfactory bulb (Cameron and McKay, 2001). In addition, multipotent stem cells capable of adult neurogenesis were detected in the cereberal cortex, optic nerve, spinal cord, and many brain stem and forebrain structures (Van Praag, et al., 2002). These neural

stem cells derived from adult brains can be propagated in vitro using a variety of cytokines, neurotrophins, and conditioned media to give rise to neurons or glia (Gensburger, et al., 1987; Arsenijvic and Weiss, 1998; Ahmed, et al., 1995; Richards, et al., 1992; Reynolds and Weiss, 1992; Lois and Alvarez Buylla, 1993; Johansson, et al., 1999; Doetsch, et al., 1999; Vescovi, et al., 1993; Kilpatrick and Bartlett, 1995; Gage, et al., 1995; Palmer, et al., 1997). However reported to exist since over three decades, the functional roles of the new cells produced by adult neurogenesis process are still largely under investigation. Knowing that hippocampus is important for some forms of learning and memory and related mechanisms of neural plasticity had directed the research to focus on finding a relationship between adult neurogenesis and memory function.

## 1.2 Extracellular matrix

Differentiation and morphogenesis of neural tissue involve a diversity of potentially important interactions between neural cells and their environment known as the extracellular matrix (ECM). ECM can be defined as a complex association of different macromolecules whose structure and function are critical for maintaining normal tissue architecture. It can be divided into *interstitial matrix* which exists in the intercellular spaces (among the cells) and *basement membranes* which are sheet-like depositions of ECM on which various epithelial cells rest (Kumar, et al., 2004). Molecular components of ECM are classified into *proteoglycans* like heparan-, chondroitin- and keratan sulafate and *non-proteoglycans* like hyaluronic acid, elastin, collagen, fibronectin, laminin, tenascins and thrombospondin molecules. Proteoglycan molecules together with hyaluronic acid in ECM form a highly hydrated, gel-like “ground substance” that resists compressive forces on the matrix while permitting the rapid diffusion of nutrients, metabolites, hormones and growth factors between the blood and the tissue cells.

Many of these components were originally discovered in non neuronal tissues but were later discovered in developing neural tissues (e.g. fibronectin, laminin, vitronectin, collagens, and thrombospondin) (Reichardt and Tomaselli, 1991). Some others like *S-laminin* and *agrin* were originally discovered in the neural tissues which exist in the basement membrane of neuromuscular junctions (Reist, et al., 1987; Hunter, et al., 1989a & b) and *F-spondin* which is expressed in the

spinal cord floor plate (Klar, et al., 1992). Early during develpoment when neural progenitors differentiate and migrate and neuronal axons elonagte, abundant ECM is present in the CNS. But by the end of development, the expression of ECM elements is substantially reduced. ECM in the developing neural tissues functions not only as a scaffold for cellular support but also as an immediate microenvironment. The interaction of cells with this microenvironment can trigger regulatory signals that influence cell proliferation, migration, and fate decision. These signals can directly regulate cells locomotory activity like polymerization of cytoskeletal components that promote extension and adhesion of lamellipodia and filopodia. In addition, these signals may also act directly on cell nuclei to alter gene expression of proteins involved in neuronal migration and morphogenesis (Letourneau, et al., 1994; Lathia, et al., 2007). Laminins generally function as potent stimulators of cell growth, migration, axon- and neurite outgrowth and myelination in addition to important roles in axonal sorting of peripheral nerves (Yu, et al., 2009; Yu, et al., 2005; Yang, et al., 2005; Cohen, et al., 1986). *Laminin-1* as a member of the laminin family is a fibrous glycoprotein member of laminin family proteins and is found in the basement membranes of the nervous tissue (Timpl and Brown, 1996; Yurchenco, 1994; Yurchenco and O'Rear, 1994). It is expressed very early during embryogenesis and becomes largely absent in adult tissues and was shown to promote cell survival, increase proliferation and maintain differentiation state (Dziadek and Timpl, 1985; Shim et al., 1996; Smyth et al., 1999; Thorsteinsdottir, 1992; Wu, et al., 1983). Another molecule is tenascin, which is implicated in neural crest and cerebellar granule cell migration and in promoting neuroblastoma cell migration (Tan, et al., 1987; Bronner-Fraser, 1988; Mackie, et al., 1988; Stern, et al., 1989; Halfter, et al., 1989; Husmann, et al., 1992). This glycoprotein is also reported to exert a neurite guidance and outgrowth promoting effect when used as a homogenous substrate for culturing neurons in vitro (Joester and Faissner, 2001; Gotz, et al., 1996; Lochter, et al., 1991; Wehrle and Chiquet, 1990; Husmann, et al., 1992).

A further example is a basement membrane-associated protein detected first in non neuronal tissues and is known as *heparin-binding growth-associated molecule* (HB-GAM, Mitsiadis, et al., 1995). In addition to its known neuronal survival and angiogenic effects (Hida, et al., 2003; Laaroubi, et al., 1994), HB-GAM in its substrate bound form shows a neurite outgrowth promoting effect on rat cerebral

neurons and is involved in neuronal maintainance and differentiation (Raulo, et al., 1992; Kuo, et al., 1990; Li, et al., 1990; Rauvala, 1989; Bradshaw, et al., 1993). In 1996, Kinnunen and coworkers were able to link this neurite outgrowth promoting effect of substrate bound HB-GAM to a specific interaction between the matrix bound protein and heparin like, highly sulfated regions of heparan sulphate chains at the cell surface (Kinnunen, et al., 1996). It was shown earlier that these cell surface proteoglycans including heparin/heparan-, chondroitin- and keratan sulafate act as cell-surface receptors or co-receptors for growth factors and molecules that mediate cell-to-ECM and cell-to-cell interactions (Rouslahti and Yamaguchi, 1991; Bernfield, et al., 1992; Lander, 1993; Lindahl, et al., 1994; Letourneau, et al., 1994; Jalkanen, et al., 1993; Yanagishita and Hascall, 1992).

There are also some of the ECM components that can exist as cell surface components where they bind the cell surface with a membrane anchor and are released or secreted into the ECM e.g. the neural cell adhesion molecule (N-CAM) (Sonderregger and Rathjen, 1992; Letourneau, et al., 1994). This protein exists as a cell surface adhesion component and is associated with ECM components. In addition, it also exists extracellularly in the cerebrospinal fluid. Concerning its functions, N-CAM was shown to exert a neurite outgrowth promoting effect on different kinds of neurons in vitro (He, et al., 1987; Doherty and Walsh, 1991).
All these examples reflect the importance of ECM bound components during the different developmental stages of the nervous system. Collectively, many ECM adhesion proteins in addition to some neurotrophic factors like nerve growth factor (NGF) and FGF-1 & -2 are characterized by playing a central role in neural development and by promoting neurite outgrowth. In the same time these molecules are identified to exert a multitude of influences on cell activities including adherence, spreading, migration, proliferation and differentiation (Ross, et al., 1991; Gospodarowics, et al., 1987; Attiah, et al., 2003).

## 1.3 Growth factors, cytokines and neurotrophic factors

### 1.3.1 Nomenclature

Growth factors and cytokines are proteins that control cell growth and proliferation by binding specific membrane receptors. This ligand-receptor interaction triggers a

cascade of intracellular biochemical signals resulting in the activation of transcription factors and hence the activation or repression of various subsets of genes (Aaronson, et al., 1990). Many growth factors stimulate cell proliferation in different kinds of cells but some others are specific for a particular cell-type. According to their structure and mode of action, growth factors can be divided into different super families as shown in the table below.

***Table 2: Examples of the super families of growth factors (McKay and Leigh, 1993).***

| Super families | Examples |
|---|---|
| 1-Large peptide factors | Transforming growth factor (TGF-β)<br>Platelet-derived growth factor (PDGF)<br>Epidermal growth factor (EGF)<br>Fibroblast growth factor (FGF)<br>Insulin-like growth factor (IGF)<br>Tumor necrosis factor (TNF)<br>Interleukin 6 (IL-6)<br>Nerve growth factor (NGF) |
| 2-Individual large peptide factors | Glial growth factor (GGF)<br>Hepatocyte growth factor (HGF)<br>Interferon alpha (IFN-α)<br>Macrophage colony stimulating factor (M-CSF)<br>Interleukin 2 (IL-2) |
| 3-Small peptide factors | Bombesin<br>Ranatensin<br>Neuromedin B (NMB)<br>Gastrin related peptide (GRP)<br>Adrenocorticotrophic hormone (ACTH)<br>Alpha-melanocyte stimulating hormone (α-MSH) |
| 4-Individual small peptide factors | Angiotensin II<br>Bradykinin<br>Vasopressin<br>Oxytocin<br>Thrombin<br>Gastrin |
| 5-Commonly used non-peptide growth factors | Androgens |

Growth factors were shown to exert their action through different modes including an autocrine and a paracrine mode of action. In the former mode the growth factor stimulates the cell that releases it and in the latter it stimulates an adjacent or a nearby cell as identified by Sporn and Todaro (Sporn and Todaro, 1980). Also an earlier known mode of action was the endocrine mode by which hormones are acting. In addition to these modes there is a condition in which some growth factors can be produced inside the cell and exert observable effects but are not secreted outside, what is known by the intracrine mode of action (Logan, 1990).

## 1.3.2 Roles of growth factors

### 1.3.2.1 General roles

Roles of growth factors are not restricted to growth and tissue formation or cell proliferation. During development, they provide important extracellular signals to regulate proliferation and determine the fate of stem and progenitor cells in CNS (Calof, 1995). For example, glial growth factor -2 (GGF-2; Marchionni, et al., 1993) can act on early neural crest cells to direct their commitment to a glial rather than a neuronal pathway of differentiation (Shah, et al., 1994). In contrast, other factors like fibroblast growth factors do not determine the cell fate of early neural progenitors during vertebrate neurogenesis, but rather they regulate the number of cell divisions a precursor cell undergoes. In olfactory epithelium cultures, many FGFs (FGF-1, -2, -4 and -7) were shown to prolong neurogenesis of immediate neuronal precursors shortly mentioned as INPs (DeHamer, et al., 1994). This effect is mostly achieved by repressing the terminal differentiation of the cells in G1 stage and permitting an extended proliferation of INPs progenitors (Clegg, et al., 1987; DeHamer, et al., 1994). This proliferation stimulating effect of FGFs was reported to be widespread in the brain. It was detected in a number of regions including E10 telencephlon (Murphy, et al., 1990; Kilpatrick and Bartlett, 1995), cerebral cortex (Gensburger, et al., 1987), corpus striatum (Cattaneo and McKay, 1990; Vescovi, et al., 1993), hippocampus (Ray, et al., 1993) and retina (Lillien and Cepko, 1992).

### 1.3.2.2 Neuron-related roles

In addition to the previously reported roles, growth factors can apparently regulate the survival of neuronal precursor cells at particular stages of differentiation. A popular example for growth factors exerting such an effect is the nerve growth factor (NGF). NGF has been long known as a survival factor for post mitotic sympathetic neurons (Korsching, 1993) that acts by signalling through tyrosine kinase A (trkA) receptors (Birren, et al., 1993, DiCicco-Bloom, et al., 1993). Roles include stimulation of proliferation and promotion of neuronal cells survival which are now reported for many other factors that are collectively termed neurotrophic factors.

Neurotrophic factors are defined as polypeptides that support growth, differentiation and survival of neurons in the developing nervous system and maintain neurons in the mature nervous system (Longo, et al., 1993, Bothwell, 1995). Recent data support the view that some neurotrophic factors may also be involved in the modification of neuronal connections in the developing brain (Thoenen, 1995). These molecules exert their effects by binding to and activating specific cell surface receptors. Activated receptors initiate a cascade of intracellular events, which ultimately induce gene expression and modify neuronal morphology and function. The following table gives a summary of some neurotrophic factors' families and their signalling receptors (Yuen, et al., 1996).

***Table 3: Some neurotrophic factors families and representative examples of each family (Yuen, et al., 1996).***

| Family | member | receptor |
|---|---|---|
| Neurotrophins | Nerve growth factor (NGF)<br>Brain-derived neurotrophic factor (BDNF)<br>Neurotrophin-3 (NT-3)<br>Neurotrophin-4/5 (NT-4/5) | TrkA<br>TrkB<br><br>TrkC, less to TrkA and TrkB<br>TrkB |
| Neuropoietins | Ciliary neurotrophic factor (CNTF)<br><br><br>Leukemia inhibitory factor (LIF or CDF/LIF) | CNTF receptor complex (CNTFRα, gp130,LIFRβ subunits)<br>LIF receptor complex (gp130, LIFRβ subunits) |
| Insulin-like growth factors | Insulin-like growth factor-I (IGF-I)<br><br>Insulin-like growth factor-II (IGF-II) | IGF Type I receptor (IGF1R), less to insulin receptor (IR)<br>IGF1R, less to IR |
| Transforming growth factor beta | Transforming growth factor b (TGFb1, TGFb2, TGFb3)<br>Glial cell line-derived neurotrophic factor (GDNF) | TGFb type I, II and III receptors<br>Unknown |
| Fibroblast growth factors | Acidic fibroblast growth factor (aFGF or FGF-1)<br>Basic fibroblast growth factor (bFGF or FGF-2)<br>Fibroblast growth factor-5 (FGF-5) | FGF receptors 1–4 (FGFR-1–4)<br>FGFR-1–3<br><br>FGFR-1, FGFR-2 |
| Other growth factors | Transforming growth factor alpha (TGF-a)<br>Platelet-derived growth factor (PDGF: AA, AB and BB isoforms)<br>Stem cell factor (mast cell growth factor) | EGFR<br><br>PDGFα- and β-receptors<br><br>c-kit |

Neurotrophins, a four-member family of neurotrophic factors, have been shown to protect against neuronal dysfunction and death in animal models of injury and

neurological disease (Yuen and Mobley, 1995). This role raised the exciting possibility that neurotrophins may act to protect neurons in diseased as well as normal neurons. It was an important step in neurosciences to realize that neurotrophic factors play important roles in the adult nervous system as well as during development (Barde, 1990; Lu and Figurov, 1997; Chao, 2000). The expression of these factors is usually very high during early development which is a time of substantial growth, differentiation, and modelling of the nervous system. In later stages, the levels of neurotrophic factors generally drop but they do not subside completely. In fact, in most cases in which it has been explored, the continued presence of these factors is substantial and is critical throughout adulthood (Maisonpierre, et al., 1990; Friedman, et al., 1991; Timmusk, et al.,1993). Neurotrophic families, particularly the NGF family, have been extensively studied for their effects on neurodegenerative diseases of both central and peripheral nervous system like Parkinson's, Alzheimer's, Huntington's and memory disorders as well as diabetic peripheral neuropathy, chemotherapy induced neurotoxicity and amyotrophic lateral sclerosis (Date, et al., 1997; O'Neill, 2001; Haque and Isacson, 2000; Brewster, et al., 1994; Gao, et al., 1995; Yah, et al., 1994; Mitsumoto, et al., 1994).

### 1.3.3 Hepatoma-derived growth factor and its related proteins

#### 1.3.3.1 Family-member overview

Hepatoma derived growth factor (HDGF) and HDGF related proteins (HRPs) represent a polypeptide family of growth factors consisting of six members belonging to different subgroups according to their length and isoelectric points (Dietz, et al., 2002). According to the classification described before in table 2, HDGF family members can be classified as individual large peptide factors. Five HDGF homologous proteins have been identified up to now (Dietz, et al., 2002; Izumoto, et al., 1997; Ikegame, et al., 1999), four of them have been termed HRP-1 to -4 (HDGF Related Proteins 1 to 4) and the fifth was termed p52/75 or LEDGF (Lens Epithelium-Derived Growth Factor). HDGF was the first member of this family to be identified. Although its sequence lacks a secretory leader sequence, HDGF was first isolated from the conditioned media of HuH-7 cells (Nakamura, et al., 1994; Ge, et al., 1998; Ikegame, et al., 1999; Izumoto, et al., 1997). HDGF and

its homologues display between 80% and 92% sequence identity among the 91 N-terminal amino acids. Because of this similarity the amino-terminal region has been termed *Homologue to Amino Terminus of HDGF* or shortly *HATH region* (Izumoto, et al., 1997). On the other hand, all the family members have no homology in the amino acid sequence of their specific C-terminal regions. All of HDGF family members show a putative nuclear localizing signal (NLS) in their self-specific regions in addition to another NLS that is found in the HATH region (Nakamura, et al., 1994; Izumoto, et al., 1997; Ikegame, et al., 1999; Ge, et al., 1998). For HDGF, this putative bipartite NLS in the self-specific region is responsible for its nuclear targeting. Any substitution of a single basic residue (lysine) in this region is sufficient to disturb nuclear targeting of HDGF.

Up to now, not much is known about the function(s) of the different members of HDGF family. Nearly most studies addressed HDGF suggesting that it plays a role in renal vascular development (Oliver and Al-Awqati, 1998) and vascular lesion formation (Everett, et al., 2000; Nakamura, et al., 1989). Extracellular HDGF was shown to signal through signal transduction pathways from the cell surface (Everett, et al., 2004, Abouzied, et al., 2005) and to act as a mitogenic factor that promotes proliferation of fibroblasts and HuH-7 cells (Nakamura, et al., 1989), endothelial cells (Oliver and Al-Awqati, 1998) and smooth muscle cells (Everett, et al., 2000). It was also shown that the nuclear localization is a prerequisite for the mitogenic activity of intracellular HDGF (Kishima, et al., 2002; Everett, 2001). These effects suggest that HDGF may be involved in tissue damage response (Marubuchi, et al., 2006).

It has also been speculated that HDGF plays a role in renal, liver, lung and heart development (Oliver and Al-Awqati, 1998; Cilley, et al., 2000; Enomoto, et al., 2002; Everett, 2001). In addition, a growing number of studies reported a possible role of this growth factor in the development of different types of cancers (Okuda, et al., 2003; Huang, et al., 2004; Bernard, et al., 2003; Hu, et al., 2003). Recently, some research groups were able to detect a role for exogenously supplied HDGF as a neurotrophic factor for hippocampal as well as motor neurons (Zhou, et al., 2004; Marubuchi, et al., 2006) when no mitogenic effect on post-mitotic neurons can be expected.

For the other members of HDGF family, very little -other than their growth factor activity- is known about their functions. HRP-1 was speculated to play a role in spermatogenesis (Kuroda, et al., 1999). LEDGF has been shown to function as a transcriptional activator that binds to and potentiates the activity of HIV integrase (Maertens, et al., 2003; Llano, et al., 2004; Cherepanov, et al., 2003 & 2004). This potentiation of HIV integrase activity has also been shown for HRP-2 (Cherepanov, et al., 2004).

#### 1.3.3.2 Hepatoma-derived growth factor related protein –3

Hepatoma derived growth factor related protein -3 (HRP-3) is a member of HDGF family of growth factors identified in 1999 by computer-aided expression sequence tag (EST) search for the homology to the HATH region (Ikegame, et al., 1999). In addition to the NLS identified within the highly conserved HATH region in all family members, the deduced amino acid sequence for HRP-3 shows a putative bipartite nuclear localizing signal (NLS) sequence in its self-specific region in a similar location to that of HDGF and HRP-1 (Nakamura, et al., 1994; Izumoto, et al., 1997). By northern blot analysis, western blot analysis and immunohistochemistry, HRP-3 expression was shown to be restricted mainly to the central nervous system tissues and to a very low extent in the testis (Ikegame, et al., 1999; Abouzied, et al., 2004). In contrast to the other family members, no functional data other than the growth stimulating activity reported by Ikegame and co-workers is known for HRP-3.

## 1.4 Aim of work

This work aimed to investigate the tissue distribution of a not widely studied member of the HDGF related protein family, HRP-3, both in embryonic and adult mice nervous tissue by using immunohistochemistry. It was also of great interest to uncover the possible intracellular roles that HRP-3 could play in the nervous system. The role(s) of HRP-3 were investigated in different cellular models including neuronal primary and clonal cell models. This was achieved by utilizing

various experimental procedures including over-expression and down-regulation of the intrinsic protein level within the cells. Due to its unique characters discovered here including tissue distribution and intracellular roles, also the extracellular roles as a trophic factor and a substrate-bound neurite outgrowth promoting factor were investigated in primary mouse cortical neuron model.

# 2. Materials

## 2.1 Instruments

| | | |
|---|---|---|
| $CO_2$ water jacketed incubator | Forma Scientifics | |
| Water bath | 1083 | GFL |
| Sterile bench | | BDK |
| Light microscope | TELAVAL 31 | ZEISS |
| Fluorescent microscope | | ZEISS |
| Confocal laser microscope | | ZEISS |
| Spectrophotometer | DU 640 | Beckman |
| Centrifuge | 5415C | Eppendorf |
| | Labofuge 400e | Eppendorf |
| | Z233 MK | Hermle |
| Vibratome | | Leica |
| Digital pH meter | Blue Line electrode | SCHOTT |
| Heating block | | STAR LAB |
| Microwave oven | Micro chef 3310 | Moulinex |
| Magnet stirrer | RCT | Ikamag |
| Ice maker | | Ziegra |
| Refrigerator | | AEG |
| Vortex device | Reox Top | Heidolph |
| Digital balance | CP 124S-OCE | Sartorius balance |
| Cold centrifuge | 5810 R | Eppendorf |
| UV lamp | FAUS NU 6 KL | |
| Electrophoresis device | electrophoresis power supply 301 | Amersham |
| Platform shaker | Rotamix 120 | Heidolph |
| PCR analyser | T3 thermocycler | Biometra |
| Sequencer | genetic analyser 310 | ABI prism |
| Protein electrophoresis cell | Protean | BioRad |
| Semi dry blotting cell | Trans-blot SD | BioRad |
| Magnetic plate | | MaTRA |

## 2.2 Equipments

| | | |
|---|---|---|
| Cell culture dish | 6 and 10 cm Φ | Falcon |
| Cell culture T-flask | 75 $cm^2$ | Falcon |
| Cell culture plate | 6 and 24 well | Falcon |
| Plastic tubes | 15 and 50 ml | Falcon |
| Reaction mini tubes | 0.5, 1.5 and 2.0 ml | Eppendorf |
| Freezing cryo-vials | 2.0 ml | Greiner |
| Sterile filter | 0.2 and 0.45 µm | Sarstedt |
| Disposable syringes | 1, 2, 5 and 20 ml | B. Braun |
| Glass pipette | 5, 10 and 25 ml | Schott |
| Glass Histobond slides | 76*26 mm | Marinefeld |
| Pasteur pipettes | 15 and 20 cm | Brand |
| Glass flasks | 50, 100, 250, 400ml | Schott |
| Filter paper | 595 ½ | Schleicher & Schuell |
| Centriplus columns | YM-30® KMWCO | Amicon |
| X-rays films | Fuji Medical X-Ray Film | |
| Nitrocellulose Transfer Membrane | Schleicher & Schuell | |
| Hemocytometer | Neubauer | |

## 2.3 Reagents

### 2.3.1 Chemicals

| **Reagent** | **Supplier** |
|---|---|
| Agarose | Gibco BRL |
| ABTS | Roche |
| Alamar blue® | AbD serotec |
| Avidin-Biotin complex kit (AB complex) | Vector |
| Bacto tryptone | DIFCO microbiology |
| Bacto yeast extract | DIFCO microbiology |
| β-mercaptoethanol | Sigma |
| BioRad DC protein assay kit | BioRad |
| Bovine serum albumin (BSA) | Sigma |
| Bromophenol blue | Sigma |
| Calcium chloride | Merck |
| Crystal violet | Sigma |

| | |
|---|---|
| DAB (diaminobenzidine HCl) | Sigma |
| DABCO (1,4-diazabicyclo(2,2,2)octan) | Roth |
| DAPI (4,6-diamidino-2-phenylindole) | Sigma |
| Dibutyryl cyclic AMP (dBcAMP) | Sigma |
| Dimethyl sulfoxide (DMSO) | Sigma |
| DNA Mini preparation kit | Qiagen |
| DNA Midi preparation kit | Qiagen |
| DPX | Sigma |
| Ethanol | Merck |
| Ethidium bromide | Sigma |
| Ethylene diamine tetra acetic acid (EDTA) | Fluka |
| Exgen 500 | Fermentas |
| Fetal calf serum (FCS) | Gibco BRL |
| Forskolin | Sigma |
| G418 | PAA |
| Gel extraction kit | Qiagen |
| Glacial acetic acid | Roth |
| Glycerol | Merck |
| Glycine | Sigma |
| HEPES | Roth |
| Histogreen | Linaris-Biologische Produkte |
| HPLC water | Merck |
| Hydrogen peroxide 30% | Sigma |
| Imidazole | Sigma |
| Isopropanol | Merck |
| Kaiser gelatine | Merck |
| L-glutamate | Gibco BRL |
| L-glutamic acid | sigma |
| Lipofectamin 2000® | Invitrogen |
| lysozyme | Sigma |
| Methanol | Merck |
| MOPS | Roth |
| Mowiol | Sigma |
| N2-supplement | Gibco |

| | |
|---|---|
| Nickel chloride hexahydrate | Fluka |
| Panceau-S | Roth |
| Paraformaldehyde (PFA) | Merck |
| PCR purification kit | Qiagen |
| Penicillin | Gibco BRL |
| Phalloidin | Sigma |
| Poly -D-lysine (PDL) | Sigma |
| Polyvinyl alcohol with DABCO® | Fluka |
| Potassium chloride | Merck |
| Potassium dihydrogen phosphate | Merck |
| REDTag™ ready mix™ PCR reaction mix | Sigma |
| SilentFect® | BioRad |
| Sucrose | Merck |
| Sodium acetate | Merck |
| Sodium azide | Merck |
| Sodium chloride | Merck |
| Sodium citrate | Merck |
| Sodium dodecyl sulfate (SDS) | Serva |
| Sodium phosphate | Merck |
| Streptomycin | Gibco BRL |
| Talon resin® | Clontech |
| Template suspending reagent (TSR) | Applied biosystems |
| Triethanolamine | Sigma |
| Tris (hydroxymethyl) aminoethane | Invitrogen |
| Triton X-100 | Fluka |
| Trypsin solution | Gibco BRL |
| Trypsin inhibitor | Gibco BRL |

### 2.3.2 Standard solutions and buffers

***Table 4: list of the standard solutions and buffers and their composition.***

| **Standard solution** | **Composition** |
|---|---|
| *150 mM NaCl* | 8.766 g NaCl/Liter $H_2O$ |
| *Phosphate-buffered saline (1x PBS)* | 150 mM NaCl, 10 mM Na-phosphate, pH 7.4 |
| *2X HEPES buffer* | 0.28 M NaCl, 0.05 M HEPES, 1.5 mM $Na_2HPO_4$ in $H_2O$, pH 7.13 |
| *2.5 M $CaCl_2$* | 277.35 gm/L $CaCl_2$ in $H_2O$ |
| *4%PFA/10% sucrose* | 4 % w/v PFA in 10 % sucrose/PBS, pH 7.4 |
| *Crystal violet staining solution* | 0.09% w/v crystal violet in 7 % alcohol |
| *Native lysis buffer* | 10 mM $Na_2HPO_4$, 1.8 mM $KH_2PO_4$ pH 7.4, 140 mM NaCl, 2.7 mM KCl, 10 mM imidazol, 0.5 mg/ml Lysozyme, 1 U/ml DNAse I, 1 mM PMSF, 2 µg/ml leupeptin, 2 µg/ml pepstatin |
| *$Ni^{2+}$-immobilization buffer* | 20 mM $Na_2HPO_4$ pH 8.0, 100 mM $Ni^{2+}$ (as $NiCl_2$. 6 $H_2O$) |
| *$Ni^{2+}$-column equilibration buffer A* | 50 mM $Na_2HPO_4$ pH 7.4, 300 mM NaCl, 20 mM imidazole |
| *$Ni^{2+}$-column elution buffer B* | 20 mM $Na_2HPO_4$ pH 7.4, 150 mM NaCl, 250 mM imidazole |
| *$Ni^{2+}$-column stripping buffer* | 20 mM $Na_2HPO_4$ pH 7.4, 300 mM NaCl, 50 mM EDTA |
| *Affigel 10® preservation buffer* | 100 mM MOPS pH 7.0, 0.02 % $NaN_3$ |
| *Saline sodium citrate buffer (2x SSC)* | 0.3 M NaCl, 0.03 M Na-citrate, pH 7.0 |
| *Sterile LB medium* | 1% (w/v) Bacto-tryptone, 0.5 % (w/v) Bacto-yeast extract, 1% (w/v) NaCl, pH 7.0 |
| *DNA electrophoresis running buffer (50x TAE)* | 2.5 M Tris base, 1 M sodium acetate, 0.1 M EDTA pH 8.0 |
| *DNA electrophoresis sample buffer* | 50 % glycerol, 50 mM EDTA, 0.25 % (w/v) bromophenol blue |

| | |
|---|---|
| *SDS-running buffer* | 192 mM glycine, 25 mM Tris, 0.1 % SDS, pH 8.3 |
| *SDS-Blotting buffer* | 10 mM Tris, 100 mM glycine, pH 8.5 and 20 % methanol |
| *4x SDS-sample buffer* | 8 % SDS, 40 % Glycerol, 240 mM Tris-HCl pH 6.8, 4 % Bromphenolblue, 4 % β-ME |
| *Panceau S* | 0.2 % (w/v) ponceau-S in 3 % trichloroacetic acid |
| *Tris buffered saline (1x TBS)* | 20 mM Tris, 137 mM NaCl, pH 7.6 |

### 2.3.3 Media

All media were purchased from Gibco BRL unless otherwise stated.

- Dulbecco's modified Eagle medium (DMEM) supplemented with 5 % foetal calf serum (FCS), 2 mM L-glutamate, 100 IU penicillin and 100 µg streptomycin.
- Freezing medium: DMEM or DMEM Nut mix-F12 containing 20 % FCS and 10 % dimethyl sulfoxide (DMSO) for storing the cells.
- Neurobasal medium (NBM) supplemented with 2% B-27 supplement.
- N2 medium: 75% DMEM + 25% Ham's F12 + 3.9 mM L-glutamate supplemented with N2 supplement: 5 µg/ml insulin, 100 µg/ml transferrin, 20 nM progesterone, 100 µM putrescin, 30 nM sodium selenite (Bottenstein and Sato, 1979).
- Hank´s balanced salt solution (HBSS).
- Opti-mem.

### 2.3.4 Antibodies

***Table 5: The primary antibodies used in immunocytochemistry and immunohistochemistry***

| **Specificity** | **Host** | **Producer/ supplier** | **Used dilution** |
|---|---|---|---|
| HDGF | Rabbit | IBMB | 1:300 of 2 µg/µl |
| HRP-3 | Rabbit | IBMB | 1:150 of 1µg/µl |
| Calbindin (Purkinje cells) | Mouse | Vector | 1:1000 |
| NeuN (Neurons) | Mouse | Chemicon | 1:500 |
| GFAP(Active astrocytes) | Mouse | Sigma | 1:100 |

| | | | |
|---|---|---|---|
| Map-2 (neurons) | Mouse | Upstate | 1 :200 |
| B-III-tubulin (Tu -20) | Mouse | Dianova | 1:100 |
| β actin | Mouse | Sigma | 1:100 |
| Anti neurofilament H | Chicken | Chemicon | 1:50 |
| Anti streptag | Cheep | Frank Dietz | 1:500 |
| Anti histag | Mouse | Sigma | 1:100 |

***Table 6: Secondary antibodies***

| **Specificity** | **Host** | **label** | **Producer/ supplier** | **Used dilution** |
|---|---|---|---|---|
| Anti-mouse | Goat | Cy2 | Dianova | 1:200 |
| Alexa fluor® 350 anti-mouse | Goat | Blue | Invitrogen | 1:100 |
| Anti rabbit | Goat | Biotin | Vector | 1:200 |
| Alexa fluor® 488 anti-rabbit | Goat | Green | Invitrogen | 1:200 |
| Anti rabbit | Goat | Cy3 | Dianova | 1:600 |
| Alexa fluor® 568 anti-chicken | Goat | Red | Invitrogen | 1:100 |
| Anti-rabbit | goat | Peroxidase | Jackson | 1:10.000 |
| Anti-mouse | goat | Peroxidase | Jackson | 1:5.000 |
| IRDye anti-rabbit | goat | Red | LiCor | 1:10.000 |
| IRDye anti-mouse | goat | Green | LiCor | 1:10.000 |

### 2.3.5 Restriction enzymes

All enzymes were purchased from Fermentas.

Restriction enzymes: HindIII, SpeI, SspI, HpaI, NotI, PstI.

Other enzymes: T4 DNA ligase.

### 2.3.6 Bacteria, cell lines and animals

| Bacteria | Genotype |
|---|---|
| BL21 | E. coli B $F^-$ dcm ompT hsdS($r_B$-$m_B$-) gal |
| XL-1 $Blue^r$ | supE44 hsdR17 recA1 endA1 gyrA46 thi relA1 lac $F'$[$proAB^+$, $lacI^q$ lacZΔM15 Tn10 ($tet^r$)] |

The used cells in culture are:

- B35 neuroblastoma cells
- Human embryonic kidney cells (HEK293T)
- Daoy medulloblastoma cells
- Mouse primary cortical neurons
- Mouse sensory neurons from dorsal root ganglia.

Animals: NMRI mice at different stages of pregnancy.

### 2.3.7 Primers

***Table 7: List of used primers***

| | | |
|---|---|---|
| HRP-3NLS1 se (5' end of the sequence | *5'-CTCGAGCTCAAGCTTGTCATGGCGCGTCCGCGG-3'* | Cloning primer |
| HRP-3NLS1 As (5' end of the sequence) | *5'-GCTACGAATATTT mGAGTTTCCAAACTTGTCTTTG-3'* | Cloning primer |
| HRP-3NLS1 se (3' end of the sequence) | *5'- CAGCAAGCTTAGCGTGTTAACCAGAACGGATTTAAT GAAGGAT-3'* | Cloning primer |
| HRP-3NLS1 As (3' end of the sequence | *5'- CTAGCATTTAGGTGACACTATAG-3'* | Cloning primer |
| HRP-3NLS2 se (480 bp fragment) | *5'-CTCGAGCTCAAGCTTGTCATGGCGCGTCCGCGG-3'* | Cloning primer |
| HRP-3NLS2 As (480 bp fragment) | *5'-TGCTGGACTAGTG TAGGACTTTTTCCGATTTGA-3'* | Cloning primer |
| HRP-3NLS2 se (294 bp fragment) | *5'-ACGCCGACTAGTAAGAAGTCTTCTAATCAGTCCCGG AACTCTCCA-3'* | Cloning primer |
| HRP-3NLS2 As (294 bp fragment) | *5'-CTAGCATTTAGGTGACACTATAG-3'* | Cloning primer |
| HRP-3siRNA1 se | *5'-CACTGCAGCCCGGTGATAGAGTAGAAGATGTTCAAG AGACATCTTCTACT-3'* | Cloning primer |
| HRP-3siRNA1 Ase | *5'-TGGCGGCCGCTTTCCAAAAAGGTGATAGAGTAGAAG ATGTCTCTTGAACA-3'* | Cloning primer |
| HRP-3siRNA2 se | *5'-CACTGCAGCCCGGAGTGAAATTTACTGGGTTTCAAG AGAACCCAGTAAAT-3'* | Cloning primer |
| HRP-3siRNA2 Ase | *5'-TGGCGGCCGCTTTCCAAAAAGGAGTGAAATTTACTG GGTTCTCTTGAAAC-3'* | Cloning primer |
| T7 sense | 5'-*GGTAATACGACTCACTATAG-3'* | Sequencing primer |
| T3 ASe | 5'-*ATTAACCCTCACTAAAGGGA-3'* | Sequencing primer |

# 3. Methods

## 3.1 Cell culture protocols

### 3.1.1 Primary mouse cortical neuron culture

Commonly used primary neurons in cultures are hippocampal, cerebellar, cortical and ganglionic neurons from rat, chicken, zebra fish and mouse. Cells are usually isolated during their developmental stage either from embryos or from newly born pups according to the cell type. In this work, cortical neurons derived from Embryonic day 14.5 mouse embryos, when undifferentiated neuron progenitors are predominant, were utilized in different experiments. For this purpose, E 14.5 NMRI mouse embryos were harvested by caesarean section from anesthetized pregnant dams. The animal protocol was approved by the Animal Care and Use Committee of the *Bezirksregierung,* Köln. Cerebral cortices were isolated in ice cold Hank´s balanced salt solution (HBSS) and digested with 0.05 % trypsin/EDTA for 12 min at 37℃ with gentle shaking after removi ng the meninges. Trypsin effect was stopped by adding an equal volume of trypsin inhibitor and 10 mg/ml BSA in PBS mixed in a ratio of 4 to 1. After a few minutes of incubation at room temperature, the supernatant was decanted carefully and the tissue pieces were dissociated with fire polished Pasteur pipette in Neurobasal medium® (Life Technologies) supplemented with 2% B-27, 500 µ*M* L-glutamine, 25 µ*M* L-glutamic acid, and 1X penicillin/streptomycin. High density cultures (9 x $10^6$ cells), plated onto 100 mm poly-D-lysine (PDL)-coated tissue culture dishes, were used for Western blot analyses. Lower density cultures (6 x $10^5$ cells), plated onto 12 mm PDL-coated glass coverslips (introduced into 24 multi-well tissue culture plates) were used for immunocytochemical studies. Tissue culture dishes were pre-coated with 100 µg/mL PDL for 1 hour at 37℃ or overnight at 4℃.

### 3.1.2 Protein coating of tissue culture vessels

Sterile 12 mm glass coverslips were pre-coated for 1 hr with PDL (100 µg /ml in water) at 37℃ then washed thoroughly with water. P re-coated coverslips (or uncoated bacterial plates in some experiments) were incubated with the purified

His-tagged protein of interest (HRP-3, HDGF or β-gal) in a concentration of 10 µg/ml at 37℃. After two hours, excess protein solu tions were aspirated and vessels were washed once with water and allowed to dry before seeding the freshly prepared mouse cortical neurons onto them.

To estimate the amount of protein bound to the PDL-coated glass surface, protein-coated, 12 mm glass coverslips as described previously were washed well to remove unbound proteins. Non-specific binding sites were blocked by incubating the coverslips with 2% BSA in PBS for 1 hr. Monoclonal antibody against His-tag diluted in the blocking solution was used to incubate the coverslips for 2 hrs. After being thoroughly washed, coverslips were incubated for 1 hr with peroxidase conjugated goat anti-mouse secondary antibody diluted in the blocking solution. Visualization of the bound peroxidase antibody was accomplished by incubating the coverslips with 2,2'-azino-di-[3-ethylbenzthiazoline sulfonate] (ABTS peroxidase substrate, Roche). The absorbance of the coloured reaction product was measured after 15-20 min using an ELISA plate reader at 405 nm according to manufacturer's instructions. Absorbance values obtained from different conditions were compared using Excel program.

### 3.1.3 Determination of neurite length

Cells (primary mouse cortical neurons or B35) were fixed after different treatments in ice cold 4 % paraformaldehyde/ 10 % sucrose (4℃ , 10 min) and immunostained using a neuronal cell marker (β-III-tubulin). Bound primary antibodies were visualized using fluorescently labelled secondary antibodies. Photos of the different cells were taken using fluorescence microscopy and the longest neurite arising from each positive cell in the captured images was measured. In some experiments also the branches arising from each positive cell were counted. Data were analysed using Excel programs and significance was calculated according to an unpaired t-test.

### 3.1.4 Neuron rescue by the addition of purified proteins

About 7 X $10^5$ freshly prepared primary cortical neurons suspended in complete NBM + B-27 were seeded on PDL coated 12 mm coverslips. Twenty four hours

after seeding, neurons were washed three times with DMEM (containing penicillin/streptomycin) to remove any residues of B-27 supplemented NBM. Afterwards, cells were incubated with a medium consisting basically of DMEM supplemented with 100 ng/ml of affinity purified recombinant His-tagged HRP-3 as a test protein or recombinant β-gal as a negative control protein. Plain DMEM medium (without any added supplements) or 5 % FCS supplemented DMEM were used as negative and positive controls respectively. Neurons were fixed three days after treatment using ice cold 4 % paraformaldehyde/ 10 % sucrose in PBS (4℃, 10 min) and non-specifically stained using cr ystal violet (0.09 % w/v in 7 % ethanol, 5 min) before mounting to analyse the general culture morphology.

### 3.1.5 Quantitative determination of cell survival using Alamar blue®

#### 3.1.5.1 Principle

Survival assays are bioassays attempting to determine the effect of an investigated factor(s) or condition(s) within a cell culture system on cell survival and/or proliferation. Colorimetric assays depending on a measurable change in the used reagent colour are reliable and easy methods to quantitatively estimate cell survival. Assays utilizing Alamar blue® incorporate an indicator dye that undergoes an oxidation-reduction (REDOX) reaction that can be photometrically measured in both forms. When it is applied to culture medium, cell growth or survival and hence respiration and electron transfer among the electron transport chain components cause a chemical reduction of Alamar blue® producing a red fluorescent reduced form. Continued growth and respiration maintain that reduced form. Inhibited growth on the other hand allows the oxidation of Alamar blue® giving a blue non fluorescent form. The measured changes in fluorescence or absorbance can be used for comparison reflecting an increased or decreased cell survival.

#### 3.1.5.2 Protocol

Survival assays used in this work were performed in a 48-well tissue culture plate format. First, neurons were seeded on PDL-coated plates in a density of 60,000 cells per well and allowed to adhere in complete NBM. After 2 hrs neurons were

washed once with warm DMEM and incubated with DMEM supplemented with the different test proteins (150 µl/well). Alternatively, neurons were seeded from the beginning in DMEM containing one of the proteins of interest. Three days after initiation of the treatment, Alamar blue® was added under aseptic conditions in a 10% ratio of the total volume and fluorescence was measured for the first time immediately after addition. Fluorescence measurements were achieved at regular time intervals using an ELISA reader at 530-560 nm excitation wave length and 590 nm emission wave length. The obtained mean fluorescence values were plotted against time and slopes of the resulting linear graphs were used for comparing the efficiency of the different supplements in promoting survival and/or cell growth.

### 3.1.6 Antibody treatment of neurons

Freshly prepared primary cortical neurons were seeded on PDL coated 12 mm glass coverslips in complete NBM+B27. Twenty four hrs after seeding neurons were washed 2x with N2 medium to remove the residual NBM. Neurons were then kept in either N2 medium alone, N2 containing 1 µg/ml polyclonal affinity purified antiserum raised against HRP-3 or N2 containing pre-absorbed anti-HRP-3. For antibody pre-absorption affinity purified antibody diluted in N2 medium (in 1 µg/ml end concentration) was incubated with an excess amount of purified recombinant His-tagged HRP-3 protein overnight at 4℃. A resin that binds to the His-tag of the protein (Talon® resin, Clontech) was then added to specifically bind the formed antibody-protein complex in the medium. By centrifugation, the medium was cleared from the resin-protein complex. After being sterile filtered, the different medium combinations were applied to neurons. Two days after treatment, neurons were fixed and non specifically stained using crystal violet solution to visualize the general morphology of cells.

## 3.1.7 Gene silencing

### 3.1.7.1 Definition and types

*Gene silencing* is a term that describes the “switching off” of a gene by a mechanism other than genetic modification within the organism aiming to regulate endogenous genes. This means, a gene which would be expressed (turned on) under normal circumstances is “switched off” by certain machinery in the cell. Mechanisms of gene silencing are a part of an ancient immune system protecting the organism's genome from infectious DNA elements (Plasterk, 2002) and it occurs at either the transcriptional or the post-transcriptional level.

*Transcriptional gene silencing* is the result of histone modifications that make the gene inaccessible to transcriptional machinery like ribonucleic acid (RNA) polymerases and transcription factors.

*Post-transcriptional gene silencing* is a result of destroying the messenger RNA (mRNA) of a particular gene and hence preventing its translation into an active gene-product (mostly a protein). RNA interference (RNAi) is considered one of the commonly used techniques for post-transcriptional gene silencing.

### 3.1.7.2 RNAi approach

RNA interference (RNAi) is a highly conserved double stranded RNA (dsRNA)-guided mechanism within living cells that helps controlling the activity level of different genes (Meister and Tuschl, 2004). There are two types of small RNA molecules controlling the process of RNA interference: *microRNA (miRNA)* and *small interfering RNA (siRNA)*. *MiRNAs* are single-stranded RNA molecules (21-23 nucleotides in length) which are partially complementary to one or more mRNA molecules, and function mainly to down-regulate gene expression. *SiRNAs* are 20-25 nucleotide-long double-stranded RNA molecules (dsRNA) with symmetric 2 nucleotide 3’-overhang that play a variety of roles like antiviral mechanisms and shaping chromatin structure of genomes. SiRNA is involved in the RNA interference (RNAi) pathway, where it interferes with the expression of specific gene(s) (Hannon, 2002; Hamilton and Baulcombe, 1999; Elbashir, et al., 2001).

SiRNA approach to gene silencing involves introducing an RNA sequence that is complementary to the mRNA transcribed from the target gene. As seen in the figure below dsRNAs are cleaved by RNAse-III-type enzymes (i.e. Dicer, Caf) into small interfering RNAs (siRNAs), probably in both the nucleus and the cytoplasm (Voinnet, 2002; Zamore, 2002).

These siRNA fragments become incorporated into various protein factors forming RNA-induced silencing complex (RISC) which become then activated. When homologous mRNAs are present in the cytoplasm, the activated RISC guided by the antisense strand of the siRNA anneals to and serves as a guide for endonucleolytic cleavage of this homologous mRNA leading to block of translation and hence blocking the production of an encoded protein (Hunter, 1999; Llave, et al. 2002; Kasschau, et al., 2003; Jana, et al., 2004).

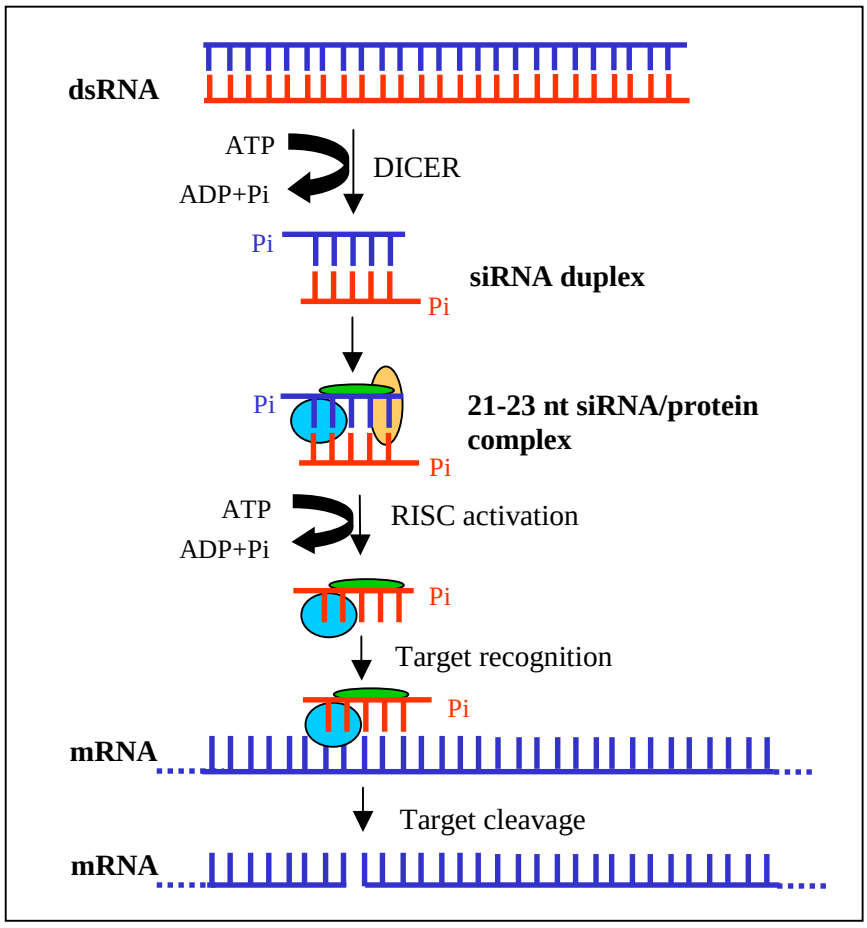


**Figure 3: A schematic diagram presenting the steps of gene silencing achieved by introducing siRNA to the cell.**

### 3.1.7.3 Transfection of neurons with siRNA oligos using lipofectamin 2000®

Transfection was done in 24 multiwell plates in triplicates using 150,000 neuronal cells per well suspended in 250 µl of culture medium. The transfection mixture per well was prepared by diluting 20 pmol siRNA (Ambion) + 5 pmol Cy3 labelled control siRNA in 50 µl Opti-mem (Gibco) in a sterile eppendorf tube. In another tube 1 µl Lipofectamin 2000® was diluted in 50 µl Opti-mem. Both solutions were mixed and allowed to stand for 20 min at RT before mixing them with the cell suspension. Afterwards, neurons suspended in transfection mix were seeded on PDL coated coverslips and final volume was filled up to 600 µl per well. Neurons were allowed to adhere to the coverslips and a medium change was done first 4-6 hrs after seeding. Neurons were fixed for staining and neurite length analysis 48 hrs after transfection.

### 3.1.7.4 Transfection of neurons with vector-based siRNA using MATra®

#### 3.1.7.4.1 Principle

Vector based siRNAs do not need the use of RNAse free chemicals and instruments. They have also other advantages including the ability to remove the untransfected cells by selecting the transfected cells using antibiotics resistance genes and the possibility to produce the vector easily by a simple transformation process (Chen, et al., 2005). When these vectors are transported into the cells they start to express the short hairpin RNA under the control of an RNA polymerase III promoter. Afterwards they are processed by the cellular machinery into 19-21 nucleotide double stranded RNA.

Magnet Assisted Transfection (MATra) approach is a new, easy-to-handle, very fast and highly efficient technology to transfect cells in culture. It can be used for all types of nucleic acids from plasmid DNA or siRNA to oligonucleotides. Using this new technique, nucleic acids are in a first step associated with specific magnetic nanoparticles (MagTag™). Exploiting magnetic force, the nucleic acid is then drawn towards and delivered into the target cells leading to efficient transfection without disturbing the membrane architecture and without causing chromosomal damage or leaving a hole in the cell membrane.

#### 3.1.7.4.2 Protocol

Freshly isolated mouse primary cortical neurons were seeded on PDL-coated 12-mm glass coverslips in a 24 well plate and kept in 500 µl complete NBM per well. One day after seeding DNA-MATra mix was prepared by diluting 0.6 µg DNA into 50 µl serum- and supplement-free medium. The diluted DNA was mixed by vortex with 0.6 µl MATra and the mixture was incubated for 20 min at RT before being applied to the cells. The mentioned amount of DNA-MATra mix was sufficient for one well of the 24 well plate so that a final volume of 550 µl/well (500 µl medium and 50 µl DNA-MATra mix) was reached. After adding the mixtures to cells, the supernatant was mixed thoroughly then the plate was placed immediately on the standard magnetic plate at 37℃ for 15 min. One to two hours after tranfection, the medium was replaced with fresh medium to remove the excess transfection mixture from cells supernatant.

### 3.1.8 Primary mouse sensory neuron culture

Sensory neuron culture is derived from dorsal root ganglia (DRG) of embryonic mice. This kind of neurons belongs to the peripheral nervous system (PNS) and originates from the embryo's migrating neural crest cells. Briefly, pregnant mice at 14.5 dpc were anaesthetized and the uterus containing the embryos was extracted by caesarean section. Embryos were released from the uterus and the amniotic sacs and they were washed before removing head, upper and lower limbs, tail and gut under a dissecting microscope. Vertebral columns from all embryos were transferred to a new Petri dish and the cartilage vertebrae were carefully removed after being opened from the ventral side using fine forceps. After exposing the neural tube and the attached DRG as seen in figure 4, an ultra fine forceps pair was used to draw the DRG away from the neural tube. Harvested DRG were transferred into HBSS in a 50-ml falcon tube using a sterile glass Pasteur pipette. To prevent adherence of the tissue pieces to the glass inner surface of the pipette, it was previously coated with 0.1 % BSA/PBS by drawing the solution up and down several times before using it for transferring the tissue.

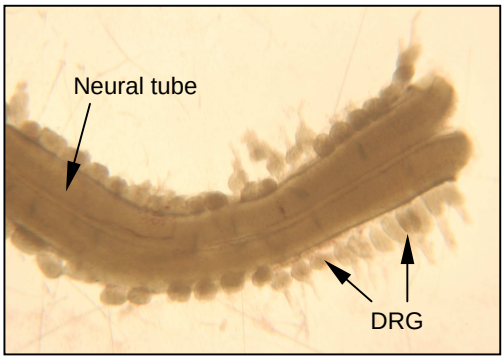


**Figure 4: A photograph showing an overview of the exposed neural tube of E14.5 mouse embryo where the attached DRG can be seen on both sides.**

To dissociate the cells, collected DRG were digested for 5 min at 37℃ using dispase/HBSS (5 mg/ml), suspended shortly with a BSA/PBS coated pipette then further incubated for another 8 min. The enzymatic reaction was stopped by adding 10 x volume of BSA/PBS solution before the suspension was centrifuged at 4,000 rpm for 5 min. After aspirating the supernatant, the cell pellet was re-suspended in NBM supplemented with 2 % B-27 and 25 ng/ml NGF and cells were counted using a haemocytometer. Cells in the needed density (about 30,000 cells/ 12-mm coverslip) were seeded on coated glass coverslips (0.1 mg/ml PDL/ 2 ng/ml laminin) and allowed to adhere. When DRG were needed in an intact form (undissociated) the step of dispase digestion and the later steps were omitted and the tissue pieces were directly seeded after isolation on PDL coated coverslips. After the required times in cultures cells were fixed in 4 % PFA/ 10 % sucrose at 4℃ and immunostained.

### 3.1.9 B35 neuroblastoma cells

#### 3.1.9.1 B35 cells in culture

B35 neuroblastoma cells represent an inducible neuronal cell line that produce a neuronal phenotype upon inducing their differentiation and can provide an alternative for primary neuron cultures. It is one of the commonly used cell lines for studying the effect of different factors on neurite outgrowth. In 1974, a panel of neuronal cell lines was derived from the neonatal rat central nervous system tumours including B35 (Schubert, et al., 1974). These cell lines offer a number of

advantages for CNS neurons research as they are simple to cultivate, differentiate, and to transfect. Under normal culture conditions with serum-containing medium, neuroblastoma cells proliferate rapidly but they have the ability to respond to serum withdrawal and increased cAMP levels by producing neuronal phenotypes bearing neurites. A known cell-permeable cAMP analog is dibutyryl cAMP (Bt2cAMP, dBcAMP) which preferentially activates cAMP-dependent protein kinase (Meyer and Miller, 1974; Boukhelifa, et al., 2001) and hence regulates neuronal differentiation, axonal guidance, neuronal survival and neurite outgrowth (Fujioka, et al., 2004; Song, et al., 1997; Hanson, et al., 1998; Meyer-Franke, et al., 1998; Neumann, et al., 2002; Cai, et al., 1999).

#### 3.1.9.2 Transient transfection of B35 cells with HRP-3 constructs

B35 cells were kept in culture under proliferative conditions using DMEM Nut mix-F12 + 5 % FCS + Penicillin/streptomycin. For transfection, about 2.5 x $10^4$ - 3.0 x $10^4$ cells suspended in culture medium were seeded on 12 mm PDL-coated glass coverslips. Twenty four hours later, Exgene 500 transfection mixtures were prepared according to the manufacturer's instructions using the different cDNA constructs. Briefly, for each well 1µg DNA was diluted in 100 µl of 150 mM NaCl before 3.3 µl Exgene 500 were added and mixed well. After 10 min of incubation at room temperature, the transfection mix was added to the cells and volume was filled up to 1 ml with culture medium. Cells were switched to fresh medium four hours after transfection. Three days later, cells were fixed and immunostained against streptag to visualize the cellular localization of the different constructs. When differentiation was required, cells were induced to differentiate 24 hrs after transfection using 1mM dBcAMP and fixed three days after induction.

### 3.1.10 Daoy medulloblastoma cells

#### 3.1.10.1 Transient transfection of Daoy cells using calcium phosphate

The calcium phosphate transfection method depends on introducing DNA to the cells via a precipitate that adheres to the cell surface. A HEPES buffer was used to

form calcium phosphate-DNA precipitate that is directly layered onto the cells. This method may be used for both transient and stable transfection of adherent cells. It introduces large amounts of DNA into the cells that pick up the DNA. One million cells were seeded 24 hrs before transfection into 10 cm plate in complete medium. For transfection, 10 µg DNA were suspended in 450 µl $H_2O$ and mixed gently with 50 µl of 2.5 M $CaCl_2$. While creating air bubbles in a tube containing 500 µl of 2 X HEPES buffer using electronic pipette, the DNA-$CaCl_2$ mixture was added drop wise to allow formation of a fine precipitate. The formed DNA-Calcium phosphate precipitate was incubated for 15-20 min at room tepmerature (RT) before adding it to the cells. After about 20-24 hrs of incubation at 37℃ in a humidified water jacketed incubator, the culture medium was exchanged with fresh medium to remove the excess precipitate from the cells.

### 3.1.10.2 Stable transfection and selection of Daoy cells

One to two days after transfecting cells with the resistance gene-encoding plasmid using calcium phosphate method, they were washed once with PBS and incubated with the selection medium. To prepare selection medium, geneticin® (G418) was diluted in the normal growth medium to a final concentration of 300 µg/ml. Selection medium was replaced every other day with fresh selection medium containing the same concentration of G418. After one week, the concentration of G418 in the medium was increased up to 400 µg/ml and cell supernatant was changed every other day for another week. Finally the concentration was increased up to 500 µg/ml and cells were kept under this concentration for one to two weeks until cell aggregates started to appear in the culture plates. For a mixed clone culture, all the colonies growing in the vessel were trypsinized together and re-plated on fresh tissue culture vessel. For single clone cultures, single clones were carefully picked up and trypsinized separately before being seeded on fresh vessels. Cells from both cases were allowed to proliferate until being semi-confluent before they were frozen and stored in liquid nitrogen for later use.

#### 3.1.10.3 Proliferation assay of Daoy cells using MTS

##### 3.1.10.3.1 Principle

Promega cellTiter® 96 $AQ_{ueous}$ Non-Radioactive cell proliferation assay is an assay to estimate cell proliferation utilizing MTS. MTS is a standard colorimetric assay (an assay which measures changes in colour) for measuring the activity of enzymes that reduce MTS + PMS to formazan, giving a purple colour. It can also be used to determine cytotoxicity of potential medicinal agents and other toxic materials which cause metabolic dysfunction and therefore decreased performance in the assay. MTS (3-(4,5-dimethylthiazol-2-yl)-5-(3-carboxymethoxyphenyl)-2-(4-sulfophenyl)-2H-tetrazolium), in the presence of phenazine methosulfate (PMS), produces a water-soluble formazan product that has an absorbance maximum at 490-500 nm in phosphate-buffered saline (Cory, et al., 1991). The reduction takes place only when reductase enzymes are active, and therefore conversion is often used as a measure of viable (living) cells.

##### 3.1.10.3.2 Protocol

To compare the viability of Daoy cells transfected with different constructs, cells were seeded into 96 well plates at a density of 5000 cells per well in 120 µl culture medium. Three days after seeding assay reagent was prepared by mixing MTS with PMS in a ration of 20:1 before 30 µl of the reagent mix were added to each well of the 96 well plate (1:5 ratio of MTS/PMS to total volume per well). Four hours later, the absorbance of the produced formazan was measured at 495 nm and the values obtained from each condition were compared.

### 3.1.11 Freezing of cells

Healthy cells growing in log phase were washed carefully with warm PBS solution then treated with trypsin solution and incubated at 37℃. After 2-3 min tissue culture plates were rocked gently to allow cell detachment then trypsin effect was stopped by diluting it with FCS containing medium. Cell suspension was placed into a sterile falcon tube and centrifuged at 3,000 to 4,000 rpm for 5 min. Under aseptic conditions supernatant was removed and cells were resuspended in ice

cold freezing medium (10 % DMSO, 20 % FCS and 70 % medium of choice) at a concentration of $2*10^6$ cells/ml. About 1-1,5 ml of cell suspension were filled into labelled cryovials and stored for one day at -80℃ before storing it in the liquid nitrogen tank.

### 3.1.12 Thawing of cells

About 10 ml of the required growth medium were placed into a 15 ml falcon tube and kept on ice while the rest of medium was warmed at 37℃. Cryovials containing the frozen cells were taken out of liquid nitrogen and thawed rapidly by swirling in a 37℃ water bath for 1-2 min. After de contaminating their outer surface, vials were taken under the laminar air flow hood and the contents were applied to the top of the previously prepared falcon tube with the cold medium. Cell suspension was centrifuged at 3,000 to 4,000 rpm for 5 min before removing the supernatant and re-suspending the cell pellet in the suitable growth medium. Cells were seeded onto 10 cm tissue culture plates and incubated at 37℃, 5 % $CO_2$ in a humidified water jacketed incubator to allow cell growth.

## 3.2 Immunolocalization protocols

### 3.2.1 Immunolocalization of interest proteins in mouse tissues

To obtain brains from adult mice, animals were deeply anaesthetized then they were perfused with 37℃ warm PBS to wash out the bl ood from the brain. After that animal tissues were fixed by perfusing it with a 37℃ warm solution of 4 % PFA in PBS. After that, heads were cut off, skulls were opened and the brains were extracted and post fixed in 4 % PFA overnight. To prepare embryonic tissues, pregnant mice at different time points of pregnancy were anaesthetized and mice embryos were extracted by caesarean section. After several washes in 37℃ warm PBS, embryos were fixed in 4 % PFA in PBS for 24 hrs. After fixation both brains and embryos were washed thoroughly in PBS before they were dehydrated through a series of increasing concentrations of ethanol (50, 60, 70, 80, 90, 100 %) using one-hour incubation in each concentration. After that, tissues

were cleared with three 60-minutes incubations in xylene before embedding in warm paraffin (56℃) overnight. Embedded tissue blo cks were allowed to solidify before being sectioned at 5-10 µm thick sections onto Histobond® glass slides (Marinefield). Slides with sections were kept at 37℃ for 24 hrs to allow for good adhesion on the glass then they were stored at 4℃. For staining, sections were deparaffinized (3 x 5 min) in xylene then rehydrated in a series of decreasing alcohol concentrations starting from 100 % down to 70 % and finally in PBS in 3 x 5 min repeats. Antibody binding sites were retrieved by heating the sections in antigen retrieval buffer (2 x SSC, pH 7.0) for 2 x 5 min using microwave oven at 600 watt. After cooling down to room temperature in the retrieval solution, sections were washed 1 x 10 min in PBS and endogenous peroxidase activity was quenched using 1 % $H_2O_2$ in PBS for 10 min. Afterwards section were permeabilized for 10 min in 0.5 % Triton X-100/PBS and washed for 3 x 5 min in PBS before blocking the non-specific binding sites with 2 % BSA/PBS for 2 hours at RT. Sections were incubated with the primary antibody diluted in the blocking solution in a humidified chamber at 4℃ overnight t hen the excess unbound antibody was washed out with PBS (3 x 5 min). Secondary antibody was diluted similarly in the blocking solution and incubated on the sections for 2 hrs at RT after which sections were washed thoroughly. For colour development of non fluorescently stained sections, tissues were further incubated with Avidin-biotin complex kit (Vector labs) for 1 hr according to manufacturer's instruction followed by Histogreen® for 1 to 5 min until a suitable colour signal with minimal background was obtained. After dehydration in xylene, sections were embedded in DPX® (Distyrene-Plasticizer-Xylene) and pictures were taken at an Axiovert zeiss microscope. When fluorescently labelled secondary antibodies were used, the peroxidase activity quenching step was omitted and direct visualization of bound antibody was possible after mounting the sections in polyvinyl alcohol with 1,4-diazabicyclo(2,2,2)octan (DABCO, Fluka) after washing for 5 min in water.

### 3.2.2 Immunolocalization of interest proteins in neuron cultures

Neurons (cortical or sensory) were fixed at different time points in ice cold 4 % paraformaldehyde/ 10 % sucrose in PBS (4℃, 10 min) , and permeabilized using 0.5 % Triton X-100 for 5 min. Non-specific binding sites were blocked using 2 %

BSA in PBS for 1 hr at room temperature after which neurons were incubated for 2 hrs with the different primary antibodies diluted in the blocking solution. After three washes in PBS, neurons were incubated with the fluorescently labelled secondary antibodies diluted in the blocking solution for 1 hr in the dark to avoid signal quenching. A nuclear counter staining with 4,6 diamidino-2-phenylindole (DAPI) was done for 2 min when required. Coverslips were finally washed 1 x PBS and 2 x $H_2O$ to remove excess salt before embedding in polyvinylalcohol with DABCO. Images were captured with an Axiovert 100M instrument (Zeiss, Jena, Germany) or by laser scan microscopy using a Leica TCS SP2 instrument (Leica, Wetzlar, Germany).

## 3.3 DNA protocols

### 3.3.1 Cloning of HRP-3 variants

Expression vectors coding for mutations in the nuclear localization signals (NLS) of HRP-3 were cloned via a two-step polymerase chain reaction (PCR) approach using a pCDNA3 vector containing the HRP-3 coding sequence as a template. For mutation of the second NLS (NLS2) as a first step, bases located 5' of the NLS site were amplified using primers *5'-CTC GAG CTC AAG CTT GTC ATG GCG CGT CCG CGG-3'* and *5'-TGC TGG ACT AGT GTA GGA CTT TTT CCG ATT TGA-3'* to produce a 480 bp fragment. This fragment was digested by HindIII/SpeI and cloned into a pBSK(-) vector. Bases located 3' of the NLS were amplified using primers *5'-ACG CCG ACT AGT AAG AAG TCT TCT AAT CAG TCC CGG AAC TCT CCA-3'* and *5'-CTA GCA TTT AGG TGA CAC TAT AG-3'* to produce a 294 bp fragment which was digested by SpeI and cloned into the pBSK(-) vector produced above (containing the 480 bp fragment).

HRP-3 mutated in its NLS1 was cloned using the primer set *5'-CTC GAG CTC AAG CTT GTC ATG GCG CGT CCG CGG-3'* and *5'-GCT ACG AAT ATT TGA GTT TCC AAA CTT GTC TTT G-3'* for the 5'-part of the sequence (HindIII/SpeI digest) and the primer set *5'- CAG CAA GCT TAG CGT GTT AAC CAG AAC GGA TTT AAT GAA GGA T-3'* and *5'- CTA GCA TTT AGG TGA CAC TAT AG-3'* (HpaI/NotI digest) for the 3'-part of the construct. Integrity of all construct were confirmed by cycle sequencing. The vector coding for the double mutant (NLS1+2)

was constructed by cutting a PstI fragment from the NLS2 mutant containing pBSK(-) vector (25 bp) and cloning it into the vector containing the NLS1 mutant. Expression vectors were constructed by subcloning into the pCDNA3 vector containing the CMV promoter for eukaryotic expression and a C-terminal signal coding for a StrepTag® peptide.

### 3.3.2 Construction of HRP3siRNA pSilencer vectors

DNA-vector-based siRNA technology, in contrast to synthetic siRNA, involves cloning of a small DNA insert of about 70 bp into a commercially available vector. This vector can be transfected into the cell by the usual transfection methods, where the DNA insert expresses a short hairpin RNA. The hairpin RNA is rapidly processed by the cellular enzyme machinery into functional double-stranded siRNA. The use of vector based siRNA provides certain advantages over chemically synthesized siRNAs, including the lower costs and the possibility of regeneration. One of the problems concerning the synthetic siRNA is the non continuous gene suppression which can be effectively overcome by using vector based siRNA. In the latter case the untransfected cells can be easily removed by selecting the transfected cells with antibiotic resistant genes. Depending on the synthetic siRNA oligos against HRP-3, two sets of oligonucleotides were designed. To amplify HRP-3siRNA1 the following set of the oligos 5´-CAC TGC AGC CCG GTG ATA GAG TAG AAG A*TG TTC AAG AG*A CAT CTT CTA CT-3´ and 5´-TGG CGG CCG CTT TCC AAA AAG GTG ATA GAG TAG AAG ATG T*CT CTT GAA CA*-3´ was used. To amplify HRP-3siRNA2 the following set of the oligos 5´-CAC TGC AGC CCG GAG TGA AAT TTA CTG GGT TTC AAG A*GA ACC* CAG TAA AT-3´ and 5´-TGG CGG CCG CTT TCC AAA AAG GAG TGA AAT TTA CT*G GGT TC*T CTT GAA AC-3´ was used. For annealing each set, five hundred picomols of each oligonucleotide in 1x ligase buffer were hybridized using the following program. 95℃ /5 min (90, 85, 80, 75, 70, 65, 60, 55℃) each for 2 min and 50℃ for 5 min. Hybridized fragments were klenow filled using 50 mM Tris-HCl (pH 7.2), 10 mM $MgSO_4$, 0.1 mM DTT, 40 µM of each dNTP, 20 µg/ml acetylated BSA and 1 unit of Klenow Fragment per microgram of DNA. The samples were incubated at

room temperature for 10 minutes then the reaction was stopped by heating the mixture for 10 minutes at 75℃.

Klenow-filled-in fragments and pSilencer vector were digested using the restriction enzymes Pst1 and Not1 according to manufacturer's recommendations. The correct size of the digested vector and annealed inserts was confirmed using 2.5 and 1% agarose gel electrophoresis respectively. The digested samples were ligated, transformed and positive clones having the insert were identified using colony screening. DNA preparation was performed on larger scale after confirming the correct sequence of insert and promoter by sequencing with the sense (T7) and antisense (T3) primers.

### 3.3.3 Ligation of DNA

DNA ligation is the process of joining linear DNA fragments together with covalent bonds. The process of ligation is catalysed by bacteriophage T4 DNA ligase, an enzyme that joins two pieces of DNA together via the formation of phosphodiester bonds between adjacent 3´-hydroxyl and 5´-phosphate termini in DNA. The enzyme catalyses ligation of DNA fragments with both blunt and single (sticky) stranded termini ends. The reaction is performed with small volumes (10-15 µl) to facilitate the annealing of two DNA fragments with compatible termini. This protocol is optimised for single strand termini ligation reactions (Sambrook, et al., 1989). The formula below is used to estimate the amount of the vector and insert needed for optimal ligation.

$$\text{X ng insert} = \frac{(\text{Y bp insert}) \cdot (50 \text{ ng vector})}{(\text{total bp in vector})}$$

Generally, vector and insert were mixed in an Eppendorf tube and T4 DNA ligase was added to them together with ligase buffer according to the manufacturer's instruction. After an incubation period that ranges from 4 hrs (at RT) to overnight (at 16℃) a small volume of the mixture was used to confirm a successful ligation by running it on an agarose gel against a suitable DNA ladder.

## 3.3.4 Transformation

### 3.3.4.1 Principle

Transformation is a process in which free DNA plasmids are introduced to bacterial cells (here E. coli were used). These bacterial cells take up the plasmids from solution and amplify them in order to produce them in large quantities because plasmids replicate by themselves by acting as extra chromosomal genomes. Only the transformed cells have to be selected from the other cells in the transformation mixture. To ensure this, plasmids containing a gene encoding a resistance to an antibiotic are usually used. Only cells containing these plasmids are able to live and multiply in a growth medium containing the same antibiotic against which a resistance gene exists. To minimise the possibility for picking cells transformed with an incorrectly inserted vector, the transformed cells were selected by the use of the α-complementation system (Sambrook, et al., 1989).

### 3.3.4.2 Protocol

About 1 ng of DNA was mixed with 100 µl competent XL-1 blue bacteria and the mixture was kept on ice for 30 minutes. A heat shock was performed by heating the mixture for 30 seconds at 42°C and suddenly cooling it on ice for 2 minutes. This heat shock enables the plasmids to enter the bacterial cells through pores in the bacterial cell wall. 900 µl of pre-warmed LB medium were added to the bacteria–DNA mix and the mixture was incubated in a shaker at 37°C for 1 hr. Afterwards, 100 to 500 µl of the DNA-bacterial cells mixture were spread on agar-LB medium plates (1.5 % w/v agar in LB medium) containing the same antibiotic used for selection and incubated at 37°C over night. Single clones arising from single bacterial cells were picked and inoculated each in 5 ml LB medium containing antibiotic (50 µg/ml penicillin) and incubated at 37°C over night. Plasmid DNA was isolated by mini prep isolation kit (Qiagen®) according to manufacturer's instructions, digested with the suitable restriction enzymes and the correct insert size was verified by agarose gel electrophoresis in comparison to a DNA standard ladder.

### 3.3.5 Colony screening

The correct clones containing the insert were verified by PCR technique using the following reaction mixture: 10 µl REDTag$^{TM}$ ready mix PCR reaction mix, 10 pmol of each forward and backward primers and volume was filled up to 20 µl with water in 250 µl PCR tubes. Using sterile tooth pickers very small amounts of the colonies to be tested were introduced into the reaction mixture. After PCR amplification using the program: [95℃ for 3 min, (95℃ for 30 se c, 55℃ for 45 sec, 72℃ for 1 min) x 30-40 cycles, 72℃ for 3 min], PCR products were separated using electrophoresis against standard DNA ladder. Clones having the correct insert size were used further for DNA isolation.

### 3.3.6 Separation of DNA by agarose gel electrophoresis

#### 3.3.6.1 Principle

Agarose gel electrophoresis is a method to separate DNA molecules migrating through an agarose matrix. The separation process depends here on the size of the migrating molecules under the effect of an electric field. Large molecules migrate slower because they have greater difficulties migrating through the pores in the gel than smaller molecules. At physiological pH, DNA is negatively charged and migrates towards the anode. DNA molecules are visualised by ethidium bromide, which intercalates between the bases in double stranded DNA so that the complex becomes fluorescent when exposed to ultraviolet light (Sambrook, et al., 1989).

#### 3.3.6.2 Protocol

Agarose gel (1 or 2,5 %) was prepared by suspending the needed amount of agarose in 1 x TAE buffer and heating in a microwave oven until the solution became clear. After cooling the solution down to about 55℃, ethidium bromide was added in a final concentration of 1 µg/ml and the mixture was allowed to polymerize in a prepared casting tray with a suitable comb size. After being completely polymerized, the gel was placed into an electrophoresis chamber filled with 1xTAE buffer. DNA samples were mixed with sample buffer and slowly loaded

into the wells before the electric current was applied (3-10 V/cm$^2$). Finally, DNA fragments were detected using a UV detector or a fluorimager.

### 3.3.7 DNA sequencing

The following reagents (all from ABI) were mixed and briefly centrifuged to spin down the droplets on the tube walls: 1 µl of 5 pmol forward or reverse primer, 2 µl Big dye and 2 µl cycle sequence buffer and the volume was filled up to 10µl with HPLC grade water. About 300-500 ng DNA were added to the previous mixture and a PCR was performed using the following protocol: 96℃ for 3 min, 30x [96℃ for 10 sec, 50℃ for 5 sec, 60℃ for 4 min].

For DNA precipitation, 10 µl HPLC-grade water, 2 µl of 3 M sodium acetate pH 5.2 and 50 µl absolute ethanol were added to PCR products, mixed well and left for 10 min at RT. After 10 min of centrifugation at 18.000 x g the supernatant was carefully removed and the DNA pellet was carefully washed with 250 µl 70 % ethanol. DNA pellets were allowed to air dry for 20 min then they were re-suspended in 25 µl of Hi Dye. Samples were applied to an ABI 310 automatic sequencer (Applied Biosystems) to verify their sequence after being denatured by heating up to 80℃ for 3 min followed by cooling down to 4℃.

### 3.3.8 Gel extraction of DNA (Qiagen®)

DNA fragments separated by agarose gel electrophoresis were extracted from the gel using a DNA gel extraction kit (Qiagen) according to manufacturer's instructions. Briefly, DNA bands were cut out and completely melt in 3 volumes of QG buffer at 50℃. One gel volume of isopropanol was added to the melted gel piece and the mixture was applied to a spin column and centrifuged for 1 minute. DNA bound to the column was washed with 750 µl of washing buffer before eluting it with 30-50 µl of elution buffer (10 mM Tris.HCl, pH 8.5) or water using a desk top-centrifuge.

### 3.3.9 Mini and midi plasmid DNA preparation (Qiagen®)

The purification was performed using Qiagen® kits according to the manufacturer's instructions.

## 3.4 Protein chemistry protocols

### 3.4.1 Purification of His-tagged proteins

#### 3.4.1.1 $Ni^{2+}$-affinity chromatography

Purification of His-tagged molecules is based on the ability of histidine to form complexes with transition metal ions, combined to a resin with a high affinity for the same transition metal ion. The high affinity of the resin for 6x His-tagged proteins or peptides is due to both the specificity of the interaction between histidine residues and immobilized metal ions and to the strength with which these ions are held to the resin. The most often used metal ions are cupric ions ($Cu^{2+}$) and nickel ions ($Ni^{2+}$) (Hi-Trap chelating column user guide, Pharmacia Biotech).

#### 3.4.1.2 Choice of lysis buffer

The native lysis buffer system recommended for the High-Trap column from Pharmacia was used for the lysis of bacterial cells induced to express the required proteins (see table of standard solutions and buffers). Tris-buffer is not recommended because it interferes with the metal-chelating system. Reagents with secondary or tertiary amines will reduce the nickel ions, and thus reduce or even eliminate the specific binding between the bound metal ion and the His-tag molecule. Other reagents that interfere with the ionic binding are HEPES, MOPS, EDTA, EGTA, DTT, SDS, Gly, Gln, Asp, His, $NH_3$.

#### 3.4.1.3 Isolation of the recombinant proteins

A Hi-Trap chelating column (1 ml column volume, from Amersham pharmacia Biotech) was charged with $Ni^{2+}$ immobilization buffer as recommended by the manufacturer and equilibrated with 5 column volumes (CV) of $Ni^{2+}$-column

equilibration buffer A. After applying the bacterial lysate to the column, unbound material was washed out with 5 CV of $Ni^{2+}$-column equilibration buffer A. Specifically bound recombinant proteins were eluted from the column with 5 CV $Ni^{2+}$-column elution buffer B and were dialysed against PBS overnight at 4℃.
Purity and correct molecular weight of the eluted proteins was proved by Coomassie staining of SDS-PAGE gels and western blotting using specific antibodies against the N-terminal histidine residue. Protein concentration was estimated by comparison to known concentrations of bovine serum albumin on Coomassie gels and with BioRad DC protein assay kit ® (BioRad).

### 3.4.2 Antibody purification protocol

Polyclonal antibodies were isolated from animal anti-sera by affinity chromatography. The bacterial protein purified by affinity Hi-Trap chelating column was dialysed against 100 mM 3-(N-morpholino) propanesulfonic acid (MOPS) buffer pH 7.0 and calcium chloride ($CaCl_2$) was added to the protein solution to reach an end concentration of 80 mM $CaCl_2$. About 2 ml of affigel 10® slurry were washed with 10 bed-volumes of 100 mM MOPS buffer pH 7.0 and mixed with the His- or GST-tagged protein. After the gel had settled down a 50 µl aliquot from the supernatant was taken as sample 1. The gel-protein mix was left on a shaker overnight at 4℃ to allow coupling of tagged protei n to gel beads and after settling of the gel another 50 µl aliquot was taken from the supernatant (sample 2). Coupling efficiency of protein molecules to the gel beads was approved by comparing protein content in sample 1 and 2. After the slurry was washed with 10 bed-volumes of 100 mM MOPS pH 7.0 to remove unbound protein molecules, it was incubated on a shaker with 1 M ethanolamine HCl pH 8.0 (0.1 ml/ml gel) for 1 hr. The produced matrix was applied to a prepared column and washed with 10 column volumes (CV) of 100 mM MOPS pH 7.0 followed by 10 CV of 100 mM MOPS pH 7.0 + 0.2 % $NaN_3$ as a preservative buffer and keep at 4℃ for later use.

Directly before using the column, it was equilibrated by washing with 10 CV of each of the following buffers respectively: 1M NaCl phosphate buffer, 100 mM glycine pH 2.5, 10 mM Tris pH 8.8, 100 mM triethanolamine pH 11.5, and 10 mM Tris pH 7.5. Animal anti-serum containing the antibodies was diluted 1:10 in 10

mM Tris pH 7.5 and centrifuged at 5,000 rpm before applying the supernatant slowly to the equilibrated antigen column. After collecting the flow through, the column was washed with 10 CV of 10 mM Tris pH 7.5 followed by 10 CV 10 mM Tris pH 7.5 + 0.5 M NaCl to remove any non-specifically bound proteins. Bound antibodies were first acidic-eluted with 5 CV of 100 mM glycine pH 2.5 and collected in 0.5 CV 1M Tris pH 8.5. In the next step, the column was washed with 10 mM Tris pH 8.8 until the pH of the column reach 8.8, the remaining antibodies were basic-eluted using 10 CV of 100 mM triethanolamine pH 11.5 and collected in 0.5 CV of 1M Tris pH 8.0.

The eluted antibody fractions from acidic & basic elutions were pooled and concentrated using spin concentrator (Centriplus YM-30® KMWCO millipore corp, Amicon) before being dialysed against 100-volumes PBS buffer three times. Dialyzed antibodies were stored in 50% glycerol and kept at –20℃. After elution of antibody, used columns were washed with 10 mM Tris-HCl pH 7.5 until pH value of 7.5 was reached and stored in the preservation buffer at 4℃.

### 3.4.3 Western blot analysis

#### 3.4.3.1 Sodium dodecyl sulfate polyacrylamide gel electrophoresis (SDS-PAGE)

Proteins possess charges as a result of acidic and basic amino acids, and in PAGE, the migration depends on the protein charge. However, in sodium dodecyl sulphate-polyacrylamide gel electrophoresis (SDS-PAGE) proteins are separated primarily according to their molecular weights because the negatively charged SDS molecules bind along the polypeptide chain and mask the charges in the molecule. During electrophoresis, migration distance of the reduced SDS-protein complex is proportional to its molecular weight and does not dependent on protein charge.

Separating gel of different percentages of acrylamide were prepared regarding the molecular weight of the separated protein according to the following table (table 8).

**Table 8: Ingredients for preparing separating SDS polyacrylamide gels.**

| Solutions | 6% | 7,5% | 10% | 12,5% | 15% |
|---|---|---|---|---|---|
| $H_2O$ | 5,79 ml | 5,42 ml | 4,79 ml | 4,17 ml | 3,54 ml |
| 40% Acrylamide | 1,50 ml | 1,88 ml | 2,50 ml | 3,13 ml | 3,75 ml |
| 1,5 M Tris-HCl pH8.8 | 2,50 ml | 2,50 ml | 2,50 ml | 2,50 ml | 2,50 ml |
| 10% SDS | 0,10 ml | 0,10 ml | 0,10 ml | 0,10 ml | 0,10 ml |
| 10% APS | 0,10 ml | 0,10 ml | 0,10 ml | 0,10 ml | 0,10 ml |
| TEMED | 0,01 ml | 0,01 ml | 0,01 ml | 0,01 ml | 0,01 ml |

Stacking gel of 5% acrylamide was prepared according to the following table (table 9)

**Table 9: Ingredients for preparing 5% stacking SDS polyacrylamide gel.**

| Solutions | Volumes (in ml) for 10 ml |
|---|---|
| $H_2O$ | 6,04 |
| 40% Acrylamide | 1,25 |
| 0,5 M Tris-HCl pH6.8 | 2,5 |
| 10% SDS | 0,1 |
| 10% APS | 0,1 |
| TEMED | 0,01 |

Using the Biorad gel casting system, the separating gel solution was filled in between the assembled glass plates. After the separating gel was polymerized, the stacking gel was poured on top and a comb with the required lane size was inserted between the glass plates then the gel was allowed to fully polymerize. polymerizaed gels were assembled in the electrophoresis cells according to manufacturer's instructions and combs were removed. Appropriate amount (30-50 µg of total protein extract) of the protein samples to be analysed were mixed with 1 volume of 2 x sample buffer containing SDS and β-mercaptoethanol. Samples were boiled for 5 min to denature the proteins. After a brief centrifugation, the samples were loaded into the lanes of the SDS-gel assembled in an electrophoresis cell (Protean, BioRad®) containing running buffer. A constant voltage of 80 V was applied to the gel until the tracking dye entered the separating gel then the voltage was increased to 120 V until the dye reached the bottom of the gel.

### 3.4.3.2 Semi dry protein transfer (blotting)

Following SDS-PAGE, separated proteins were transferred to nitrocellulose membrane having 0.45 µm pore size (Schleicher & Schuell) in a semi-dry blotting apparatus (BioRad) at 0.8 mA/cm$^2$ for 90 min using Tris/glycine/methanol blotting buffer. After transfer, the membrane was washed twice with 1 x TBS and stained with Ponceau-S to ensure proper loading and blotting as recommended by the supplier. Free protein binding sites on the membrane were blocked by incubation in 5 % skimm milk in TBS containing 0.05 % Tween-20 (TBS-T) at RT for 1 hr or over night at 4℃. After washing three times with T BS-T, the membrane was incubated with affinity purified primary antibody diluted in TBS-T containing 0.5 % skimm milk for 1 hr at RT. Unbound antibodies were removed by triple wash in TBS-T. Membrane was then incubated for 1 hr at RT with a peroxidase labelled secondary antibody against rabbit diluted similarly in TBS-T containing 0.5 % skimm milk. After three washings in TBS, bound antibodies were visualized by the ECL system (Amersham Pharmacia Biotech) according to manufacturer's protocol.

# 4. Results

## Part I: Cellular localization of HRP-3

### I.1 Expression of HRP-3 under physiological conditions

### I.1.1 HRP-3 expression in adult mouse nervous system

#### I.1.1.1 HRP-3 expression in adult mouse brain

In the work done before (diploma thesis, Eltahir) the immunolocalization of different HDGF related proteins was shown using vibratome free floating brain sections of adult mice. Immunostaining using affinity purified polyclonal antibodies raised against the investigated proteins showed a different expression pattern for each protein. Whereas HDGF was widely expressed throughout all brain areas, HRP-3 showed more restricted expression mostly in the cerebellum and hippocampus.

Starting with the cerebellum, the schematic diagram represented in figure 5 shows the cellular organization and architecture of a cerebellar lobe. It consists basically of three layers that differ in their cellular content including the molecular cell layer, Purkinje cell layer and internal granular layer arranged starting from outside. The *molecular cell layer* (MCL) contains two types of inhibitory interneurons: the *stellate cells* and *basket cells*. It also contains the dendritic arbours of Purkinje neurons and parallel fibre tracts from the granule cells in addition to axons of Golgi cells. Both stellate and basket cells form GABAergic synapses onto Purkinje cell dendrites.

The middle layer, Purkinje cell layer (PCL), contains only one type of neuronal cell bodies, that of the large Purkinje cell. Purkinje cells are primary GABAergic integrative neurons of the cerebellar cortex having dendrites that are large arbours with hundreds of spiny branches reaching up into the molecular layer and exist in one plane (flat). Both basket and stellate cells (found in the cerebellar molecular layer) provide inhibitory (GABAergic) input to the Purkinje cell, with basket cells synapsing on the Purkinje cell axon initial segment and stellate cells onto the dendrites. Purkinje cells send inhibitory projections to the deep cerebellar nuclei, and constitute the sole output of all motor coordination in the cerebellar cortex.

The third, innermost, layer is the granular cell layer which consists of two cell types: the numerous and tiny *granule cells* and the larger *Golgi cells*. Granule cells are glutamatergic neurons that account for nearly half of the neurons in the central

nervous system and are found in cerebral cortex, olfactory bulb, dentate gyrus and hippocampus in addition to the cerebellum. They send their T-shaped axons - known as parallel fibres- up into the superficial molecular layer where they form hundreds of thousands of synapses with Purkinje cell dendrites. Golgi cells on the other hand are GABAergic neurons providing inhibitory feedback to granule cells, forming a synapse with them and projecting an axon into the molecular layer (Fine, et al., 2002; Muller and O'Rahilly, 1990).

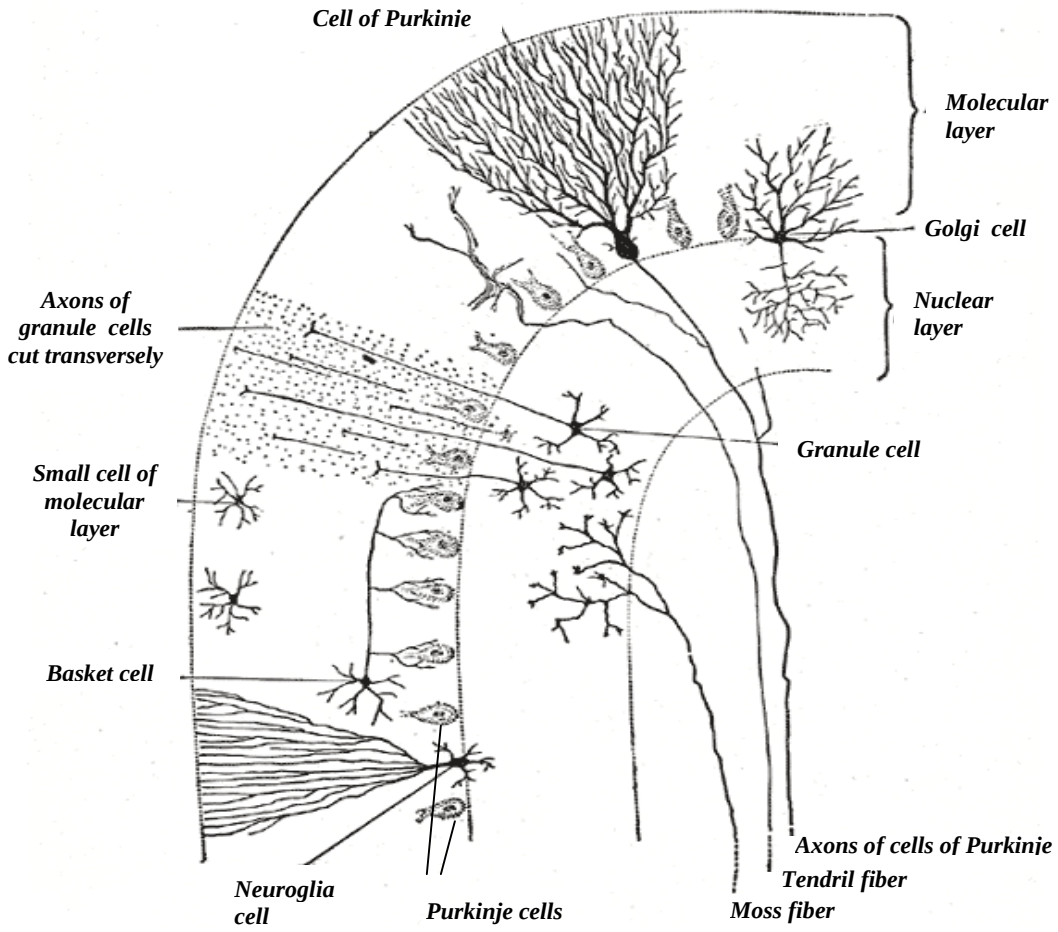


**Figure 5: Schematic diagram of a lobe of the cerebellum.** The mammalian cerebellum consists of three layers ordered from the outer to the inner: the molecular cell layer which contains basket and stellate cells, the dendritic arbors of Purkinje cells and the parallel fibers of the granule cells, Purkinje cell layer which contain the largest neuronal cells (Purkinje cells) and the nuclear (internal granular) layer which contains the small granule cells and the larger Golgi cells (Grey's anatomy, 1918).

Sagittal sections of paraffin embedded brains obtained from adult mice were used to immunolocalize HDGF and HRP-3. To proof the identity of the different cell types specific neuronal markers were used for double staining and bound

antibodies were visualized by different fluorescently labeled secondary antibodies. First, brain sections were stained against HDGF or HRP-3 together with a granular cell marker (NeuN, figure 6) to examine if both proteins were expressed by this cell population or with calbindin as a Purkinje cell marker to test for their expression in Purkinje cells (figure 7). Analysis using laser scan microscopy showed that most of the cells were expressing HDGF including granular cells and Purkinje cells of the cerebellum in addition to cells in the molecular cell layer (figures 6A, 7A). On the other hand, a very restricted expression pattern was detected in HRP-3 stained sections. HRP-3 was expressed in the Purkinje cell layer similar to HDGF but surprisingly only few NeuN negative cells were expressing it in the granular cell layer. These HRP-3 positive cells are most likely Golgi cells (arrow heads in figures 6F, 7D).

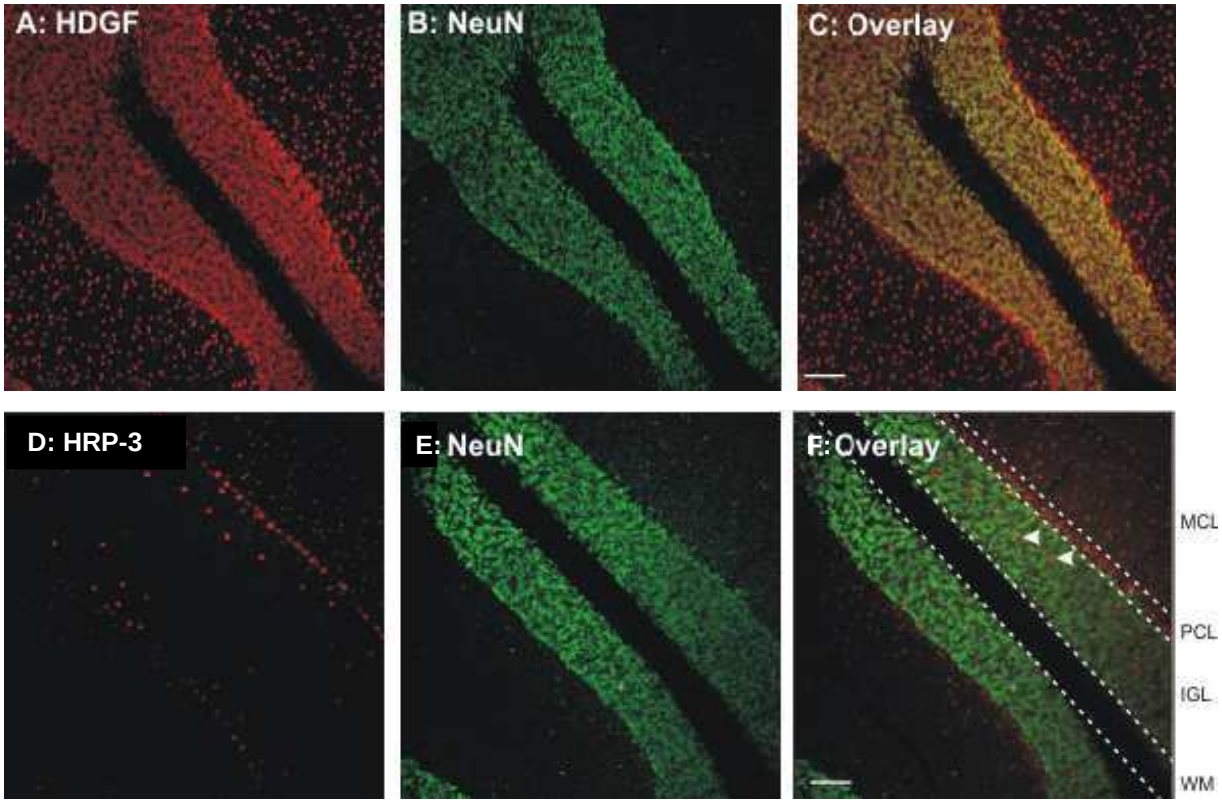


**Figure 6: Expression of HDGF and HRP-3 in granular cells of the mouse cerebellum**. Antibodies against HDGF (A) or HRP-3 (G) together with NeuN (B, E) were used to detect the expression of both proteins in paraffin embedded brain slices from adult mice. Double staining of HDGF or HRP-3 with NeuN demonstrated that in contrast to HDGF which was widely expressed in most of the cells, HRP-3 was not expressed in NeuN positive granular cells of the cerebellum. Only few distinct NeuN negative cells in the IGL, most likely Golgi cells, were detected to be HRP-3 positive (F, arrowheads). HRP-3 was also clearly expressed in the PCL and weakly in some cells of the MCL (F). MCL:

molecular cell layer; PCL: Purkinje cell layer; IGL: internal granular cell layer; WM: white matter. Bars are 80 µm.

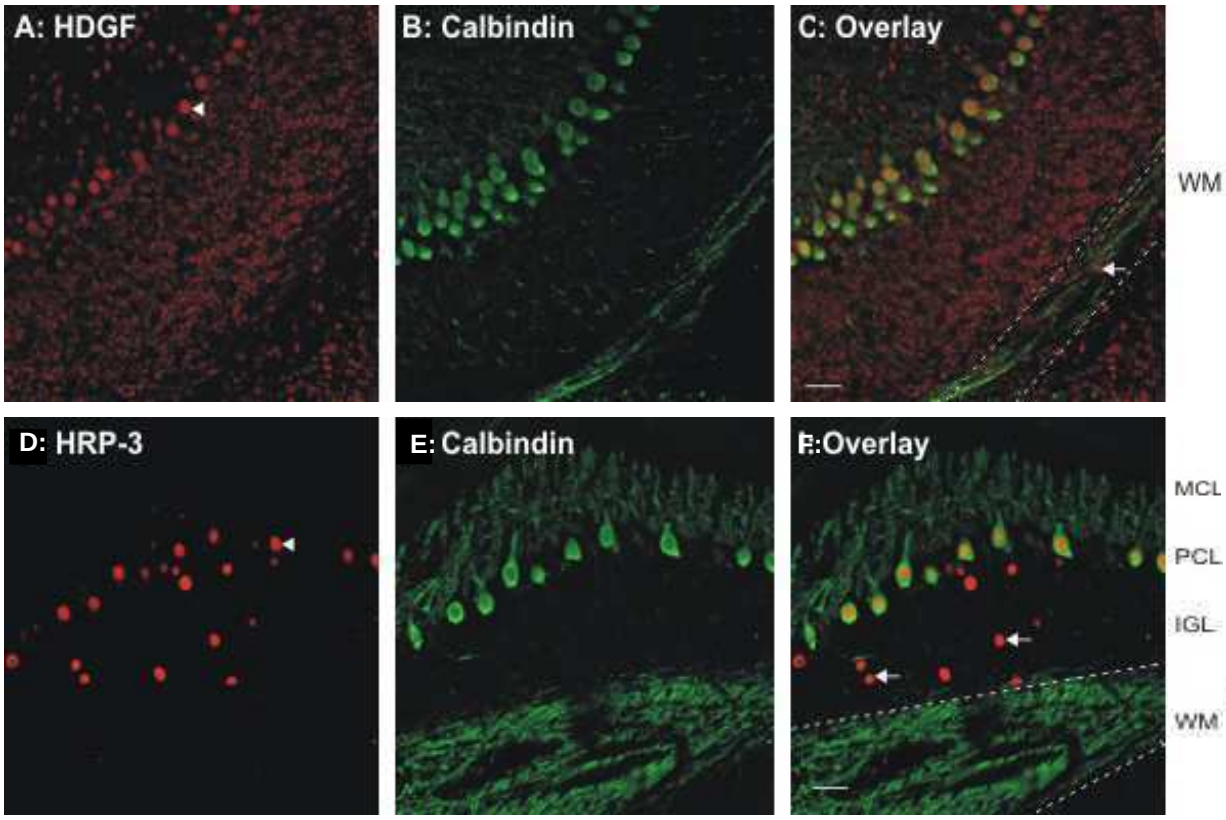


**Figure 7: Expression of HDGF and HRP-3 in Purkinje cells of mouse cerebellum.** Antibodies against HDGF (A) or HRP-3 (D) together with Calbindin (B, E) were used to detect the expression of the respective proteins in paraffin embedded brain slices from adult mice. Double staining of either proteins together with Calbindin (Purkinje cell marker) demonstrated that both members were expressed in nuclei of Calbindin positive cells of the cerebellum (arrowheads in A and D). Arrows in C indicate HDGF positive cells in the white matter. Arrows in F point to HRP-3 expressing cells in the IGL. MCL: molecular cell layer; PCL: Purkinje cell layer; IGL: internal granular cell layer; WM: white matter. Bars are 40 µm.

Detecting HDGF positive cells in white matter tracts was behind a more detailed investigation about the expression of HDGF and HRP-3 in glial cells. So that, the specific antisera directed against both proteins together with a monoclonal antibody recognizing glial fibrillary acidic protein (GFAP) were applied to sections from adult mouse brain. Immunostaining showed that cells with HDGF positive nuclei also expressed GFAP (arrowheads, figure 8). In contrast, HRP-3 did not localize to GFAP positive cells. Therefore, astrocytes express HDGF but no HRP-3. To investigate the expression of HDGF and HRP-3 in oligodendrocytes a co-immunostaining on brain stem sections was performed for both proteins together

with an antibody against 2,3-cyclonucleotid-phosphodiesterase (CNPase, Figure 9).

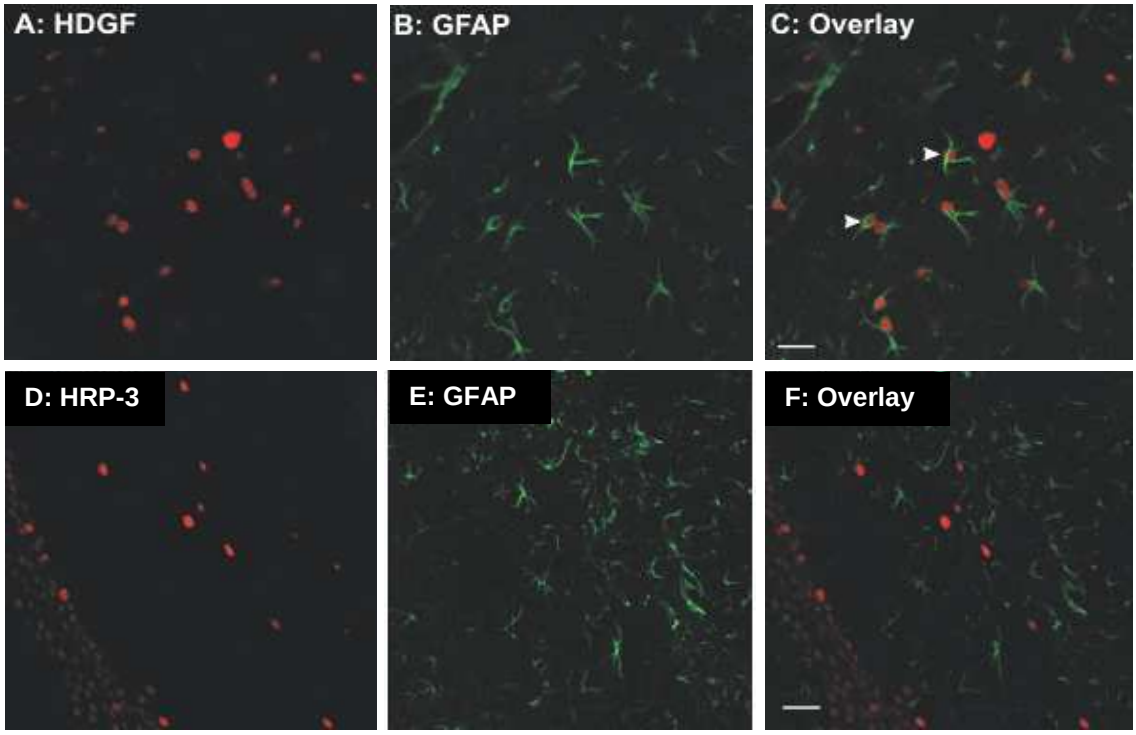


**Figure 8: Expression of HDGF and HRP-3 in astrocytes**. Antibodies against HDGF (A), HRP-3 (D) and GFAP (B & E) were used to detect the respective proteins in the hippocampal region of adult mice brain. Double immunfluorescence demonstrates that HDGF (C, arrows) was expressed in cells positive for GFAP. On the other hand, no GFAP positive cells could be detected as HRP-3 positive (F). Bars are 40 μm.

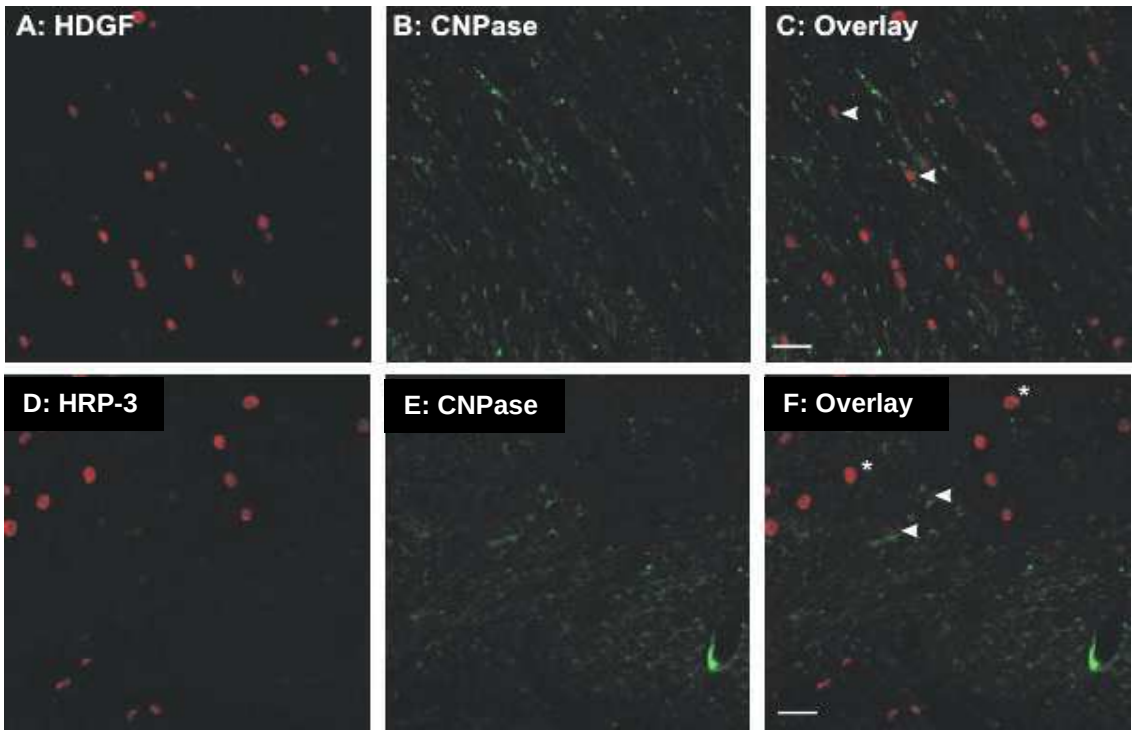

**Figure 9: Expression of HDGF family members in oligodendrocytes**. Antibodies against HDGF (A), HRP-3 (D) and CNPase (B & E) were used to detect the respective proteins in fibre tracts in the brain stem of adult mice brain. Double immunfluorescence demonstrates that HDGF (C, arrowheads) was strongly expressed by cells also positive for CNPase. In contrast HRP-3 was only very weakly expressed by this cell type (F, arrowheads) when compared to other HRP-3 positive cells which most likely represent brain stem neurons (F, asterisks). Bars are 25 μm.

Also in this staining HDGF was strongly expressed by CNPase positive cells (arrowheads in Figure 9) whereas these cells showed only very limited HRP-3 expression when compared to cells most likely representing neuronal cells of the brain stem that are strongly HRP-3 positive.

To examine whether beside the described differences there were also cell populations that simultaneously express both proteins, double staining of paraffin embedded adult brain sections using sheep antiHDGF together with rabbit antiHRP-3 was performed. A set of two different fluorescently labelled goat anti sheep and goat anti rabbit secondary antibodies was used to visualize the bound primary antibodies. Using laser scan microscopy, the expression of both proteins in cerebellum showed a low degree of co-localization. HRP-3 was expressed only in Purkinje cells and Golgi cells of the IGL but not in the white matter or in the rest of granular cells (figure 10E). Although HDGF was expressed in most of IGL cells, some of the possibly Golgi cells did (arrow heads) and some did not express HDGF (asterisk) as shown in figures 10B & C.

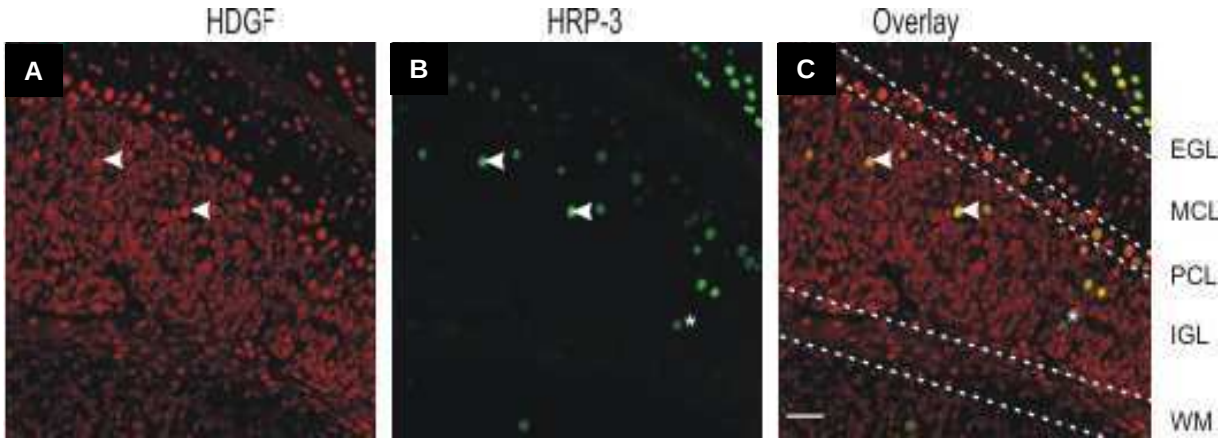


**Figure 10: Simultaneous expression of HDGF and HRP-3 in adult mouse brain cerebellum.** Antibodies against HDGF (A) and HRP-3 (B) were used to detect both proteins in the cerebellum of an adult mouse brain. Comparison of the double immunfluorescence demonstrated a low degree of co-expression. Whereas HRP-3 was

only expressed in Purkinje cells and in Golgi cells of the IGL (B), HDGF was expressed in most of cerebellum cells (A) including some of the HRP-3 positive Golgi cells (D-F, arrowheads). Some of HRP-3 positive Golgi cells did not express HDGF (B+C, asterisks). EGL: external granular layer; MCL: molecular cell layer; PCL: Purkinje cell layer; IGL: internal granular cell layer; WM: white matter. Bars are 40 µm.

The simultaneous expression of HDGF and HRP-3 was tested in two other brain structures: hippocampus and cortex. Hippocampus is a part of the forebrain that plays an important role in short term memory. It can be divided mainly into three structures: the *dentate gyrus* (DG), *subiculum* (Sub) and *Cornu ammonis* (CA). *DG* consists of three cell layers: a molecular, a granular and a polymorphic layer. *Sub* is composed of tightly packed pyramidal neurons (striatum pyramidale) which extend their dendrites into the second layer of subiculum, the striatum moleculare. The third structure, *CA*, consists of five layers: Stratum lacunosum-moleculare (I), Stratum radiatum (II), Stratum pyramidale (III), Stratum oriens (IV) and Alveus (V, only axons = white matter) mentioned from inside to outside as seen in figure 11 (Amaral, 1978; Amaral and Lavenex, 2006; Andersen, et al., 1971).

Double staining against HDGF and HRP-3 in the hippocampus area demonstrated that neurons in the different hippocampal structures co-expressed both HDGF and HRP-3 in varying degrees. Whereas HDGF was more evenly expressed in the whole hippocampal structures (figure 12A), HRP-3 showed a weak expression signal in the DG when compared to its signal in the rest of the hippocampus including sub and CA1 (figure 12B). In addition, the cells lining the ventricular wall of the hippocampus showed a lack of HRP-3 expression in the same time they expressed HDGF clearly (arrow in figure 12C).

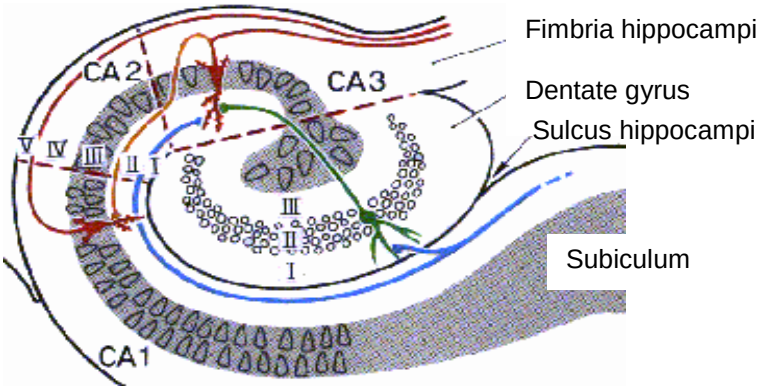


**Figure 11: A Schematic diagram showing the laminar structure of the hippocampus.** The hippocampus consists of three regions: the dentate gyrus, cornu ammonis CA1-3 and the subiculum. The dentate gyrus can be divided into lamina molecularis (I), lamina granularis (II) and hilus (III); and the cornu ammonis into: stratum lacunosum-moleculare (I), stratum radiatum (II), stratum pyramidale (III), stratum oriens (IV) and Alveus (V).

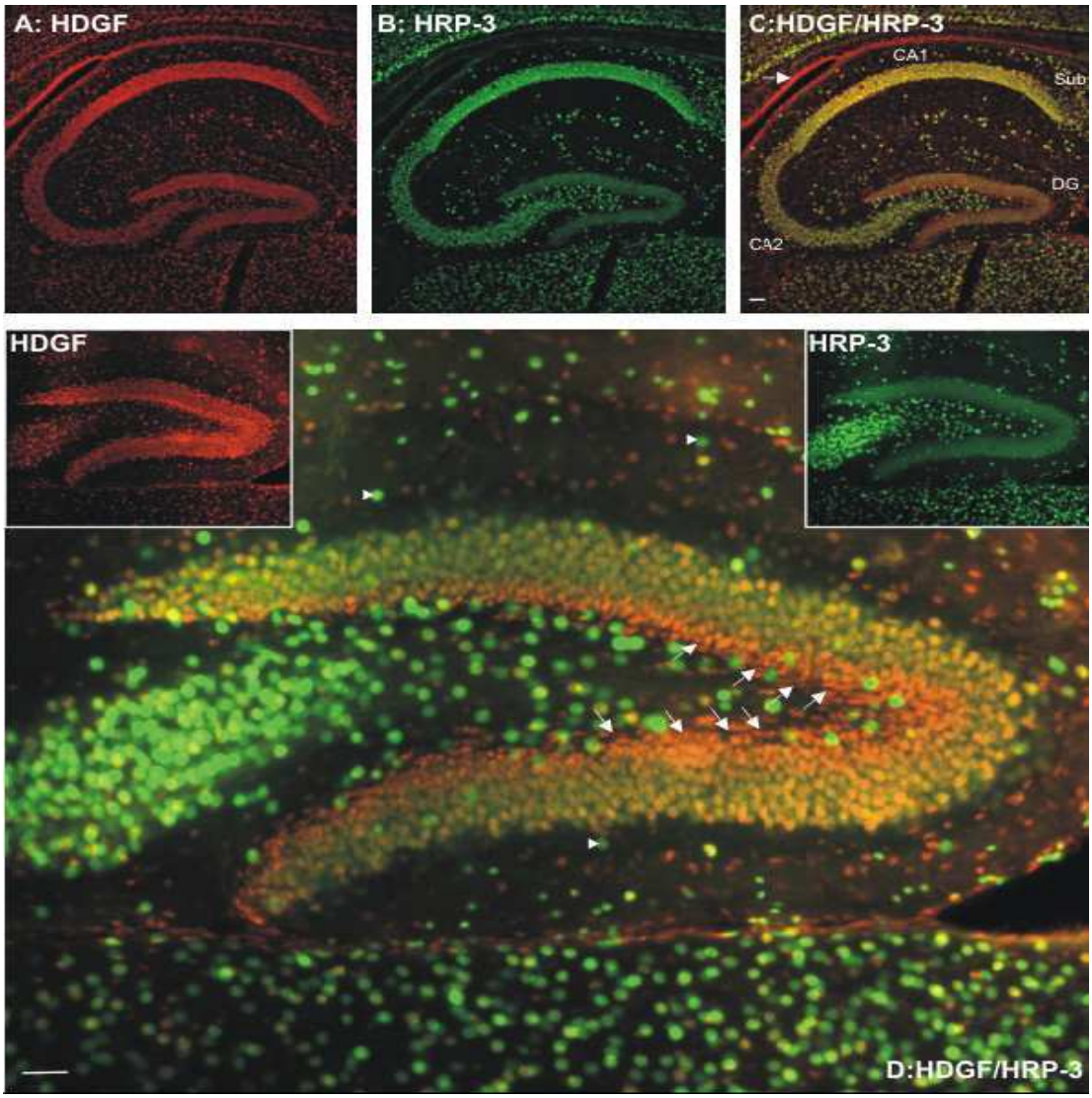


**Figure 12: Comparison of HDGF and HRP-3 expression in mouse hippocampus.** An antibody against HDGF raised in sheep (A) was used together with the rabbit raised antibody against HRP-3 described before (B) to detect both proteins in the hippocampus of adult mouse brain. Cells covering the ventricular wall of the hippocampal region (arrow in C) did not express HRP-3, whereas HDGF was clearly expressed in this cell type. Hippocampal neurons co-expressed both family members. Whereas HDGF was almost evenly expressed in all neurons of the hippocampus (A), neurons of the DG showed only weak expression of HRP-3 compared to the rest of the hippocampus (B). Arrow heads in D (D is a higher magnification of C) show cells that predominantly expressed HRP-3 whereas arrows show a cell layer that was only positive for HDGF. CA: cornu ammonis; Sub: subiculum; DG: dentate gyrus; Bar in C is 80 µm; bar in D is 40 µm.

Arrow heads in figure 12D show cells that predominantly expressed HRP-3 whereas arrows show a cell layer that was only positive to HDGF. The Pia mater represents the innermost layer of the meninges enveloping and protecting the brain and is derived from neural crest cells on the surface of the neocortex. Immunostaining demonstrated that cells forming the Pia mater (PM, figures 13A &

C), expressed HDGF but not HRP-3. Some cells in layer I were HRP-3 negative whereas cells in the rest of the cortex showed a high degree of co-expression of both HDGF and HRP-3 (figures 13A-C).

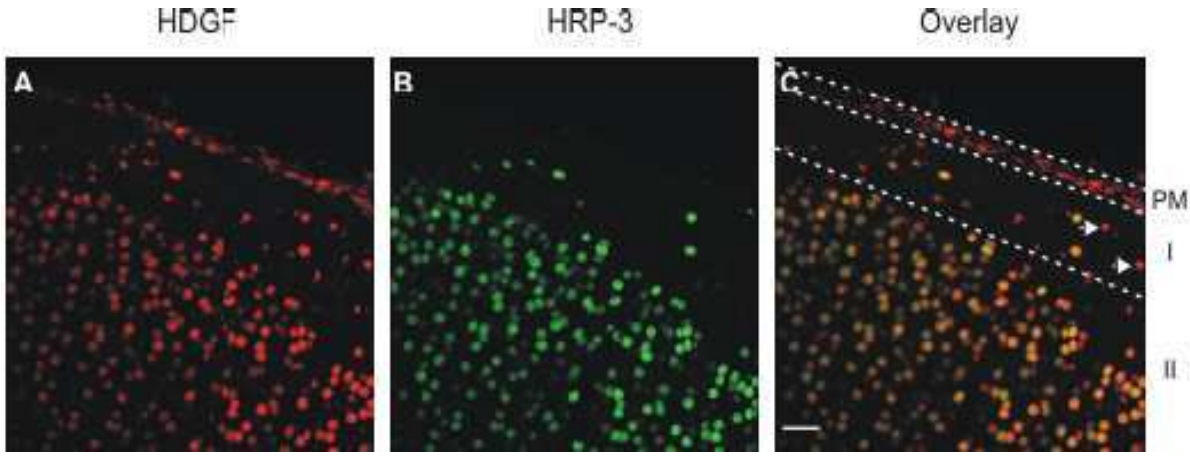


**Figure 13: HDGF and HRP-3 expression in adult mouse brain cortex.** Antibodies against HDGF (A, D) or HRP-3 (B, E) were used to detect both proteins in the neocortex of an adult mouse. Comparison of the double immunfluorescence demonstrated the lack of expression of HRP-3 in cells building the pia mater at the surface of the cortex (PM in C) and some cells in layer I (C, arrows). Cells in the rest of the cortex showed a high degree of co-expression of HDGF and HRP-3. PM: Pia Mater; I+II: layer I and II. Bars are 40 µm.

As it was shown before in fluorescently stained free floating sections from adult brain, HRP-3 was expressed in the processes of hippocampal neuron. To have a more detailed view, a better structure preservation was required. So that paraffin blocks prepared from PFA perfused and fixed adult mouse brain were used to prepare 5 to 10 µm thick sagittal sections. These sections were deparaffinized and immunostained as mentioned in the Methods part using a biotin labelled anti-rabbit secondary antibody. Bound antibodies were visualized with Histogreen® as a substrate (chromogen) for the Avidin-biotin reaction. This method of staining provided a very good structure preservation. Examination by light microscopy interestingly demonstrated a cytoplasmic localization of HRP-3 in addition to the expected nuclear signal in some brain regions. Arrows in figures 14A & D point to cells in the cerebral cortex that beside the nuclear signal also showed a signal in some of their processes. These cells represented most probably neuronal cells of the third cortical layer (layer III) which are usually characterized by the vertically-oriented intracortical axons. In the Sub and CA (in hippocampus) also, extranuclear expression signals for HRP-3 were detectable (figure 14B & E) .

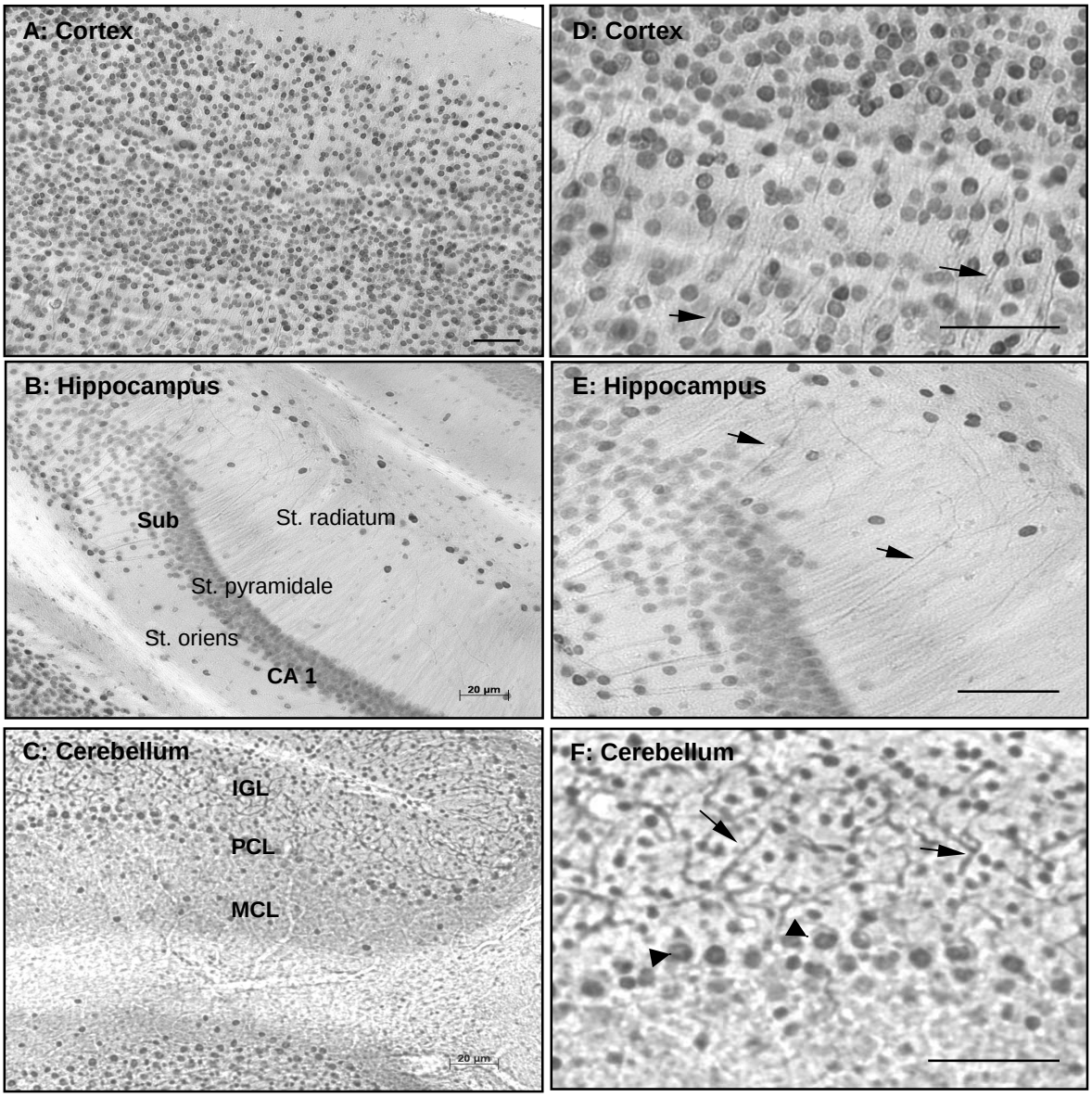


**Figure 14: Extranuclear expression of HRP-3 in different areas of adult mouse brain.** Five to ten micrometer-thick paraffin embedded adult mouse brain sections were immunostained against HRP-3 using biotin labelled secondary antibody. Avidin biotin complex kit followed by Histogreen® as a chromagen were used to visualize the immunreaction. Examination under a light microscope showed an expression of HRP-3 in the nuclei as well as in the cytoplasm including cell body and/or cell processes in the deeper layers of the cortex (A), stratum pyramidale and stratum radiatum layers of the hippocampus (B) and in Purkinje cells in the cerebellum (C). Arrows point to areas of cytoplasmic expression whereas arrowheads point to nuclear signal of HRP-3. D, E and F are higher magnifications of the 20x photos A, B and C. CA 1: cornu ammonis 1; Sub: subiculum; IGL: internal granular cell layer; PCL: Purkinje cell layer; MCL: molecular cell layer. St. radiatum: stratum radiatum; St. pyramidale: stratum pyramidale; St. oriens: stratum oriens. Bars are 20 µm.

In the different hippocampal structures, HRP-3 was expressed in the nuclei of the pyramidal cells (stratum pyramidale, layer III) and possibly in the nuclei of some cells of striatum oriens (layer IV) as seen in figures 14B & E. In addition, an

extranuclear expression of HRP-3 in the Stratum radiatum was detected, which contains septal and commissural fibers (arrows in figure 14E) together with some interneurons (basket cells, bistratified cells, and radial trilaminar cells).

In a third region, the cerebellum, also a cytoplasmic signal for HRP-3 was clearly detected in the largest neurons found there, Purkinje cells. These cells which have characteristic highly branched processes showed a very impressing HRP-3 staining in their dendritic trees. In the same way, this extranuclear expression pattern was accompanied by a more prominent nuclear HRP-3 signal as shown by the arrows in figures 14C & F.

### I.1.1.2 HRP-3 expression in adult mouse spinal cord

The spinal cord is a long, thin tubular bundle of nerves that represents an extension of the central nervous system arising from the brain. Its main function is to transmit neural inputs and outputs between the brain and the periphery. It consists mainly of an outer envelope called the white matter and an inner core named the grey matter which can be distinguished by the naked eye due to the color difference. The white matter consist mainly of the myelinated nerve axon fibers traveling long distances from the spinal cord to the brain and vice verse in addition to a minor population of cells, some astrocytes, oligodendrocytes and endothelial cells from blood vessels. On the other hand, the grey matter is made up mainly of different types of neuronal cell bodies together with their dendrites. Grey matter can be divided roughly into two ventral and two dorsal horns.

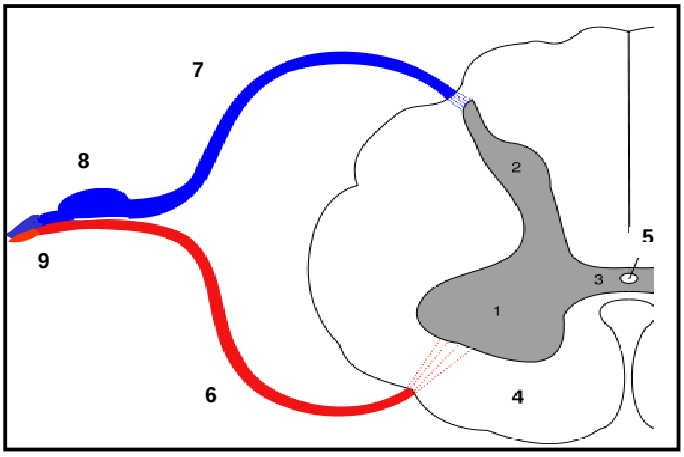


**Figure 15: Schematic diagram of the adult spinal cord in mammals**. Spinal cord consists of white matter (the outer part, white in diagram) and grey matter (inner core, grey in diagram). Numbers represent the following structures: 1 ventral horn, 2 dorsal horn, 3

Gray's commissure, 4 white matter, 5 central canal, 6 ventral root, 7 dorsal root, 8 dorsal root ganglion, 9 spinal nerve.

Motor neurons are located in the ventral horns on the ventral side of the spinal cord (structure 1, figure 15) giving rise to the ventral roots (structure 6, figure 15) which are bundles of nerve axons innervating target muscles. The sensory neurons (projection- and interneurons), on the other hand, exist in the dorsal horns of the spinal cord (structure 2, figure 15) and deal with the sensory perception signals from allover the body transmitted to them through the dorsal roots (structure 7, figure 15).

Along their length, these dorsal roots show cell aggregations named the dorsal root ganglia (DRG, structure 8 in figure 15). DRG consist of afferent (receptor) spinal neuron cell bodies that send their dendrites to the periphery to take up the sensory signals and send their axons in a bundled form called the dorsal roots to the spinal cord to conduct the received signals. In the intermediate area between both horns, the autonomic neurons which innervate muscles and glands are located (Nolte, 2002). As a part of the nervous system, it was interesting to know if HRP-3 was expressed in the spinal cord. To check for HRP-3 expression in this organ, paraffin embedded transverse sections from adult mouse spinal cord were stained against HRP-3 using a non fluorescent avidin-biotin based immunostaining technique. A moderate expression signal was detected in many areas including both white and grey matter. As mentioned above, HRP-3 was expressed in the adult mouse brain in both nuclear and extranuclear patterns in some cell populations. Similarly, adult spinal cord showed nuclear and extranuclear expression patterns. Here, HRP-3 was distributed between nuclei in the majority of cells on one side as shown by arrows in the figures 16D & E, and the cytoplasm and cell processes in a minority of cells on the other side as shown by arrow heads in these figures. It can also be noticed that the expression level of HRP-3 was higher in motor neurons area in the ventral horn (figures 16D & E) than in the sensory neurons area in the dorsal horn (figure 16C). Also axons in the white matter showed a fibrous staining pattern for HRP-3 as seen in figure 16E. No significant signal for HRP-3 expression was detected in the ependymal cells surrounding the central canal through which the cerebrospinal fluid runs in the middle of the grey matter (figure 16B). No immunoreactivity was observed when only the secondary antibody was used for immunostaining.

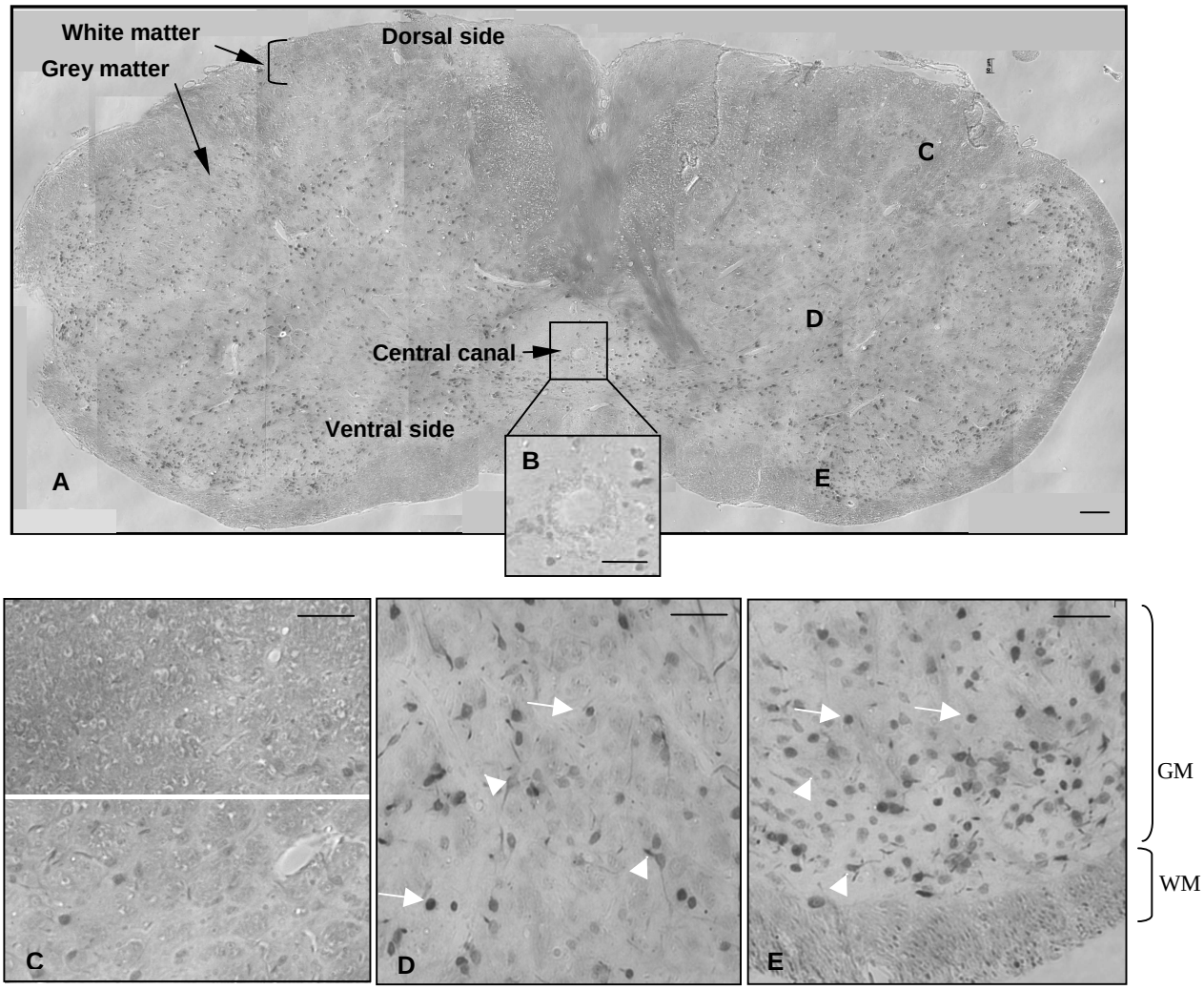


**Figure 16: Expression of HRP-3 in adult mouse spinal cord.** Transverse sections from adult mouse spinal cord were stained against HRP-3 using avidin-biotin system followed by Histogreen®. Figure A represents a mosaic overview of the whole section assembled from multiple, low magnification pictures (10x, A). C, D and E represent shots from three different areas taken at a higher magnification. A clear expression signal was detected for HRP-3 in the areas D and E (motoneuron areas) in the nuclei of many cells (arrows) as well as in the cell cytoplasm and processes of other fewer cells in the grey matter (arrow heads). A fibrous expression pattern for HRP-3 was also noticed in the white matter, WM (E). The area of sensory neurons (C) showed a weaker HRP-3 signal detected in fewer cells compared to motoneuron areas. Ependymal cells surrounding the central canal did not express HRP-3 (B). GM: grey matter, WM: white matter. Bars are 50 µm.

### I.1.1.3 HRP-3 expression in adult mouse sciatic nerve

HRP-3 expression up to this point was detected in the central nervous system (CNS) but whether it is expressed in the peripheral nervous system (PNS) needed further examination. The sciatic nerve is a part of this PNS and is the largest and thickest nerve in the body emerging from the spinal cord at the lumbar part. It represents the main nerve supply for the lower limb and consists of a large

number of myelinated fibers (myelinated nerve axons). Myelination process of the peripheral nerves includes the enwrapping of the axons with layers of special, lipid enriched membranes (myelin) which act as an insulator for the transmitted signals. In the periphery, myelin production is taken over by Schwann cells that lie among the nerve axons. Each single axon (fiber) is individually wrapped with a very delicate layer of connective tissue called the endoneurium produced by fibroblasts. These individual fibers are collected into numerous bundles and each nerve bundle is surrounded by a layer of connective tissue known as the perineurium separating it from other bundles. These wrapped bundles are then collected all together to form the nerve by an external layer of connective tissue: the epineurium.

To examine for HRP-3 expression in the PNS, sciatic nerve was prepared from the lower limb of an adult mouse and cut into longitudinal sections. These sections were stained against HRP-3 and HDGF for comparison using immunofluorescent staining technique. As expected from a protein expressed by axons, HRP-3-stained nerve sections showed a fibrous staining along the nerve as shown by arrow heads in figure 17A. In contrast, HDGF-stained sections showed only a nuclear pattern of staining (figure 17B) probably corresponding to the nuclei of Schwann cells present along the nerve fibers.

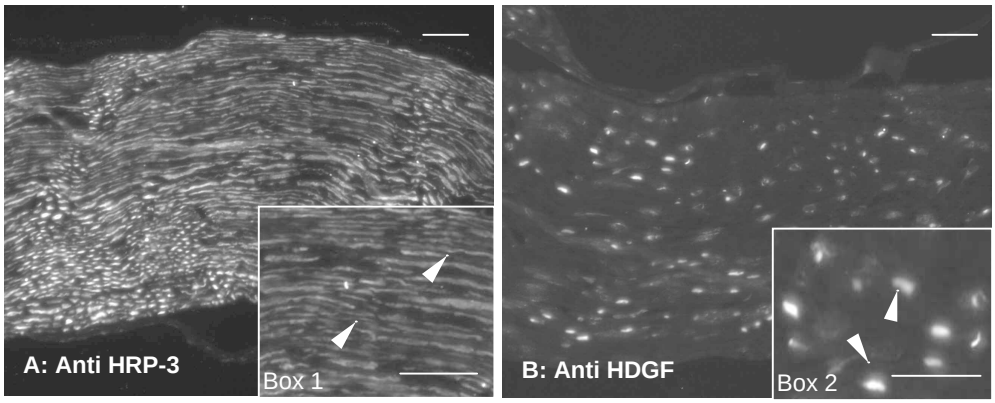


**Figure 17: Expression of HRP-3 and HDGF in adult mouse sciatic nerve.** Paraffin sections obtained from adult mouse sciatic nerve cut along its length were stained against HRP-3 or HDGF using specific primary antibodies and fluorescently labelled secondary antibody. Boxes in A and B represent a higher magnification of the original pictures. A fibrous pattern of staining was observed in the sections stained for HRP3 as shown by the arrow heads in box 1. On the other hand, a staining of what is likely to be Schwann cell nuclei was observed in case of HDGF stained sections with a complete absence of axonal staining as seen in box 2. Bars are 20 µm.

## I.1.2 HRP-3 expression in the embryonic mouse

### I.1.2.1 General expression of HRP-3 in mouse embryo

All the previously presented data showed that HRP-3 was expressed in both adult CNS and adult PNS. The expression signal was detected primarily in cell nuclei but in some cell populations HRP-3 was also expressed in the cell cytoplasm.

To check for a possible expression of HRP-3 during the development of the nervous system, immunhistochemistry was performed on sections prepared from mouse embryos at different developmental stages. First, transverse sections in the neck region of an E11.5 mouse embryo were stained against HRP-3. Staining showed a strong expression signal that was highly restricted to nervous tissues (Figure 18A). At this time point of the embryonic life, the neural plate had already folded itself into a neural tube. This tube can be distinguished into a dorsal part and a ventral part. The dorsal part contains the sensory neurons which receive sensory inputs from the different organs through axon bundles known as the posterior or dorsal roots (these axons develop from the cells of the neural dorsal ganglia). The ventral part contains the motor neurons which extend their axons in the form of bundles known as the anterior or ventral roots to the different organs as seen in the schematic diagram (figure 18B). Immediately beyond the dorsal root ganglion (DRG, neural ganglion), both ventral and dorsal roots join to form a spinal nerve which later on is split into anterior, posterior, and visceral divisions (Kandel, et al., 2000).

Immunostaining against HRP-3 in figure 18 shows that the motor neurons (MN) and their axons (anterior nerve root, ANR) expressed higher amounts of HRP-3 than the sensory neurons (SNC) which resembles the pattern represented before in the adult spinal cord. In the posterior nerve root (PNR), a much weaker signal was detected, however, the oval bundle (OB) which is the area where the PNR penetrates the neural tube showed a comparatively high expression signal. The expression was also high in the spinal nerve (SN) and its visceral branch (VB). Comparing the expression in the sympathetic ganglia (SG) and in the dorsal root ganglion (DRG) showed that the former ones, SG, expressed higher amounts of HRP-3 than the latter, DRG. A weaker signal was detected in the rest of the neural tube cells including the roof and floor plates (RP & FP, respectively) and the neuroepithelium forming the major mass of the neural tube. In the same time, no detectable expression signal for HRP-3 was found in the other structures

comprising the rest of the embryonic tissue seen in these sections other than those related to the nervous system. Similar observations in the neural tube were obtained from free floating, PFA fixed transverse sections using fluorescent secondary antibody (see supplementary data, figure S1).

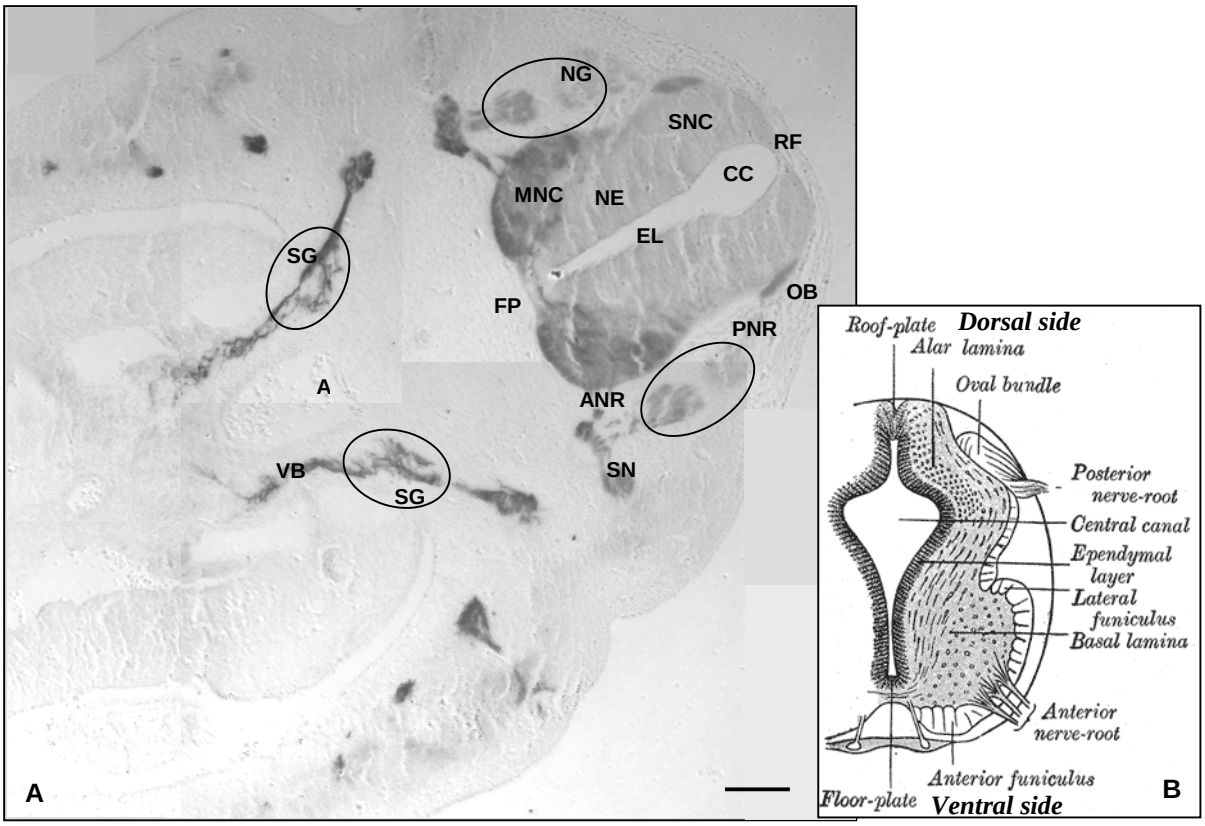


**Figure 18: Expression of HRP-3 in transverse section of E11.5 mouse embryo.** Picture A represents a transverse section from an E11.5 mouse embryo in the neck area showing the neural tube immunostained against HRP-3 using avidin-biotin technique. A strong expression signal for HRP-3 was detected in most of the neural tube structures including oval bundle (OB), sympathetic ganglion (SG), anterior nerve root (ANR, Efferent motor neuron axons), spinal nerve (SN) and motor neuron (MN) cell bodies. A weaker HRP-3 signal was detected in neural ganglion (NG), floor and roof plate (FP, RP), posterior nerve root (PNR) and neuroepithelium (NE). B: schematic diagram represents the different structures in the neural tube (Grey's anatomy). A: aorta, CC: central canal, SNC: sensory neurons cell bodies, EL: ependymal layer, VB: visceral branch of the spinal nerve. Bar is 100 µm.

Staining of sagittal section near the middle line of an E15.5 whole mouse embryo against HRP-3 underlined the results regarding the restriction of HRP-3 expression to nervous tissue (Figure 19). All brain divisions, prosencephalon (I), mesencephalon (II) and rhombencephalon (III) were positive for HRP-3. In addition, a signal was detected in the exposed parts of the spinal cord (arrows in figure 19A) and in the dorsal root ganglia (DRG, figure 19B) together with the

fibres connecting them to the spinal cord (dorsal roots, posterior nerve roots) as pointed out with arrow heads in figure 19B.

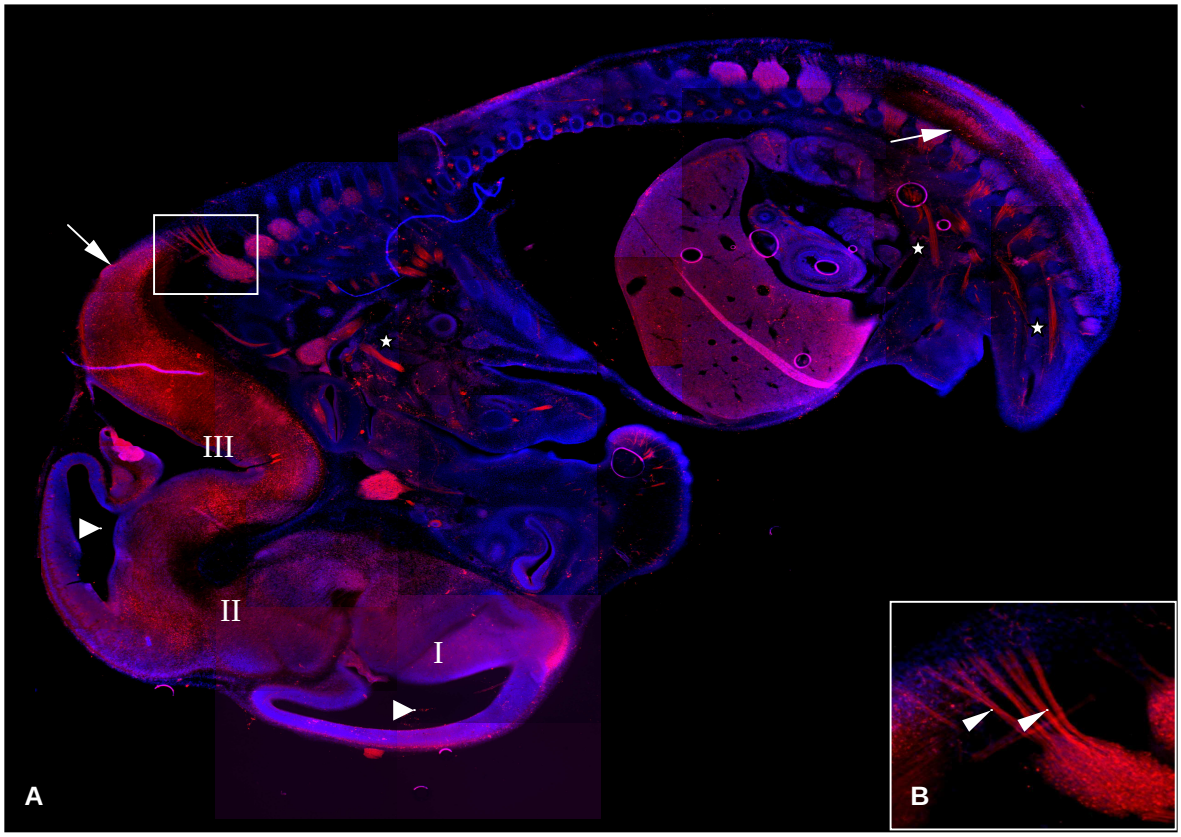


**Figure 19: Expression of HRP-3 in E15.5 mouse embryo.** Sagittal section in E15.5 paraffin embedded mouse embryo was stained against HRP-3 using a red fluorescent secondary antibody together with the blue fluorescent DNA stain 4,6-diamidino-2-phenylindole (DAPI). HRP-3 expression was restricted to the nervous tissue including brain, spinal cord and dorsal root ganglia. A fibrous staining of HRP-3 in posterior nerve roots at DRG level (B) can be seen. Other fibrous structures representing mainly organ innervations were recognized as HRP-3 positive structures in A. Red signal in liver was not considered to be a positive HRP-3 expression signal as the same signal was obtained when the secondary antibody was used alone. I, II and III represent the three brain divisions: prosencephalon, mesencephalon and rhombencephalon, respectively. White triangles represent brain ventricles.

In addition to these tissues, some fibrous structures in many organs were detected to be strongly HRP-3 positive as shown by the asterisks in figure 19A. From the previously represented HRP-3 expression pattern it can be speculated that these structures probably represent nerve fibers (innervations) supplying these organs. On the other hand, positive HRP-3 signal was neither detected in the skin and muscles of the embryo nor in the inner organs except for some background staining detected in liver which was also detected in similar sections incubated with the secondary antibody only.

### I.1.2.2 HRP-3 expression in embryonic mouse DRG

Dorsal root ganglia (DRG) are collections of nerve cells on the posterior roots of the spinal nerves and consist mainly of spinal neurons from which the fibers of the posterior root take origin and travel to the spinal cord. As mentioned before, directly beyond the ganglion both the anterior and posterior roots join to form the spinal nerve.

Staining of sagittal sections cutting through the DRG from embryos at different developmental stages (E10.5, E11.5, E13.5 and E15.5) against HRP-3 showed that the protein was strongly expressed in DRG (as shown by arrow heads in figures 20A, B, C and D) and in the spinal nerves (as shown by arrows in figure 20B & C) in all time points examined.

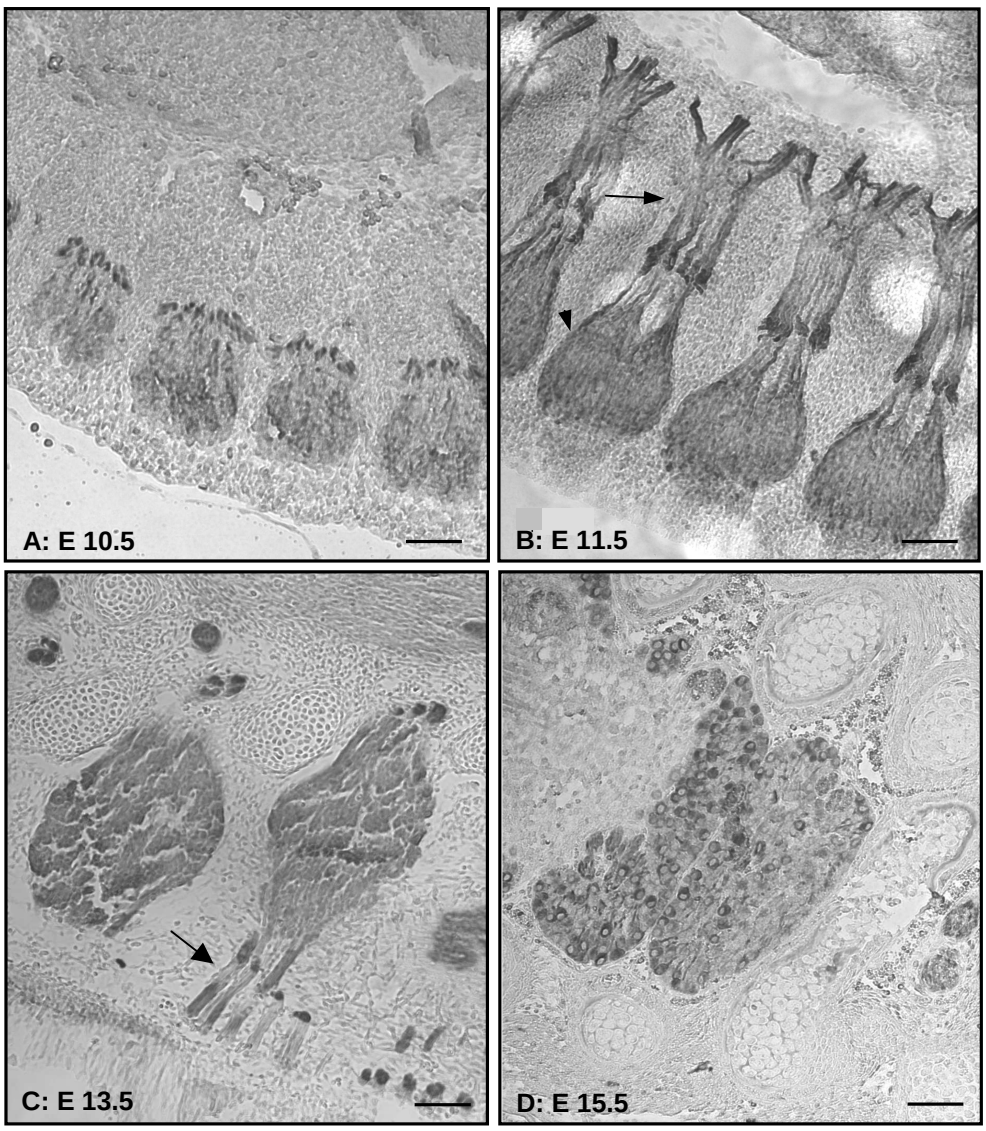

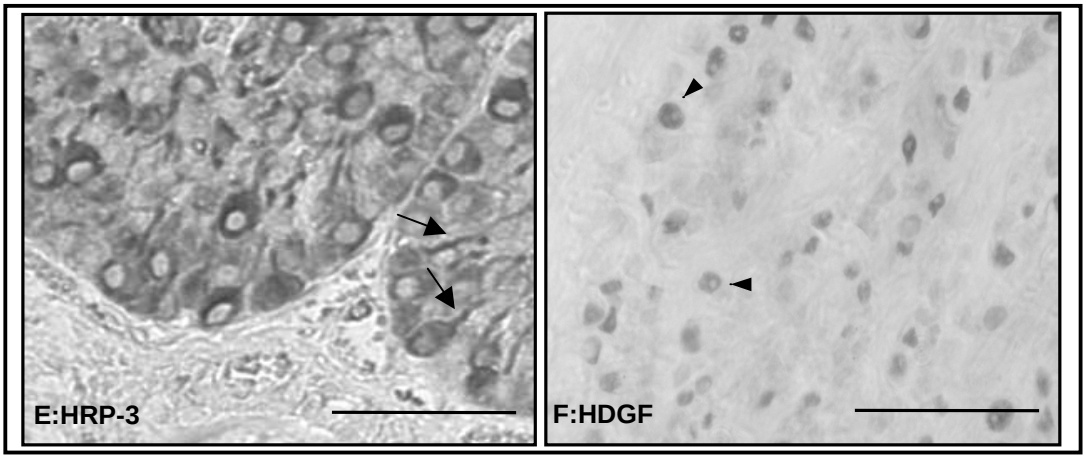


**Figure 20: HRP-3 expression in embryonic mouse dorsal root ganglia**. Sagittal sections in the DRG area from paraffin embedded mouse embryos at E10.5, E11.5, 13.5 and E15.5 were stained against HRP-3 (A-E) or HDGF (F). HRP-3 signal was strong in all time points in both: DRG (arrow heads A-D) and connected nerves (arrows in B & C). E and F represent higher magnification of DRG at E13.5 stained against HRP-3 or HDGF respectively. HRP-3 showed a strong signal in the cytoplasm and processes of a cell population bearing a single process (arrows in E). HDGF expression was restricted to the nuclei of some cells in the ganglion (arrow heads in F). Bars are 20 µm.

When higher magnification was used to examine HRP-3 expressing cells within the DRG of E13.5 mouse embryos, many cells with minor morphological differences (representing mostly the same cell population) were detected to be HRP-3 positive. These cells showed a prominent cytoplasmic signal that extended to a single cell process as shown by arrows in figure 20E giving the outline of unipolar-looking cells. In contrast, tissue sections stained for comparison against HDGF -which is the parent member in this protein family- demonstrated an exclusive nuclear signal for HDGF (figure 20F, arrowheads). Comparing the pictures E and F in figure 20 indicates a clear and basic difference in the subcellular distribution of both proteins. Whereas HRP-3 showed a characteristic intense signal in the cytoplasm in addition to the positively stained fibers, only a nuclear expression signal was detected for HDGF suggesting different functions for both growth factors.

### I.1.2.3 HRP-3 expression in the developing mouse cerebral cortex

Taking a closer look into the embryonic brain, it was noticed that HRP-3 at the early life stage exists in nearly all cortical cells including neurons, radial glial cells and their progenitors as both types exist at this age (Choi, 1988). In these cells, HRP-3 localized mainly in the cell cytoplasm including cell body and cell

processes (figure 21E, arrows). When this pattern was compared to the expression pattern in adult mouse brain, a clear difference in the pattern of HRP-3 expression between both cases could be noticed. HRP-3 in the adult brain cortex was expressed by a limited number of cortex cells and the expression signal was predominantly restricted to nuclei of these cells (arrow heads in figure 21F). The gradual change in the pattern of expression through the examined time points points to a possible developmentally regulated role for HRP-3. In the same time, this may also underline an initial importance of HRP-3 for most cell populations in the developing mouse cerebral cortex and a more specific role(s) for HRP-3 in certain populations of mature neural cells.

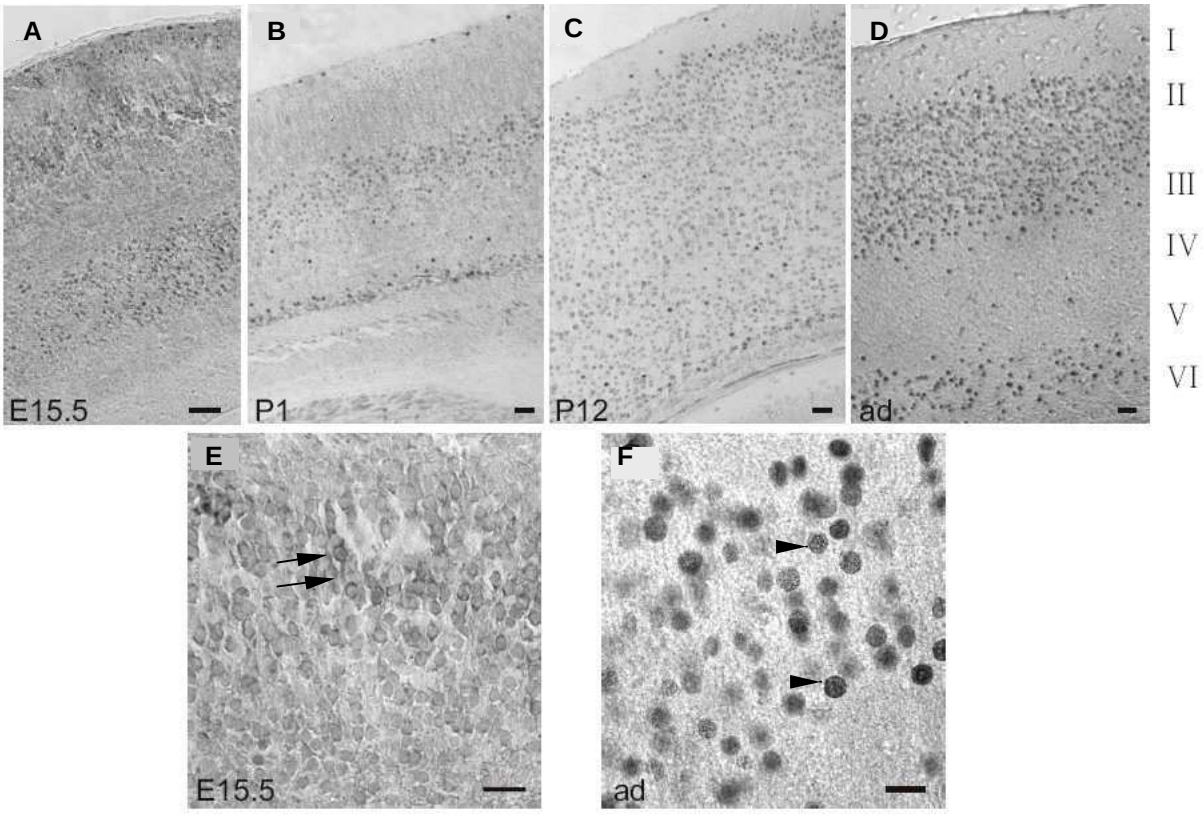


**Figure 21: A comparison of HRP-3 expression pattern between developing and adult mouse brain cortex.** Sagittal paraffin E15.5, P1, P12 and adult mice brains were stained against HRP-3 using avidin-biotin based technique. Under light microscope, pictures were taken of an area of the neocortex above the hippocampal structure. During the embryonic and early postnatal stages (E15.5 and P1, A and B) cortical neurons showed an extranuclear HRP-3 signal that was strongly reduced at later time points (P12 and adult, C and D). Numbers on the right side refer to the different cortical layers in adult mice. E and F represent higher magnification of E15.5 and adult cortex demonstrating the cellular changes in HRP-3 expression during development. Arrows in E point to cytoplasmic signal of HRP-3 and arrow heads in F point to nuclear signal of the protein. Bars are 40 µm in A-D and 20 µm in E & F.

## I.2 Expression of HRP-3 under pathological conditions

### I.2.1 HRP-3 expression in medulloblastoma tumor

The high level of HDGF expression in the EGL of the cerebellum and the fact that HDGF was found to be over-expressed in a number of cancer types (Okuda, et al., 2003; Huang, et al., 2004; Bernard, et al., 2003; Hu, et al., 2003) raised the question whether tumors in this layer would show an increased level of HDGF. To answer this question, a mouse model with medulloblastoma tumor was used. Serial paraffin sections of the cerebellar tumor were deparaffinized, rehydrated and immunostained against HDGF or HRP-3. Tumor tissue was visualized by hematoxylin staining (figure 22A).

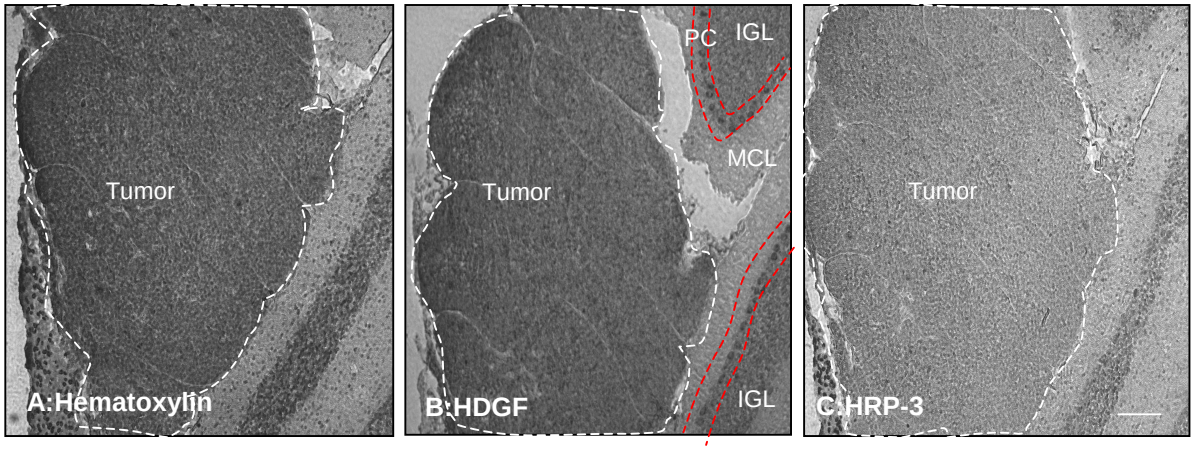


**Figure 22: Expression of HDGF and HRP-3 in medulloblastoma tissue**. Serial paraffin sections from cerebellum of a medulloblastoma mouse model were stained against HDGF or HRP-3. Shown is a part of the cerebellum with a massive rosette shaped medulloblastoma pointed out with the white dotted lines. Tumor cells showed an intense signal for HDGF in the area of granular cells (EGL) as seen in B compared to the healthy surrounding areas. No increase in the signal of HRP-3 was detected in the tumor tissue compared to the healthy surrounding tissue in C. Tumor area was identified with the intense hematoxylin staining of the cancerous cells (A). PC: Purkinje cells, MCL: molecular cell layer, EGL: External granular layer. Bar is 100 µm.

Immunostaining revealed an increased signal for HDGF in tumor cells (figure 22B) whereas the signal for HRP-3 was unchanged compared to its expression signal in the neighboring healthy part of the tissue (figure 22C).

This pattern of staining points to a possible relation between the increased HDGF expression and tumorigenesis or increased rate of cell proliferation. For many cell types like fibroblasts, HuH-7 cells (Nakamura, et al., 1994), aortic endothelial cells (Oliver and Al-Awqati, 1998), and vascular smooth muscles (VSM) (Everett, 2000) a mitogenic effect for HDGF was already shown. To test the mitogenic effect of

HDGF on tumor cells, Daoy medulloblastoma tumor cells were stably transfected with HDGF-GFPC3, HRP-3-GFPC3 or GFPC3 and seeded into a 96 well plate (10.000 cells per well) in normal culture medium using 24 wells for each stable cell line. After three days, cell proliferation of the different stable lines was estimated using Cell titer 96® $AQ_{ueous}$ non radioactive cell proliferation assay (Promega) according to the manufacturer's instructions. The mean absorbance at 490 nm was measured using an ELISA plate reader and the results were compared for the different cases. It was found that HDGF over-expressing cells showed a significantly higher proliferation ($P \leq 0.0001$, unpaired t-test) compared to the control-transfected cells (figure 23).

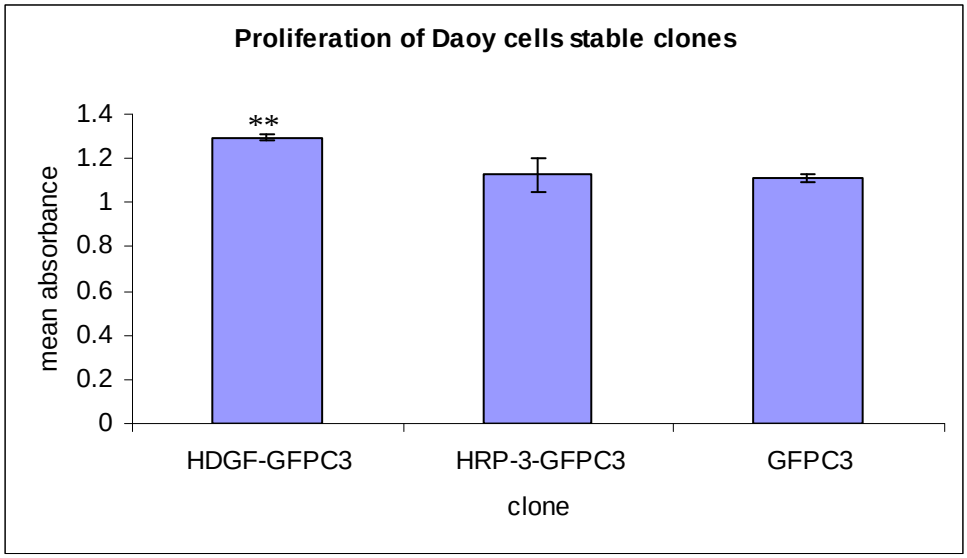


**Figure 23: Increased proliferation of Daoy medulloblastoma cells over-expressing HDGF**. Daoy medulloblastoma cells were transfected with HDGF-GFPC3, HRP-3GFPC3 or GFPC3 and kept under genticin-containing medium to select for the positively transfected cells. The expression of the respective genes in mixed clones prepared from each condition was controlled by fluorescence microscopy. Cell proliferation was determined three days after seeding 10.000 cells /well in 96 well plates, using Promega non-radioactive cell proliferation assay. Light absorbance of the colorimetric reaction was measured on an automated ELISA plate reader at 490 nm. A significant increase in the proliferation of HDGF over-expressers compared to both HRP-3 over-expressers and the control transfected cells was detected. Bars on the columns represent the standard error. Asterisks represent $p<0.0001$.

On the other hand, HRP-3 over-expressers did not show a significant increase in proliferation compared to the control cells, a finding that can be expected from the immunohistochemistry staining of tumor tissue done before.

### I.2.2 HRP-3 expression in crushed sciatic nerve

Another type of pathological changes in the nervous system is nerve injury which is usually accompanied by many sub-cellular changes. From the previous data it was found that HRP-3 was expressed in mouse sciatic nerve and DRGs under physiological conditions. So that it was interesting to investigate any possible changes in its expression after injury and during the healing process. In cooperation with professor H. W Müller and Dr. Frank Bosse, Molecular Neurobiology institute, University of Duesseldorf, the sciatic nerve of adult mice was exposed using surgical procedures under anesthesia and crushed before re-suturing the animal skin (trans). As a control (sham), the animal was exposed to the same surgical procedures of cutting and suturing but without the step of nerve crushing. Seven days after the procedures animals were sacrificed and the sciatic nerves were extracted together with the attached ganglia, fixed and paraffin embedded before they were cut in transverse sections. Section were cut so that the sections contained both, the ganglion and the nerve as shown in the schematic diagram in figure 24.

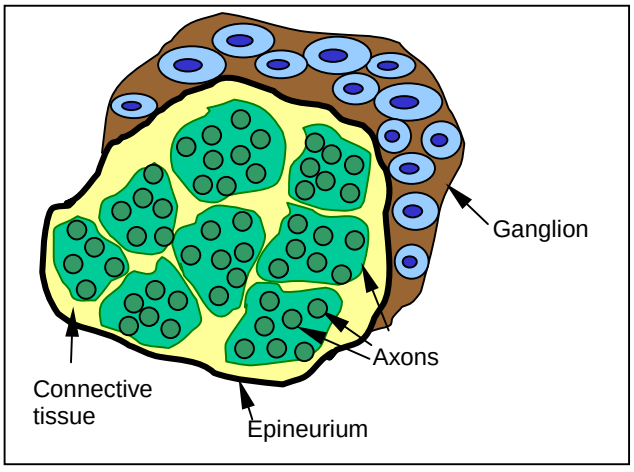


**Figure 24: A schematic diagram for a transversely cut nerve with part of an adjacent ganglion.** Nerve bundles (represented as green colored areas) which consist of many axons (represented as dark green circles) are normally separated by a layer of connective tissue (yellow). All nerve bundles and the separating connective tissue are enwrapped with a layer of connective tissue named the epineurium (thick black outline). The ganglion is shown as a brown structure adjacent to the nerve.

Sections from both conditions, trans and sham, were stained against HRP-3 using avidin-biotin technique and histogreen® as a chromogen. Examining the control sections under transmitted light microscope showed that HRP-3 was strongly expressed in the nuclei of nearly half of the ganglion cells adjacent to the

undamaged nerve (sham, arrow heads in figure 25B). This was in addition to a signal for HRP-3 in the cytoplasm of a population of bigger cells ranging from very intense to much lighter expression signal (arrows in 25B). Also in the transversely cut nerve fibers, a strong HRP-3 signal was clearly detectable (figure 25C).

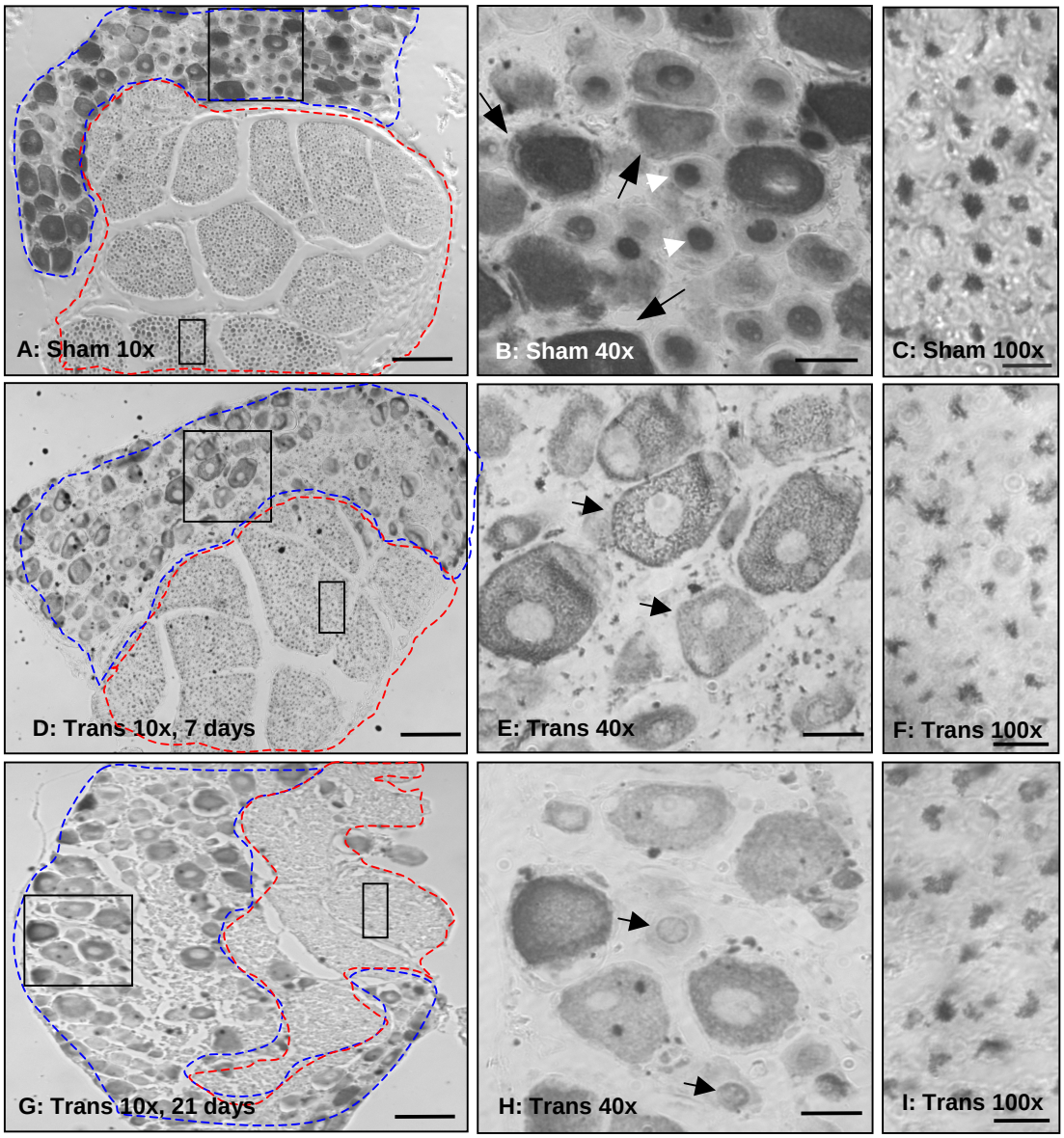


**Figure 25: Changes in HRP-3 expression pattern after sciatic nerve injury.** Transverse sections from either control treated (sham, A-C) or crushed (tarns, D-F) adult mice sciatic nerve seven days after the surgical manipulation were stained against HRP-3. Sections showed a part of the ganglion (blue dotted line) adjacent to the nerve (red dotted line) as explained in figure 22. In the control treated nerve, ganglion cells showed an intense nuclear signal for HRP-3 in almost half of the positive cells. A population of significantly bigger cells showed varying degrees of a cytoplasmic signal of HRP-3. Seven days after nerve damage, almost no nuclear signal for HRP-3 was detected and a comparatively weak, structured cytoplasmic signal was detected in nearly all ganglion cells (E). However, three weeks after damage initiation the nuclear HRP-3 signal was partially retained beside its cytoplasmic signal (H). Although not many differences were detected in the expression pattern of HRP-3 in nerve fibers between sham and trans models, a relative reduction in

signal intensity in damaged nerve axons was detected (compare C+F). Bars are 100 µm in A, D and G, 25µm in B, E and H and 10 µm in C, F and I.

Interestingly, however no change in its pattern was seen, the expression signal of HRP-3 in the crushed nerve fibers (axons) showed a relative reduction in its intensity compared to undamaged nerve expression signal (figures 25C, F & I). To determine if this decrease in intensity was resulting from a down regulation of protein expression or because of the wallerian degeneration of the nerve needs further investigations. On the other hand, a clear difference in the expression pattern of HRP-3 in ganglion cells was observed between the control and the damaged nerve. It was found that the cell population expressing HRP-3 in their nuclei before nerve damage (arrow heads in 25B) either disappeared or remodeled its expression pattern after damage leaving the bigger cells with a significantly weaker cytoplasmic signal and almost HRP-3 negative, eccentric nuclei (arrows in 25E). By the time, the missed nuclear signal of HRP-3 started to appear in a small sized cell population as pointed out with arrows in figure 25H.

## I.3 HRP-3 expression in vitro

### I.3.1 HRP-3 expression in mouse primary DRG (sensory) neurons

As described before, HRP-3 was found to be expressed very early in mouse embryo and due to the intense and interesting signal detected in the embryonic DRG, it was important to investigate the expression of HRP-3 in DRG neurons in vitro. Therefore, primary cultures of these sensory neurons were prepared from embryonic DRG isolated from E 14.5 mouse embryos as described in the Methods part and were allowed to proceed in culture in the form of aggregates (explants). After about three days some cells had already migrated away from the main cellular aggregation and started to differentiate. Starting from this time point cells were fixed at three days intervals in ice cold 4% PFA/ 10% sucrose and stained against HRP-3. To prove the neuronal identity of the fixed cells, a neuron specific marker (β-III-tubulin) was used and nuclei were visualized using the DNA-stain DAPI. Under fluorescence microscope, it was very interesting to observe that HRP-3 was expressed in the DRG neurons at all examined time points. However, a clear change in the expression pattern of HRP-3 was observed. While in the young DRG neurons (three to six days in culture) the expression signal was

almost cytoplasmic as seen in figure 26A and D, a strong nuclear expression signal was noticed in older neurons (figure 26E & F). It was also noticed that the intensity of the cytoplasmic signal was decreasing with time. In three days old neurons, HRP-3 was detected along the whole neuronal cell processes and in the growth cones (arrow heads, figure 26B & C) whereas the older neurons showed a weaker signal in cell soma as well as a much weaker signal for HRP-3 that was hardly detectable in cell processes.

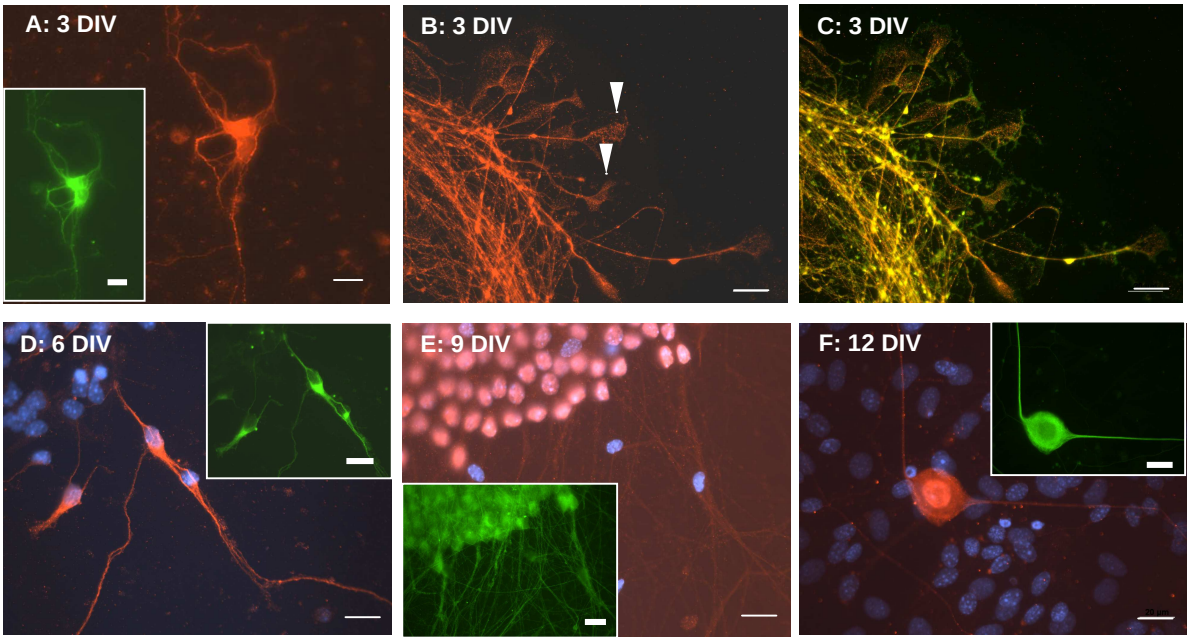


**Figure 26: HRP-3 expression in mouse primary sensory neurons at different time points.** Sensory neurons obtained from DRG of E14.5 mouse embryos were brought into culture as aggregates and kept under complete NBM + 20 nM NGF. Neurons were fixed at different time points (3, 6, 9 and 12 days) and immunostained against HRP-3 (red channel) and the neuronal cell marker β-III-tubulin (green channel) together with the DNA-stain DAPI (blue channel). Figure A represents the predominant cytoplasmic signal of HRP-3 in β-III-tubulin positive neurons after three days in culture whereas B and C represent expression signals of HRP-3 in neuronal processes and growth cones (arrow heads) at the same time point. A nuclear expression signal for HRP-3 started to appear after 9 days in culture (E) and was also detectable after 12 days (F). Bars are 20 µm.

### I.3.2 HRP-3 expression in mouse primary cortical neurons

It was also very interesting to investigate whether HRP-3 was still expressed in cortical neurons kept in vitro and whether its expression in these neurons exhibited changes over the time similar to which was noticed in vivo. For this purpose, primary cortical neurons were prepared from mouse embryos and taken into culture in Neurobasal medium (NBM) containing B27 supplement as a standard

culture medium (Brewer, 1995). After trying to prepare neurons from embryos of different ages, E14.5 gave the best results regarding cell yield and survival in culture.

Neurons obtained after enzymatic and mechanical dissociation were plated onto thoroughly washed PDL coated vessels in standard NBM. As early as four hours after plating many cells were starting to differentiate showing filopodia or even minor processes. For the various experiments neurons were fixed at different time points and immunostained using antibodies against HRP-3, MAP-2 and neurofilament-H or with the DNA-stain DAPI to visualize cell nuclei when needed. Figure 27 demonstrates HRP-3 expression in dendrites stained for MAP-2 (arrows heads, figure 27B) as well as axons stained for neurofilament-H (arrows, figure 27C) of mouse cortical neurons.

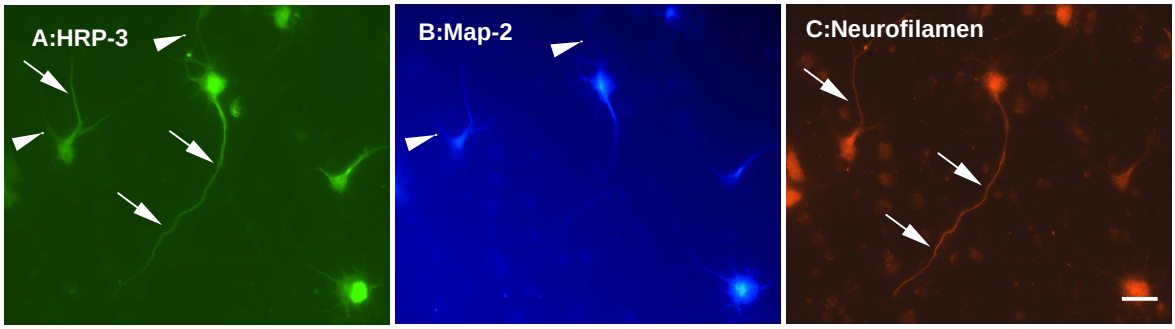


**Figure 27: HRP-3 expression in both axonal and dendritic compartments of mouse primary cortical neurons**. Cultured cortical neurons were stained for HRP-3 (red), MAP-2 (blue) as a dendritic marker, and neurofilament-H (red) as an axonal marker. Staining showed that HRP-3 at this time point was expressed in cell bodies, dendrites (MAP-2 positive processes) and axons (neurofilament positive processes). Bar is 20 µm.

This staining showed that HRP-3 was expressed in cultured cortical neurons and also resolved the question about HRP-3 expression in both types of neuronal cell processes, dendrites and axons. This triple immunostaining was able to confirm that HRP-3 (green signal in figure 27A) was expressed in both, Map-2 positive dendrites as shown by arrow heads in figure 25B and neurofilament positive axons as shown by arrows in figure 27C.

When primary neurons are grown in culture, they undergo a sequence of morphological changes that have been well documented (Dotti, et al., 1988). After dissociation and within a few hours after plating, cortical neurons look rounded and exhibit lamellipodia. After about five hours in culture, the neurons start to extend minor processes. After one day in culture, the axons elongate and the dendrites

start to develop, and both acquire large growth cones at their tips. After four days in vitro (DIV), cortical neurons reach morphological maturation, with numerous dendrites, synaptic contacts, and axonal branches. To investigate HRP-3 localization during neuronal differentiation stages in culture, immunofluorescence staining and imaging were performed using cultured cortical neurons fixed after different periods of time starting from 9 hrs up to 12 DIV.

The interesting pattern of expression of HRP-3 shown before in mouse embryonic and postnatal brain cortices was behind the idea of a detailed, time point based series of cultured cortical neuron immunocytochemical analysis. For this purpose, primary cortical neurons were prepared as mentioned before and seeded on PDL coated glass coverslips in a 24-well tissue culture plate in the complete culture medium. At different time points (9 hrs, 24 hrs, 48 hrs, 72 hrs, 5 DIV and 12 DIV), neurons were fixed in ice-cold 4% PFA/ 10% sucrose solution. Neurons were immunostained against HRP-3 together with Map-2 as a marker for neuronal cells. Fluorescently labelled anti-rabbit and anti-mouse secondary antibodies were used to visualize bound primary antibodies. Pictures taken for the stained neurons at each stage showed that HRP-3 expression in cortical neurons in vitro started as early as 9 hrs after seeding showing a clear signal in their cytoplasm as seen in figure 28A. By this time, some neurons had already started to be polarized and extend some minor processes, of which a single one should grow rapidly to form the future axon. After 24 hrs in culture, most of neurons were extending a long axon and shorter dendrites. HRP-3 signal at this time was highly concentrated in the cell body and along all the extending processes (figure 28B) and no signal was detected in the cell nucleus (arrow head, figure 28B). A stronger signal was also noticed at this time at the base of the longest process representing probably the axonal hillock as shown by the arrow in figure 28B. By the time neurons were two days in culture, an intense nuclear signal started to appear in some cells in addition to the cytoplasmic one which remained with an unchanged intensity until this time point (figure 28C). From this time onwards, the intensity of the nuclear HRP-3 signal increased until five DIV (arrow heads in figures 28D and E). In the same time, HRP-3 expression signal started to fade out gradually in the cytoplasmic compartments but it did not completely disappear, as the axons remained clearly HRP-3 positive until five days in culture (arrows in 28D & E). After 12 days in culture, neurons were fully mature and the process network was

highly developed as proved by the clear immunopositivity for MAP-2 (green signal in figure 28F). However, at this time point it was noticed that only the nuclear signal for HRP-3 was detectable (arrow heads in figure 28F).

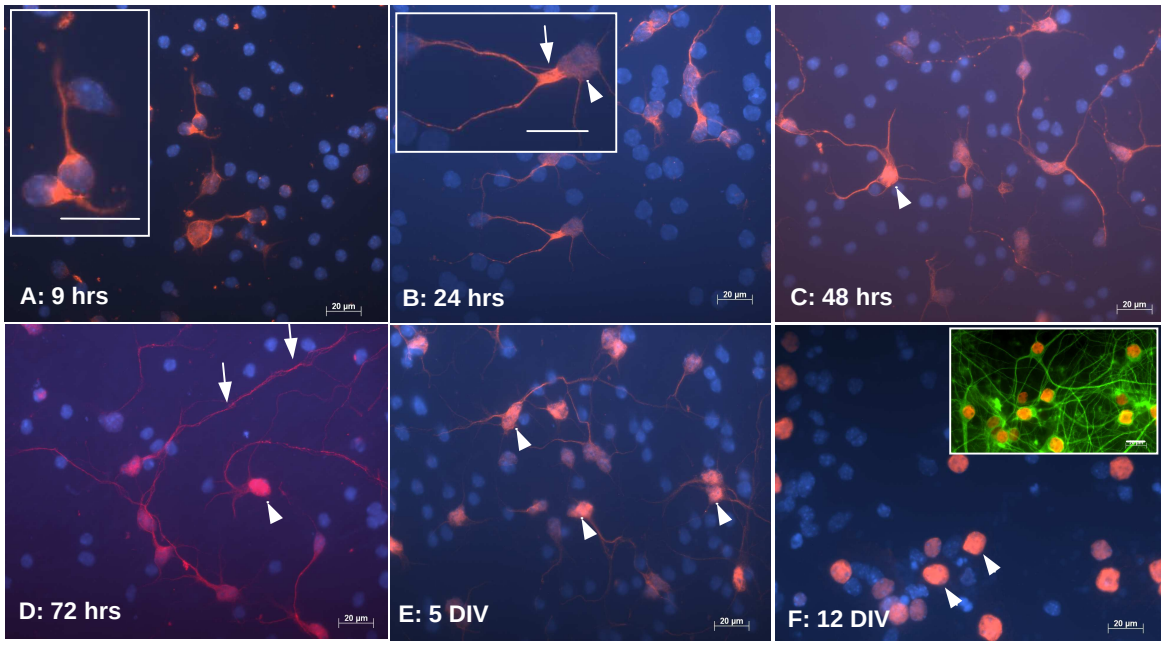


**Figure 28: HRP-3 expression dynamically changed over time in cultured primary cortical neurons**. Primary mouse cortical neurons prepared and fixed at different time points (9 hrs, 24 hrs, 48 hrs, 72 hrs, 5 DIV and 12 DIV) were stained against HRP-3 (in red) together with a DNA stain (DAPI, in blue) or MAP-2 (in green). At 9 and 24 hrs HRP-3 signal was exclusively cytoplasmic including cell processes (A & B). After two to five days of culture in vitro, neurons showed a nuclear signal for HRP-3 in addition to the cytoplasmic signal that started to fade out. Older neurons (12 DIV) expressed HRP-3 only in their nuclei however the neurite network was still intact. Box in F indicated a neuron culture with an intact processes network after 12 days. Arrows in B point to HRP-3 signal at the axonal hillock and arrow head points to an HRP-3 negative nucleus at day 1 and to an HRP-3 positive nucleus at 3 and 12 days in D and F respectively. Arrows in D point to an HRP-3 positive axon. Bars are 20µm.

These results were similar to data obtained from immunolocalization of HRP-3 in mouse brain neocortex in vivo at different developmental stages. In these tissues, almost a nuclear HRP-3 expression signal was found in the adult animal brain (in which the cortical neurons were already mature, much resembling the 12-days old neurons in culture) whereas a predominant extranuclear signal for HRP-3 was detectable in various regions of the cortex in the embryonic and early postnatal stages (in which the cortical neurons were still developing, resembling the neurons in earlier time points of the cortical neurons culture, figure 28). Interestingly, the changes in HRP-3 expression pattern in cultured cortical neurons was also very similar to the changes observed in the cultured primary DRG neurons except for a

slight time shift in the onset of the nuclear expression signal that appeared earlier in primary cortical neurons.

The expression of the structurally related growth factor of the same family, HDGF, was also examined in cultured cortical neurons and compared to HRP-3 expression by immunocytochemistry. Using specific antibodies raised against either one of them together with the neuronal marker MAP-2 to prove neuronal cell identity, the expression patterns of both proteins were compared.

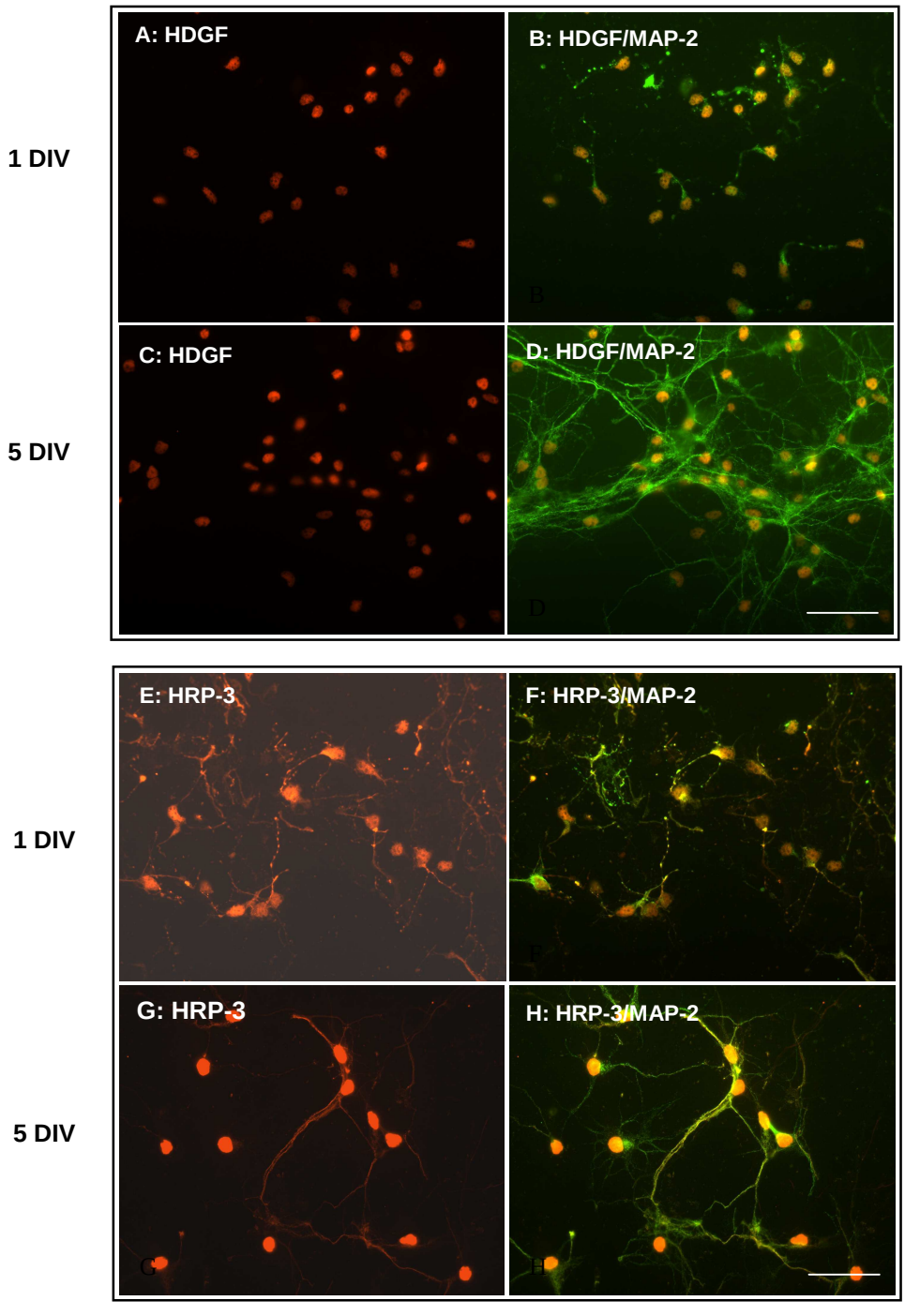


**Figure 29: Comparison between HDGF and HRP-3 expression patterns in cultured mouse cortical neurons after 1 and 5 days in vitro**. Primary mouse cortical neurons were

fixed after one or five days and immunostained against HDGF or HRP-3. MAP-2 was used to prove the neuronal identity. A set of fluorescently labeled secondary antibodies was used to detect bound antibodies (red labeled for HDGF or HRP-3 and green labeled for MAP-2). Under fluorescence microscope, HDGF was expressed only nuclear at both time points (A & C) but HRP-3 was showing a dynamic change, being expressed in the cytoplasm after one day (E) and started to be expressed in the nuclei after five days (G). Bars are 40 µm.

As can be expected from the previous immunohistochemistry of brain sections, both factors were also expressed in the primary cortical neurons in culture. But interestingly, HRP-3 showed, as previously mentioned, a dynamic change in the expression pattern over the time. Neurons showed only a cytoplasmic signal for HRP-3 in the early time point (24 hrs) but in the later time points an additional nuclear signal was detectable (figure 29E & G). On the other hand, HDGF was expressed at both time points (one day and five days after seeding) only inside cell nuclei showing no changes in its localization (figure 29A & C).

# Part II: Possible roles of HRP-3

## II.1 Intracellular roles

### II.1.1 Knockdown of endogenous HRP-3 protein level

After detecting the developmentally regulated expression pattern of HRP-3 in vivo in the different mouse nervous tissues and in vitro in primary sensory and cortical neurons culture it was very interesting to get an idea about the possible functions of this protein inside neuronal cells in vitro. One of the most useful tools used today to determine the possible roles and importance of a certain gene are the approaches depending on post-transcriptional gene silencing using small interfering RNA (siRNA, Fire, et al., 1998). They produce their selective effects on the target gene by destroying the gene's mRNA and hence preventing its translation into an active protein. To knock down the expression of HRP-3, three different siRNAs targeting three different regions of the coding sequence of HRP-3mRNA were designed:
siRNA1: 5'*GGTGATAGAGTAGAAGATG-3'*
siRNA2: 5'*GAGTGAAATTTACTGGGT-3'*
siRNA3: 5'*GGGAGAAGGTGGAAATACT-3'*

These oligos were tested first on HEK293T cells. As these cells do not express HRP-3, first, cells were stably transfected with HRP-3-GFPC3. After that, the resulting HRP-3-GFPC3 stable clones were seeded in 24 well plate and transfected with 50 nM of siRNA solution per well using Silentfect® reagent according to manufacturer's instructions. For the pooled siRNA mixture 20 nM of each siRNA were used to give a total of 60 nM of siRNAs. Three days after transfection cells were collected and lysed in ice cold RIPA buffer and equivalent protein amounts were used to estimate the knock down efficiency by Western blot analysis. Separated proteins were blotted onto a nitrocellulose membrane and probed with specific antibodies against HRP-3 and β-actin as a quantitative control for the loaded protein amounts. Using two different fluorescently labelled secondary antibodies, bound primary antibodies were detected using a LiCor fluorescent scanning system. The signals obtained for HRP-3 under the different conditions were normalized against the intensity of the corresponding β-actin bands. Quantitative analysis of the obtained bands showed that in HRP-3siRNA

transfected cells the expression level of HRP-3-GFPC3 was reduced (band at ≈63 kDa, lanes 1, 2, 3 and 4 in figure 30A) by a ratio of about 40 to 50% (figure 30B) in comparison to cells transfected with a scramble siRNA (an RNA that is not directed against any known gene, lane 5 in figure 30A).

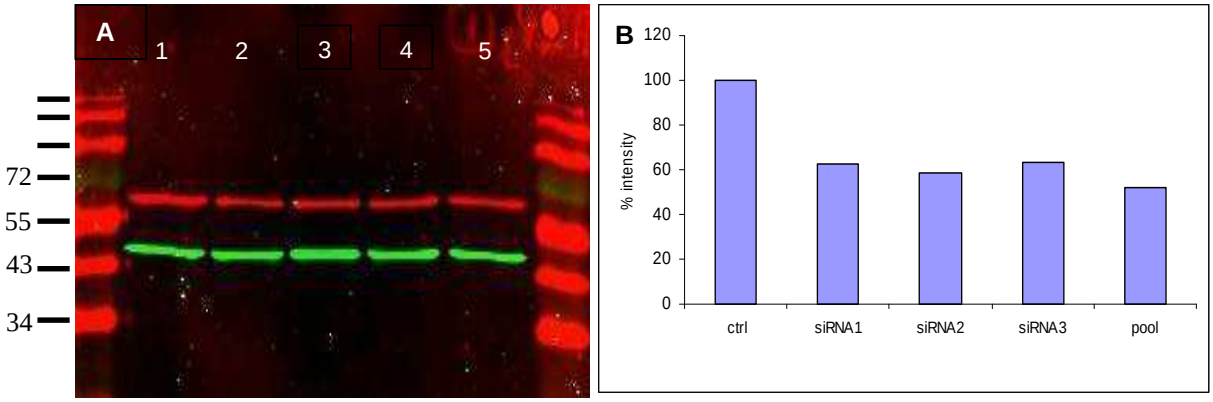


**Figure 30: HRP-3siRNAs reduced HRP-3 level in HEK293T cells.** HEK293T cells stably expressing HRP-3-GFPC3 seeded into a 24 well plate were transfected with either the different siRNA targeting HRP-3 or a control siRNA. Three days after transfection cells were lysed and protein contents were separated by SDS-PAGE. (A) represents a Western blot analysis of the cell lysate of the different conditions using an HRP-3 specific antibody recognizing the HRP-3-GFPC3 fusion protein (upper band, 63 kDa) and a β-actin specific antibody (lower band, 42 kDa). Lanes are: 1: HRP-3siRNA1, 2: HRP-3siRNA2, 3: HRP-3siRNA3, 4: pooled HRP-3siRNA, 5: scramble siRNA. (B) Quantification of the detected protein bands using the Odyssey quantification system shows that HRP-3siRNAs decreased HRP-3 expression level within the selected stable HRP-3 GFPC3 clone to various degrees.

After proofing the ability of the chosen HRP-3siRNA sequences to reduce HRP-3 protein content in HEK293T cells, they were used to transfect primary cortical neurons to test for possible effects. Neurons were transfected using Lipofectamin 2000® at the same time of seeding in a 24 well plate-format. A red fluorescent (Cy3) control siRNA was co-transfected to label targeted cells. Two days after transfection, neurons were fixed and immunostained against HRP-3 and β-III-tubulin using green and blue fluorescently labelled secondary antibodies. Under a fluorescence microscope more than 200 labelled cells were randomly photographed from each condition. The length of the longest neurite arising from each cell was measured and the number of neurites arising from single neurons was counted and the obtained data were analysed in a blind way. Interestingly, cortical neurons transfected with the specific HRP-3siRNAs exhibited significantly shorter neurites compared to control siRNA transfected neurons (figure 31A). In

addition to the shorter neurites, reduced HRP-3 levels resulted in neurons bearing less number of neurites as shown by the accumulation curve in figure 31B.

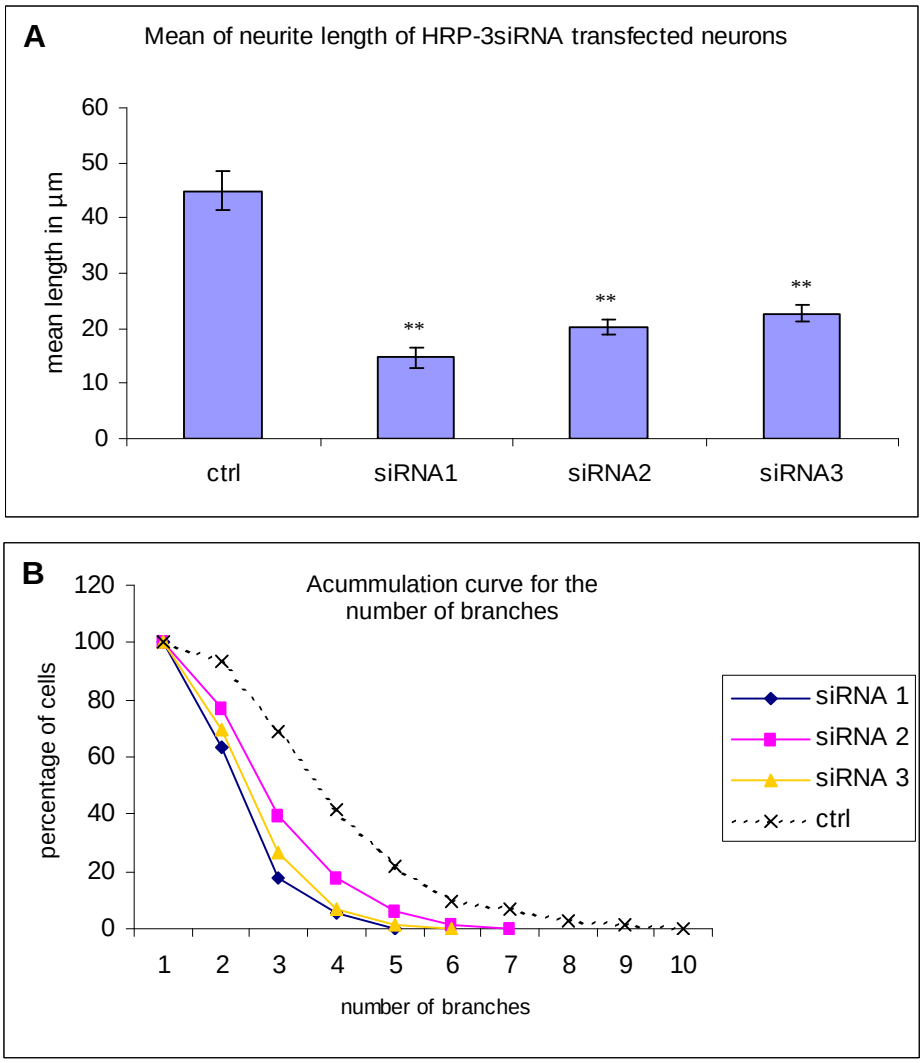


**Figure 31: Reduction of the intracellular HRP-3 level resulted in neurons bearing shorter and fewer neurites**. Primary cortical neurons were transfected with different HRP-3siRNAs directly before seeding. A scramble, Cy3 labelled siRNA (ctrl siRNA) was used as a negative control. Two days after transfection cells were fixed and immunostained against HRP-3 and β-III-tubulin to verify the identity of the transfected cells. More than 200 randomly chosen neurons were analysed from each condition in a blinded way. Data analysis showed a highly significant reduction in both the mean neurite length (A) as well as the number of neurites arising from the cell body (B) of HRP-3siRNA positively transfected neurons compared to control transfected neurons (represented by two asterisks in A). The experiment was repeated four times with similar results every time (see supplementary data, S2). ** $p<0.0001$

Repeating the experiments resulted each time in the same results with minor variations related to the culture-to-culture differences (see supplementary data, figure S2).

### II.1.2 Increasing the endogenous HRP-3 protein level

There are many neuronal cell lines that provide many properties similar to in vivo neuronal tissues like B35 (rat neuroblastoma cells), PC12 (rat pheochromocytoma cells) and P19 (mouse teratocarcinoma cells). Most of these cell lines have the ability to differentiate into a neuronal phenotype after certain treatments. Rat B35 neuroblastoma cell model (Schubert et al., 1974) is one of these lines which proliferates normally under serum supplemented medium. As soon as the serum is withdrawn and culture medium is supplemented with 1 mM of dBcAMP which is a membrane permeable analogue of cAMP, cells start to differentiate into a neuron-like phenotype with extended neurites (Boukhelifa et al., 2001*).* Due to the ease of transfecting this cell line in comparison to primary cortical neurons and in addition to its rapid proliferation rate and easy differentiation procedures, B35 cell line was chosen as a convenient cellular model for studying the possible roles of increasing the intracellular expression of HRP-3. Under normal culture conditions in DMEM:F12 medium supplemented with 5 % FCS and 2 mM L-glutamate, B35 cells were allowed to grow and proliferate.

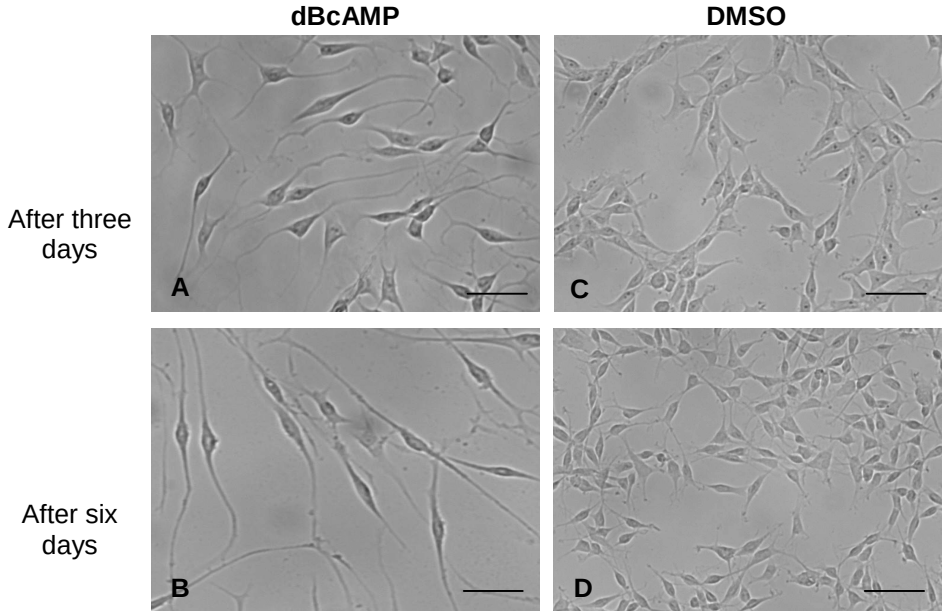


**Figure 32: B35 neuroblastoma cells differentiated into a neuronal phenotype induced by an increased cAMP level**. B35 cells treated with 1mM dBcAMP in serum free medium showed neurite outgrowth and a neuron-similar morphology after three (A) and six days (B) compared to cells treated with the vehicle alone for the same period of time (C & D). Bars are 100 µm.

Cell differentiation was started in culture by keeping cells under serum-free medium supplemented with 1 mM of dBcAMP. Shortly after treatment, cells started to show longer cell processes and after 3 days nearly all cells showed a neuronal morphology (figure 31A). After a further three-days interval the extended processes were much longer forming a network of extensions (figure 32B).

To check for the endogenous HRP-3 expression of these cells, normally proliferating undifferentiated B35 cells cultured on glass cover-slips were fixed in ice-cold 4% PFA for immunostaining. Immunocytochemistry analysis was done by shortly permeabilizing the fixed cells with 0.5% Triton X-100 solution then blocking the non specific antibody binding sites before incubating the cells with specific antibody against HRP-3. Bound antibodies were visualized by a second incubation with a Cy3 fluorescently labeled secondary antibody. Under normal proliferation conditions no endogenous HRP-3 expression signal could be detected by microscopic examination (figure 33A). Interestingly, a positive HRP-3 expression signal could be detected within B35 cells when they were exposed to differentiating conditions for three or six days before being stained against HRP-3 (examined using the same exposure time figures 33B & C). A change in HRP-3 protein distribution was observed during the differentiation process.

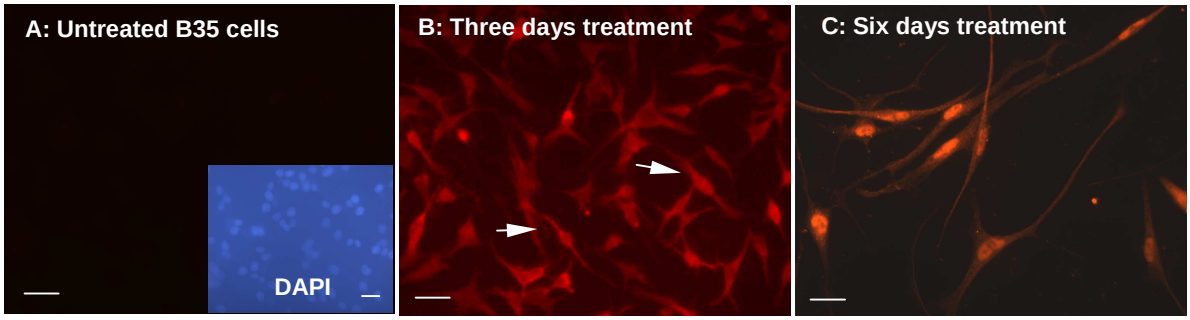


**Figure 33: Endogenous HRP-3 expression in B35 cells.** B35 rat neuroblastoma cells were either untreated for 6 days (A, kept under 5% FCS supplemented DMEM:F12) or treated for three (B) or six days (C) with 1mM dBcAMP supplemented, FCS free DMEM:F12. At these time points cells were fixed and immunostained for their endogenous HRP-3 content using a specific antibody against HRP-3. A fluorescent secondary antibody was used to visualize bound antibody. Cells were examined using the same exposure time under a fluorescence microscope. Undifferentiated proliferating cells (A) did not express HRP-3. Early after differentiation, B35 cells showed an HRP-3 signal distributed over the whole cytoplasm (B). Three days later a strong nuclear signal was detected in addition to the cytoplasmatic signal (C). Bars are 20 µm.

Whereas B35 cells allowed to differentiate for three days showed a clear cytoplasmic signal for HRP-3 (arrows in figure 33B), most of the cells allowed to

differentiate for longer time showed a visible nuclear signal of endogenously expressed HRP-3 as shown in figure 34C in addition to the cytoplasmic signal. These observations mean that only differentiating B35 cells expressed HRP-3 and that the expression pattern of the protein was dependent on the differentiation stage in which the cells were.

Interestingly, also B35 cells transfected with a streptagged wild type HRP-3 showed a change in the expression pattern over time when they were allowed to differentiate. When HRP-3 transfected B35 cells were kept under proliferating conditions, HRP-3 signal remained nuclear after three or six days in culture (figures 34C & D). But when HRP-3 transfected cells were allowed to differentiate, HRP-3 signal showed a change in its distribution pattern. Three days after inducing differentiation, the signal of transfected HRP-3 was seen both nuclear and cytoplasmic (figure 34A). As differentiation continued, the cytoplasmic signal faded out leaving a more prominent nuclear signal after six days (figure 34B).

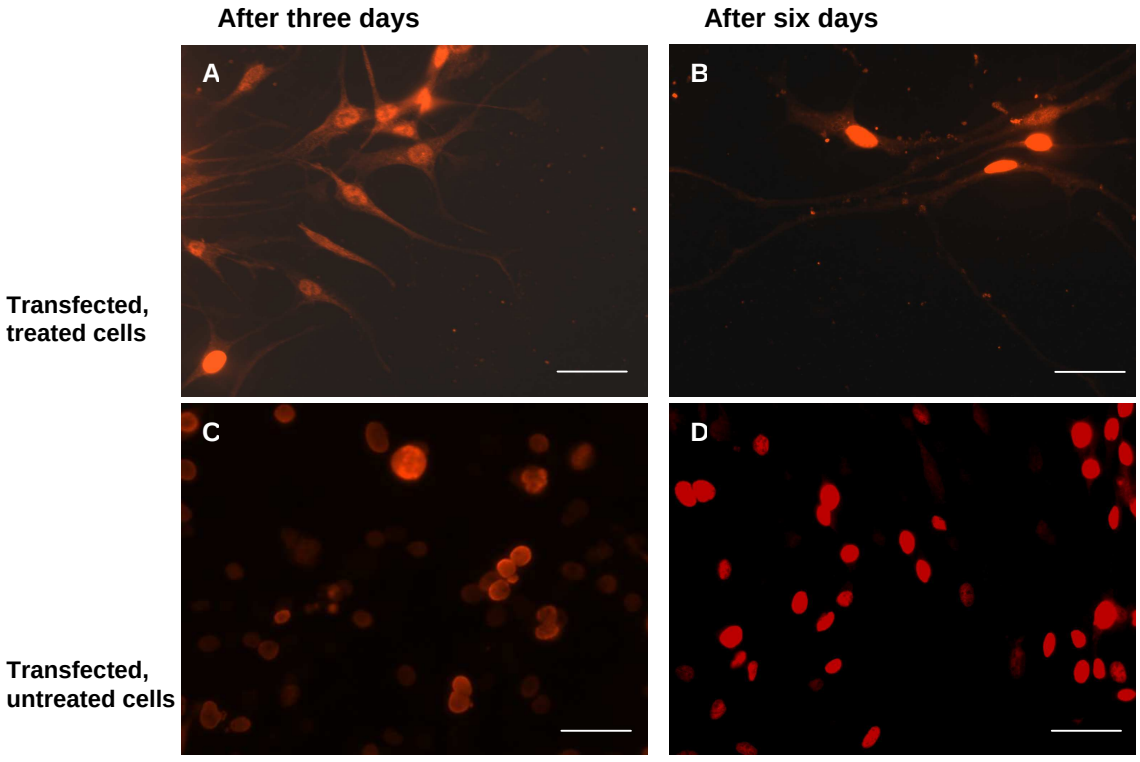


**Figure 34: Expression pattern of wild type HRP-3 transfected into B35 showed a differentiation-dependent distribution pattern.** B35 neuroblastoma cells were transfected with cDNA encoding wild type HRP-3 with a streptag. Cells were either allowed to proliferate or induced to differentiate into a neuron phenotype using dBcAMP. Comparing the streptag signal after three and six days in both conditions showed that proliferating cells expressed transfected HRP-3 only in their nuclei (C & D). Differentiating cells on the other hand showed both nuclear and cytoplasmic signals after three days (A) but almost only a nuclear signal after six days (B). Bars are 20 µm.

Expression of transfected wtHRP-3 in proliferating B35 nuclei can be due to the nuclear localizing signals in its sequence. HRP-3 has -like the other HDGF family members- two nuclear localization signals (NLS). One is located in the conserved N-terminal HATH region (NLS1) and one in the non conserved C-terminal part of the protein (NLS2). In this aspect HDGF was shown to achieve its proliferative activity by the nuclear translocation of the protein through its NLS2. To investigate which of the two NLSs was responsible for the nuclear localization of HRP-3 in B35 cells, they were mutated by exchanging the Lysine residues in the NLS to Asparagine residues.

Polymerase chain reaction (PCR) technique was utilized to introduce three point mutations at $Lys^{74}$, $Lys^{77}$ and $Lys^{79}$ (lysines) changing them to Asn (asparagines) in NLS1 to produce the construct HRP-3mutNLS1.The same strategy was used to construct HRP-3mutNLS2 where the three amino acids $Lys^{144}$, $Lys^{156}$ and $Lys^{160}$ were replaced by Asparagine. To produce the double mutated NLS HRP-3 construct, all six Lysines in both NLS1 and NLS2 ($Lys^{74}$, $Lys^{77}$, $Lys^{79}$, $Lys^{144}$, $Lys^{156}$ and $Lys^{160}$) were replaced with Asparagine (figure 35).

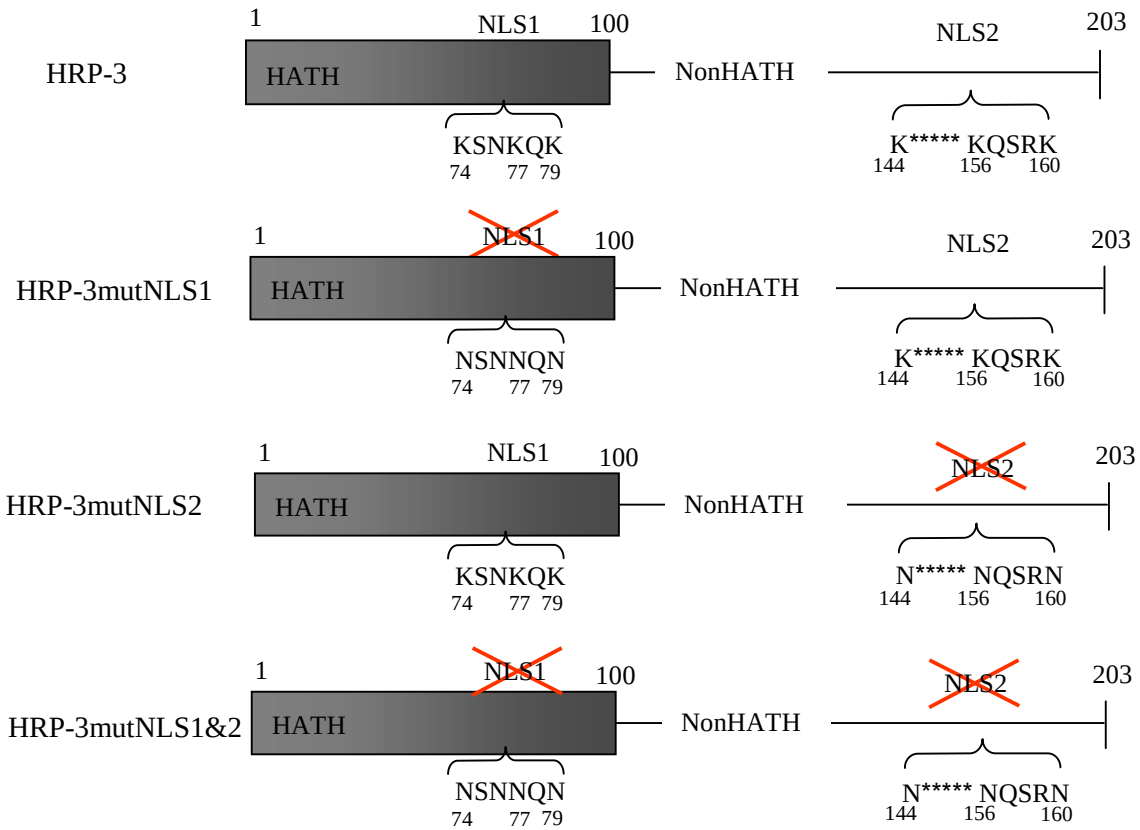


**Figure 35: Schematic diagram of NLS mutant HRP-3 constructs**. Schematic diagram showing the position of the different NLSs and positions of the created point mutations in HRP-3 molecule. In HRP-3mut NLS1 or HRP-3mutNLS2 three lysine amino acids in

either NLS1 (74, 77 and 79) or NLS2 (144, 156 and 160) respectively were replaced by three asparagines. In the double mutant construct (HRP-3mutNLS1&2) all six lysines (of both NLS1 and NLS2) were replaced by asparagines using a primer based PCR technique.

All constructs were cloned into a vector coding for a C-terminal StrepTag. The integrity of the constructs was confirmed by cycle sequencing before they were transfected into proliferating B35 neuroblastoma cells seeded on glass cover-slips. Three days after transfection, cells from each transfection condition were fixed using ice-cold 4% PFA, permeabilized, blocked with 2% BSA and immunostained against Streptag. A red fluorescently labeled secondary antibody was used to visualize the bound antibody and nuclei were counter stained with DAPI. Under microscope, it was found that immuno-positive B35 cells were able to completely translocate wtHRP-3StrepTag to the nucleus (arrow heads in figures 36A, B & C).

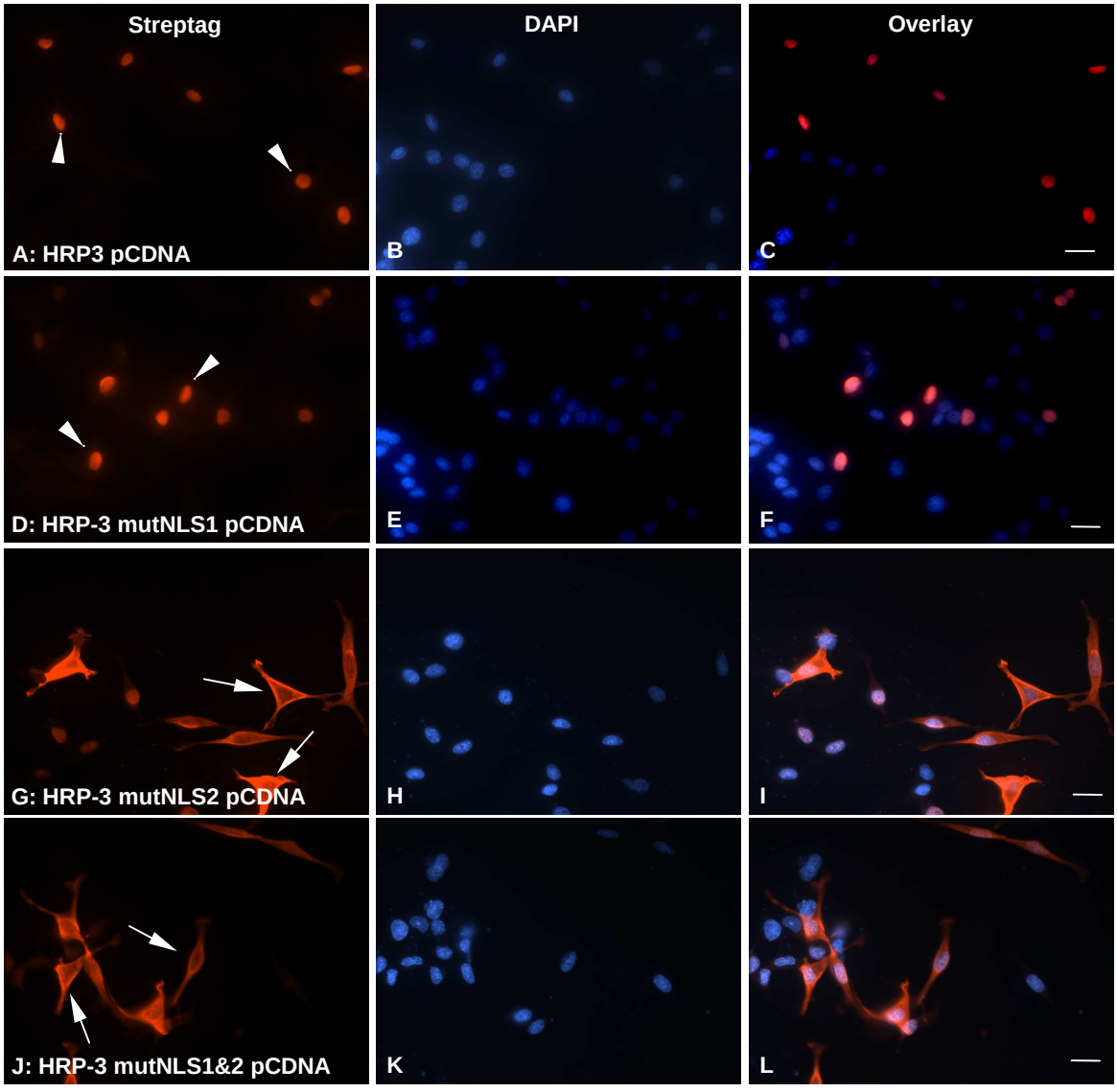


**Figure 36: Subcellular localization of wild type or NLS-mutant HRP-3 constructs transfected into B35 neuroblastoma cells**. B35 neuroblastoma cells under normal

proliferation conditions were transfected with the wild type or the different NLS-mutant HRP-3 constructs (cloned in streptag pCDNA3 vector) using Exgen 500 reagent. Three days after transfection, cells were fixed and immunostained using an antibody against streptag. DAPI was used as a nuclear counter stain. Both wild type HRP-3 and HRP-3mutNLS1 were able to localize to the nuclei of positively transfected cells (arrow heads in A & D) whereas HRP-3mutNLS2 and HRP-3mutNLS1&2 failed to target the nucleus and localized only to the cytoplasm in most of the cells (arrows in G & J). Bars are 20 µm.

This observation was found to be in accordance with the data shown by Ikegame concerning the nuclear translocation of transfected HRP-3 (Ikegame, et al., 1999). Interestingly, whereas cells expressing HRP-3mutNLS1 were indistinguishable from the wtHRP-3 expressing ones, most cells failed to translocate HRP-3mutNLS2 into their nuclei showing a streptag signal only in the cytoplasm (arrows in figures 36G, H & I). This last finding was similar to the behavior of NLS2mutHDGF which failed to target the nucleus when transfected into 293 cells (Kishima, et al., 2002) indicating the importance of the NLS2 in the nuclear targeting ability of at least HRP-3 and HDGF within this protein family. As expected, constructs mutated at both NLSs were unable to translocate to the nucleus most probably due to the deficient NLS2 (figures 36J, K & L).

The data presented before showed that reducing the level of endogenous HRP-3 resulted in negative effects on neurite length and sprouting ability of cells. In addition, data from previous experiments on the same cell line (see diploma Thesis, El-Tahir) showed that increasing the intracellular level of HRP-3 in B35 cells had a neurite outgrowth promoting effect upon dBcAMP-induced differentiation. To investigate whether localization of HRP-3 could be responsible for these effects, B35 cells were transfected with the different NLS mutant constructs of HRP-3 described before. WtHRP-3 transfected cells were used as a positive control and cells transfected with the empty vector (pCDNA3) as a negative control. Twenty four hours after transfection, cells were induced to differentiate using 1 mM dBcAMP and they were fixed 3 days after induction. Cells were co-transfected with an eGFPC3 plasmid in a ratio of 10% of total DNA amount of the different constructs used so that transfected cells could be detected under the fluorescence microscope by their GFP signal. Randomly chosen pictures were taken under the microscope from the different conditions. The length in micrometer of the longest neurite arising from about 100 randomly chosen positive transfected cell in each condition was recorded. Analysis of the obtained data showed as expected a highly significant increase in the mean neurite length

in wtHRP-3 transfected cells compared to the negative control. Interestingly, also HRP-3mutNLS2 transfected cells which failed to translocate the protein into their nuclei showed a nearly equal and significant increase in the mean neurite length ($p<0.001$, unpaired t-test) when compared to the negative control cells. Surprisingly, however located to cell nuclei similar to the wild type HRP-3, no significant increase in the neurite length was observed over the negative control when B35 cells were transfected with HRP-3mutNLS1 ($p=0.9$) or the double mutant construct HRP-3NLS1&2 ($p=0.1$; figure 37). The same observations were obtained when the experiment was repeated under the same conditions (see supplementary data S 3).

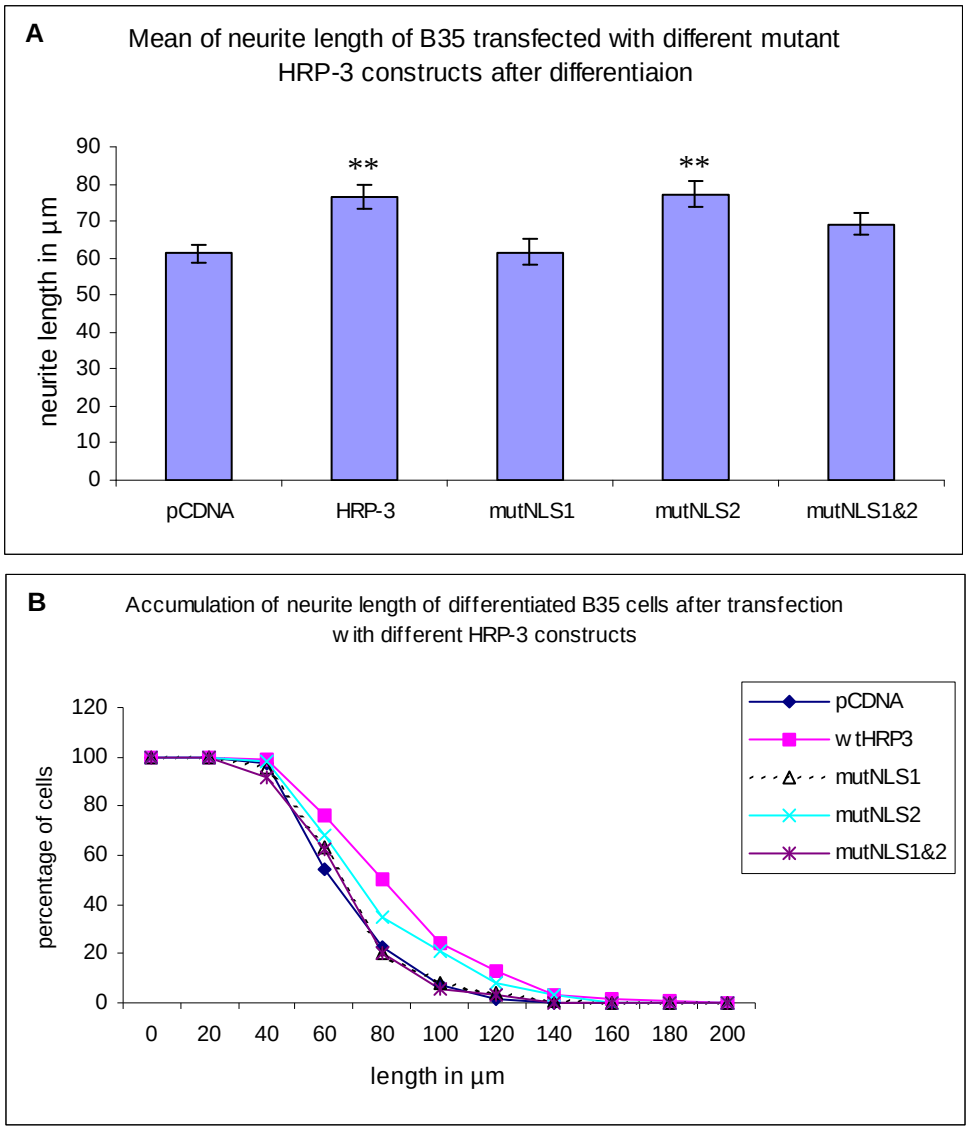


**Figure 37: NLS1 is responsible for the neurite outgrowth promoting effect of HRP-3 in B35 cells.** B35 neuroblastoma cells were transfected with different NLS mutant constructs, wild type HRP-3 or the empty vector together with eGFPC3 in a DNA ratio of 10 to 1 to detect the positively transfected cells under a fluorescence microscope. Twenty

four hours after transfection, differentiation was induced with 1 mM dBcAMP and cells were fixed and stained three days later. The length of the longest neurite arising from about 100 randomly chosen positively transfected cells was estimated in a blind assay. Repeating the experiment under the same conditions resulted in the same tendency. In the first graph bars represent the standard error and asterisks indicate a significant mean over the control. **$p \leq 0.001$.

## II.2 Extracellular roles

### II.2.1 Role of HRP-3 in neuronal cell survival

Zhou and co-workers reported that in the central nervous system HDGF was produced mainly in neurons and retained in their nuclei. They found that this protein was released by cultured primary hippocampal neurons under physiological conditions and that its release was accelerated under necrosis conditions. They reported also a similar observation concerning the secretion of a well known neurotrophic factor, HMG1 (Zhou, et al., 2004). From the data shown here before, beside the structural similarity of HRP-3 and HDGF, cortical neurons expressed both proteins in parallel. Therefore it was interesting to know if neurons release HRP-3 into their supernatant in a similar way to that observed for HDGF. For this experiment, neurons were freshly prepared from mouse embryos and seeded onto PDL coated 10 cm cell culture plates. Thirty to sixty minutes after seeding cells were washed twice with DMEM then NBM/B27 medium was replaced by DMEM medium supplemented with 200 ng/ml affinity purified recombinant HDGF. Neuron supernatant was collected after 3 or 5 days. After being concentrated by centrifugation through a filter with MWCO 10 kDa, supernatant contents were separated by SDS-PAGE. Medium not incubated with cells was used as control. Western blot analysis using a polyclonal antibody against HRP-3 detected HRP-3 in supernatant (figure 38A) indicating that it was released by primary cortical neurons into the supernatant similar to HDGF. Control medium (medium without cells) showed no immunoreactivity against HRP-3 (figure 38A, lane 8). Bands obtained at 72 kDa were identified using mass spectrometry as bovine serum albumin (BSA) which was used in relatively large amounts during the preparation of primary cortical neurons as a trypsin inhibitor.

Neurons in primary cultures are very sensitive to the absence of nutrients and they may show survival difficulties under these conditions. It was shown before by many research groups that many proliferating and/or differentiating factors affect the survival of neurons (Oppenheim, 1996; deLapeyrier and Henderson, 1997;

Giehl, 2001). Zhou and Marubuchi and their co-workers reported that the addition of HDGF (the structurally similar to HRP-3) to the culture medium of mouse hippocampal neurons (Zhou, et al., 2004) or rat motor neurons (Marubuchi, et al., 2006) was able to promote cell survival and neurite extension in an equivalent way to those of well known neurotrophic factors like CNTF and BDNF (Arakawa, et al., 1990; Sendtner, et al., 1990, 1992a & 1992b; Oppenheim, et al., 1991 & 1992; Yan, et al., 1992; Henderson, et al., 1993; Koliatsos, et al., 1993; Mitsumoto, et al. 1994). To investigate whether HRP-3, like HDGF, was involved in neuronal survival, the protein released by the neurons into their supernatant was blocked 24 h after seeding by adding a specific antiHRP-3 antibody. Pre-absorbed antibody was used as a negative control. After 48 hrs of treatment, neurons were fixed and visualized by an unspecific crystal violet staining to analyze general cell morphology (figure 38B) by transmitted light microscopy.

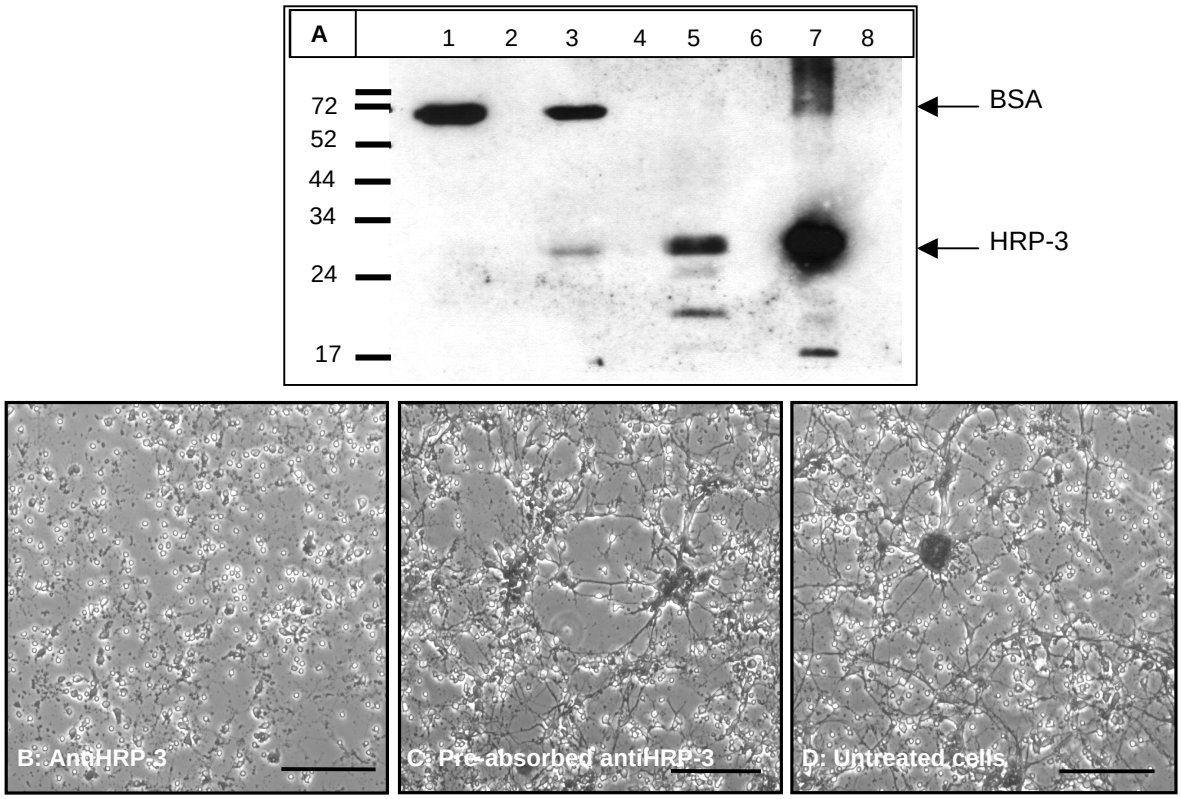


**Figure 38: Endogenous HRP-3 promoted primary cortical neurons survival after being released into the cell culture supernatant.** (**A**) supernatants from primary cortical neurons were collected at different time points (3 and 5 days after seeding) and concentrated. One eighth of the total supernatant volume from both time points was separated by SDS-PAGE and separated proteins were detected using specific polyclonal antiHRP-3 antibodies. A protein migrating at a molecular weight of ≈ 30 kDa was detected as HRP-3. No immunoreactivity was detected in the cell-free medium. Lane 1 & 3: supernatant collected after 3 and 5 days respectively, 5: mouse brain lysate, 7: affinity purified bacterially expressed HRP-3, 8: cell free medium, 2, 4 and 6 are free lanes. Bands

at 72 kDa were identified as BSA using mass spectrometry. (**B**) One day old primary cortical neurons were treated for 48 hrs with 1 µg/ml of the affinity purified HRP-3 antibody (AntiHRP-3) or the antibody pre-absorbed against recombinant HRP-3 protein (Pre-absorbed antiHRP-3) or an equivalent amount of the vehicle used for diluting the antibody (Untreated cells). Antibody treated neurons showed a massive loss of the neurite network compared to the cells treated with the blocked (pre-absorbed) antibody or those treated with the vehicle alone. Bars are 100 µm.

It was noticed that neurons treated with the medium supplemented with an equivalent amount of the antibody-diluting vehicle (50 % glycerol/PBS) alone did not show any change in their morphology and proceeded normally like untreated neurons (figure 38D). On the other hand, blockage of HRP-3 in neuron supernatants resulted in time dependent deterioration of neurite network of the neurons and finally led to cell death within three to four days of HRP-3 depletion indicating its importance for maintaining culture health (figure 38B). The specificity of HRP-3 survival promoting effect was proved by the possibility to completely block the effect of the added antiHRP-3 antibody by pre-absorbing it before being applied to neurons. Neurons under this condition were not distinguishable from those incubated with the vehicle supplemented medium (figures 38C & D).

Taking in consideration the previous experiment's results and the possible neurotrophic effect of HRP-3, it was interesting to test the ability of HRP-3 to rescue neurons kept under nutrient deficient conditions. In the preliminary trials to configure this effect cells were cultured in complete N2 medium. Culture medium was daily exchanged with fresh medium which was either complete N2 medium, His-tagged HRP-3 supplemented N2 medium (100 ng/ml) or β-gal supplemented N2 medium (100 ng/ml). As an additional control for comparison, neurons in some wells were kept under unchanged complete N2 medium for the whole period of the experiment. Under these conditions only a little difference between the test protein and the different controls (β-gal supplemented or un-supplemented medium) was obtained probably due to the nutrient-rich medium used (complete N2). To get a clearer difference, a nutrient-free Dulbecco's Modified Eagle Medium (DMEM, GIBCO) with neither serum nor growth factors was used as the basal medium (negative control). Plain DMEM was supplemented either with 100 ng/ml of affinity purified recombinant His-tagged HRP-3, 100 ng/ml of affinity purified recombinant β-gal or 5% FCS. Having the experiment done in this way resulted in significant differences between HRP-3 treated cells on one hand and β-gal treated or nutrients free medium treated cells on the other hand regarding neurons survival

and consequently integrity as well as the degree of complexity of neurite network. As expected, keeping neurons under nutrient-free medium resulted in degeneration and loss of neurite network over time and finally cell death within 3-4 days (figure 39D). Surprisingly, neurons kept under HRP-3 as the only supplement in culture medium (figure 39A) looked as healthy as those under 5% FCS supplemented DMEM during the whole period of experiment (figure 39B).

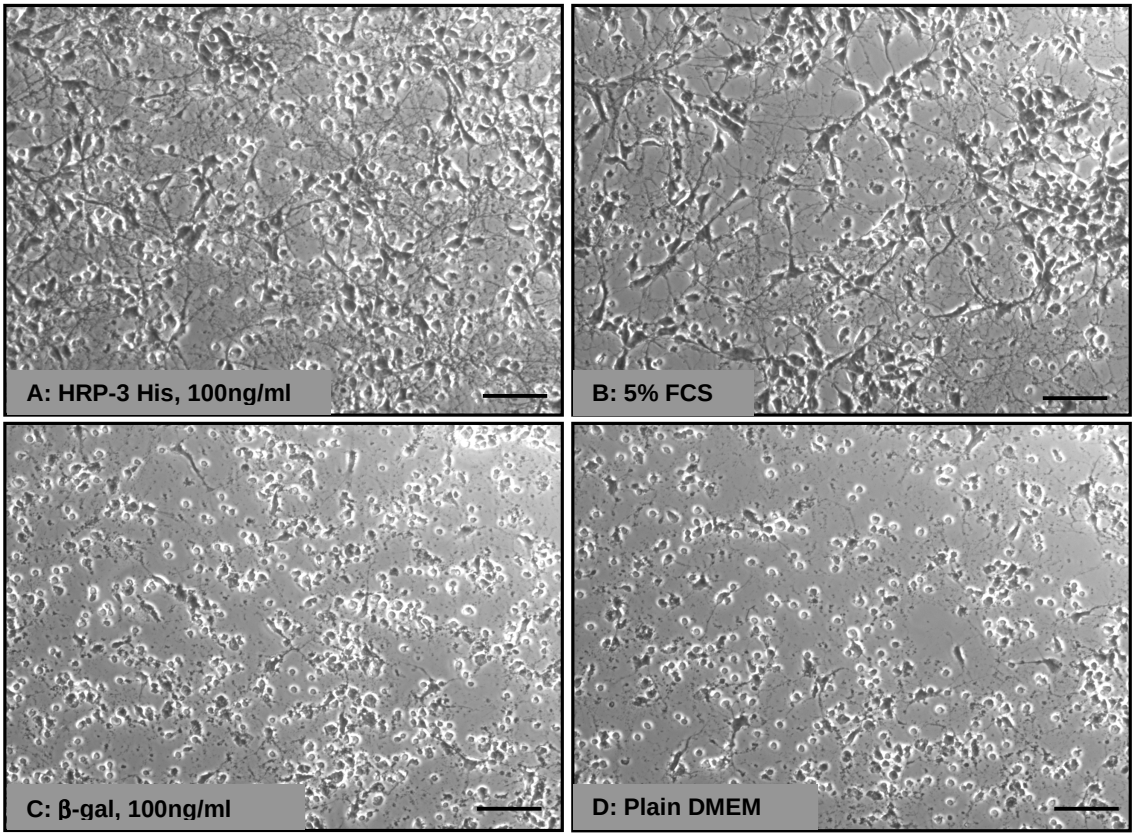


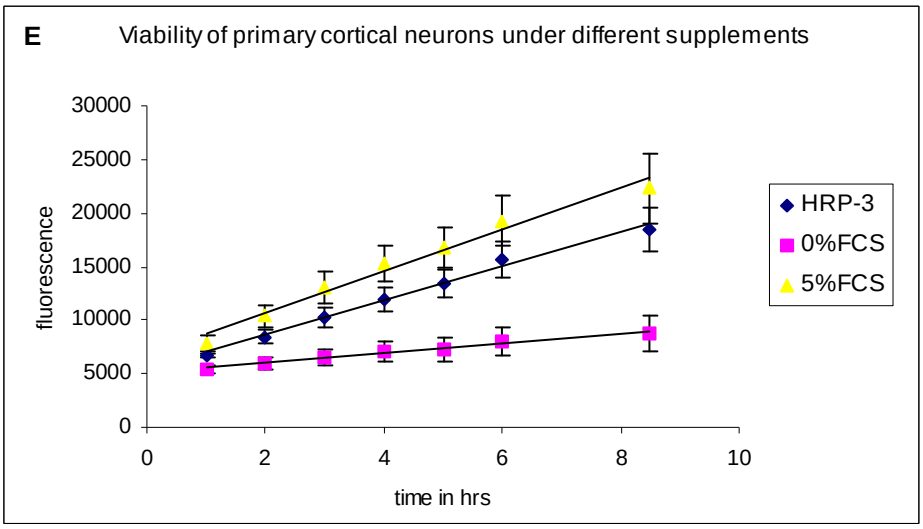


**Figure 39: Exogenously-supplemented HRP-3 rescued mouse primary cortical neurons cultured under supplement-free conditions**. Primary cortical neurons were seeded on PDL coated glass coverslips in complete NBM medium. One day later cells

were thoroughly washed and incubated in supplement-free DMEM or DMEM supplemented with 100 ng/ml HRP-3, 100 ng/ml β-gal or 5% FCS. After three days of treatment cells were fixed and non-specifically stained using crystal violet. Pictures taken using light microscopy demonstrated the ability of recombinant HRP-3 to rescue primary cortical neurons (A). Neither another recombinant protein similarly purified from bacterial culture (C) nor DMEM medium alone (D) were able to rescue neurons from death. FCS supplemented DMEM was used as a positive control (B). E represents a quantitative estimation of the survival promoting effect of HRP-3 on cortical neurons compared to the other supplements using Alamar blue®. Bars are 50 µm.

Unlike HRP-3, The presence of a control protein, like β-gal, purified after bacterial expression using the same protocol was unable to protect the neurons from cell death when used under the same conditions (figure 39C). Quantitative estimation of this effect was achieved using colorimetric Alamar blue® proliferation assay three days after keeping neurons under the different conditions. Measuring the fluorescence of the reduced form of the added dye (which is in a direct relationship with the cell viability) showed that neurons under HRP-3-supplemented medium were surviving better compared to those under no supplement (figure 39E). The results of the quantitative estimation were reproducible when the experiment was repeated (see supplementary data, figure S 5). These data together with the data obtained from depleting the medium from secreted HRP-3 suggested that HRP-3 either secreted by the neurons themselves or artificially added to their supernatants exerted a neurotrophic effect on mouse primary cortical neurons. These experiments point to an important role played by HRP-3 in neuronal cell survival.

### II.2.2 Role of HRP-3 in neuritogenesis

#### II.2.2.1 Effect of soluble HRP-3 on neuritogenesis

After detecting a role for HRP-3 in supporting neuronal cell survival, it was important to determine whether this growth factor in addition to its survival promoting effect also has an influence on neuritogenesis. To answer this question, the protein in its soluble form was applied to neuron supernatant. For this purpose neurons seeded in complete NBM culture medium were supplemented with 1.5 µg/ml of either affinity purified recombinant HRP-3 or β-gal. After 48 hrs, neurons were fixed and immunostained against the neuronal marker β-III-tubulin to label neuronal processes. Using fluorescence microscopy, pictures were taken for

neurons under both conditions. The length of the longest neurite arising from randomly chosen β-III-tubulin positive neurons was measured and the number of processes (branches) arising from these cells were counted. Blind analysis of the data obtained from both conditions showed that the addition of HRP-3 in its soluble form to the culture medium did not result in a statistically significant enhancement neither in the mean neurite length nor in the number of branches produced by these neurons when compared to those produced by neurons treated by adding β-gal (figure 40).

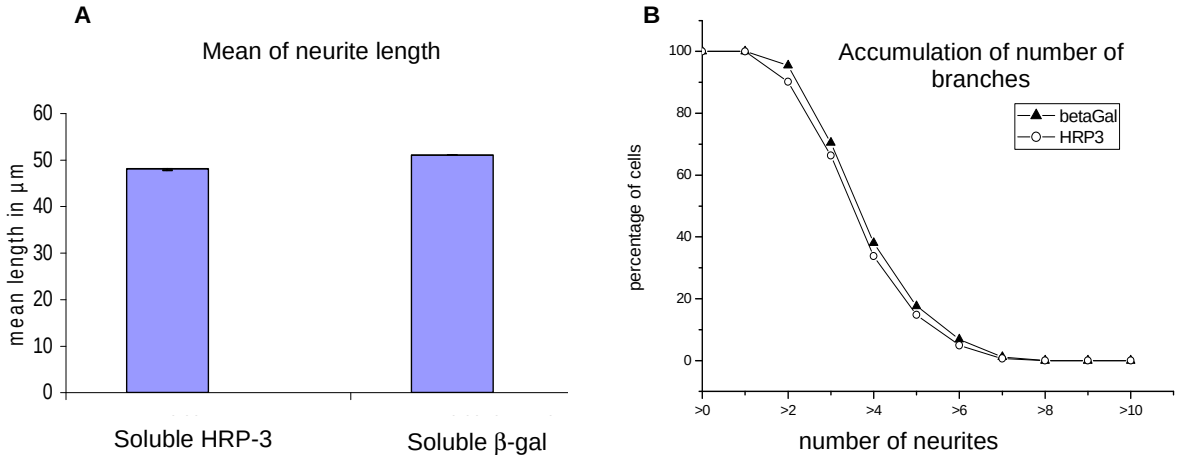


**Figure 40: Soluble HRP-3 did not show a neurite outgrowth promoting effect on cultured primary cortical neurons.** Primary cortical neurons were seeded on PDL coated glass coverslips in complete NBM medium. The complete growth medium was supplemented with recombinant HRP-3 or β-gal as a control protein (1.5µg/ml). After 48 hours cells were fixed and immunostained against β-III-tubulin. Random pictures were taken from each condition under a fluorescence microscope. The neurite length (A) and number of branches arising from β-III-tubulin positive neurons (B) were analyzed independently. HRP-3 was unable to induce any significant increase regarding both parameters when compared to the control protein. n = 200.

### II.2.2.2 Effect of substrate-bound HRP-3 on neuritogenesis

As HRP-3 in its soluble form proved not to play a role in neuritogenesis, it was important to exclude the possibility that it may bind the substrate and exert other effects. It was shown before that some molecules like HB-GAM or chondroitin/dermatan sulfate were able to promote neurite outgrowth under conditions when they were coated on a cell culture dish surface but not when they were used in soluble form (Rauvala, et al., 1994; Kinnunen, et al., 1996; Raulo, et al., 2005; Li, et al., 2007). To test whether this case would apply also for HRP-3,

two questions were investigated. The first question was to know if HRP-3 helped the cells at all to adhere to an unfavourable substrate coated only with HRP-3. The second question was to find out the consequences of this adherence if it exists at all. To get an answer for these questions, primary mouse cortical neurons were seeded onto an unfavourable substrate for cells, non adhesive sterile bacterial plates. These plates do not provide an appropriate surface for cell adhesion and cell growth, resulting in the inability of neurons to start differentiation due to the lack of a supporting substrate. Before seeding, plates were pre-treated for 1 hr with the purified recombinant His-tagged proteins HRP-3, HDGF or β-gal (10 µg/ml). The amount of bound proteins was estimated using an ELISA based enzymatic assay (supplementary data, figure S 6). Equal numbers of freshly prepared neurons were seeded on the different substrates after being washed and incubated in complete NBM. A few hours after seeding cells showed nearly the same number of neurons adhering on the different protein coats. After 48 hrs on the bacterial plates, neurons were fixed and stained using crystal violet.

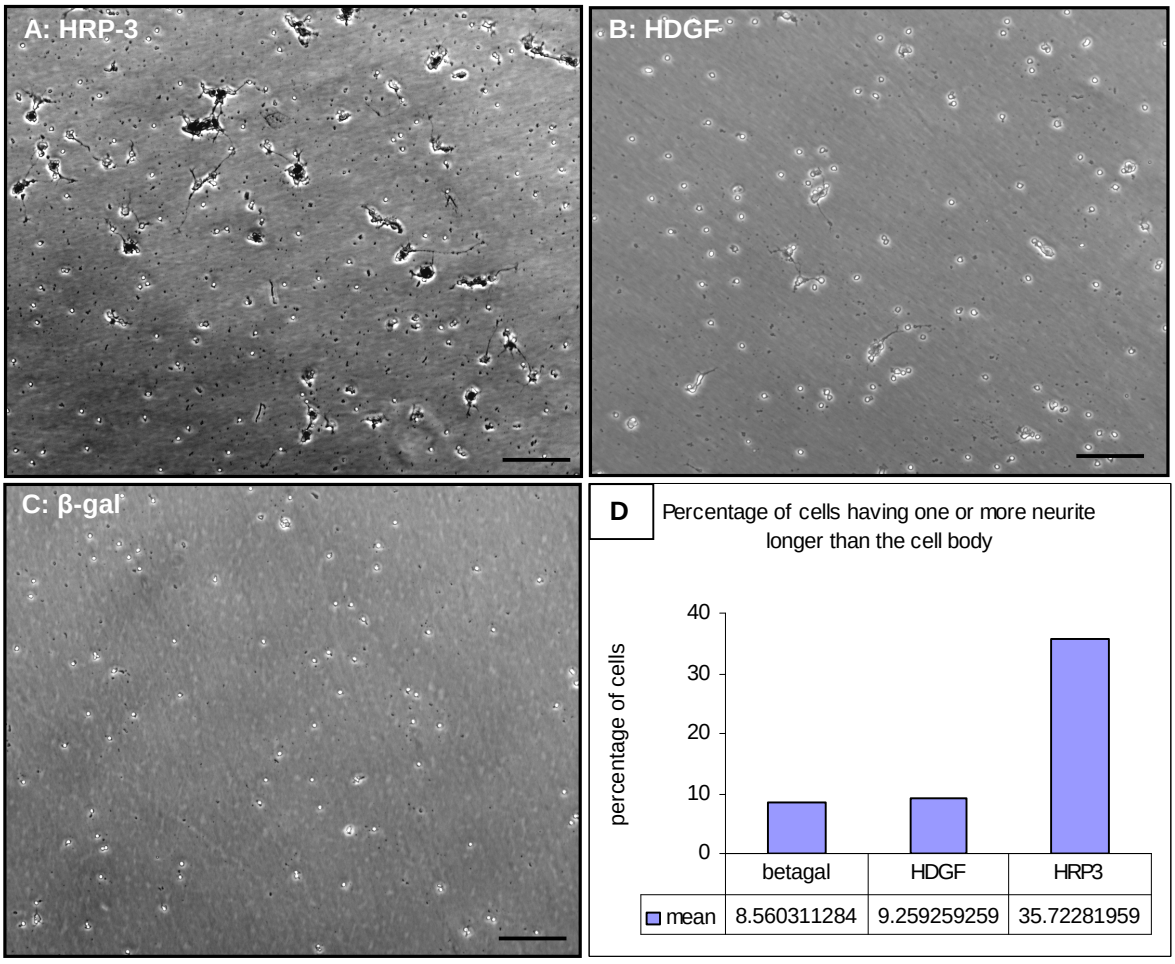


**Figure 41: Surface-immobilized HRP-3 promoted neurite outgrowth of primary cortical neurons seeded on bacterial plates**. Freshly prepared primary cortical neurons

were seeded on bacterial plates pre-coated for 1 hr at 37°C with 10 µg/ml of affinity purified recombinant His-tagged HRP-3, HDGF or β-gal. Morphological examination initially revealed a similar amount of cells attached to the different coated culture substrates. Only on HRP-3 coated plates a substantial amount of cells started to differentiate compared to HDGF or β-gal (A-C). Quantitative analysis of cells producing neurites longer than their cell bodies underlined the neurite outgrowth promoting effect of HRP-3 on cultured primary cortical neurons. Bars in A, B, C are 100 µm.

Plates were examined under transmitted light microscope for morphological differences of neurons on the different substrates. It was found that the presence of any of the three proteins as a substrates was enough to allow the adherence of nearly the same number of cells in all conditions. But interestingly, only in case of HRP-3 matrix a significant number of neurons was able to sprout and began to produce neurites (figure 41A). On the other hand, neurons that were seeded on HDGF coat were not distinguishable from those on the control protein coat (β-gal). In both cases (HDGF and β-gal coats) very few cells were able to spread their processes and differentiate (figures 41B & C). Statistically, about 100 randomly chosen cells in different shots from each condition were analyzed concerning the production of at least a single cell process that was equal to or longer than the cell body. A highly significant increase in the number of differentiating cells was observed when HRP-3 was used as a coat (4-time increase) compared to HDGF or β-gal coats (figure 41D). An effect that may be explained by a facilitated penetration of the growing processes only on HRP-3 matrix.

To compare the proteins effect on neurons, two days after seeding on the protein-coated PDL-coated coverslips, neurons were fixed and immunostained against β-III-tubulin to visualize their morphology. Using fluorescence microscopy more than 200 positively stained cells from each condition were randomly chosen, photographed and analysed. Analysis parameters were the length of the longest neurite arising from neurons and the number of neurites arising from each neuron. The analysis revealed that HRP-3 as an extracellular matrix exerted a significantly stronger neurite outgrowth promoting effect compared to the other coats. Data showed a highly significant increase in the mean length of the processes produced by the neurons seeded on HRP-3 coat as well as in the number of neurites produced by these cell (figure 42A & B). On the other hand, neurons seeded on HDGF and β-gal coats did not show significant differences regarding both

parameters (mean length of longest neurite and number of produced neurites per neuron) when compared to each other or to neurons seeded on PDL coated coverslips.

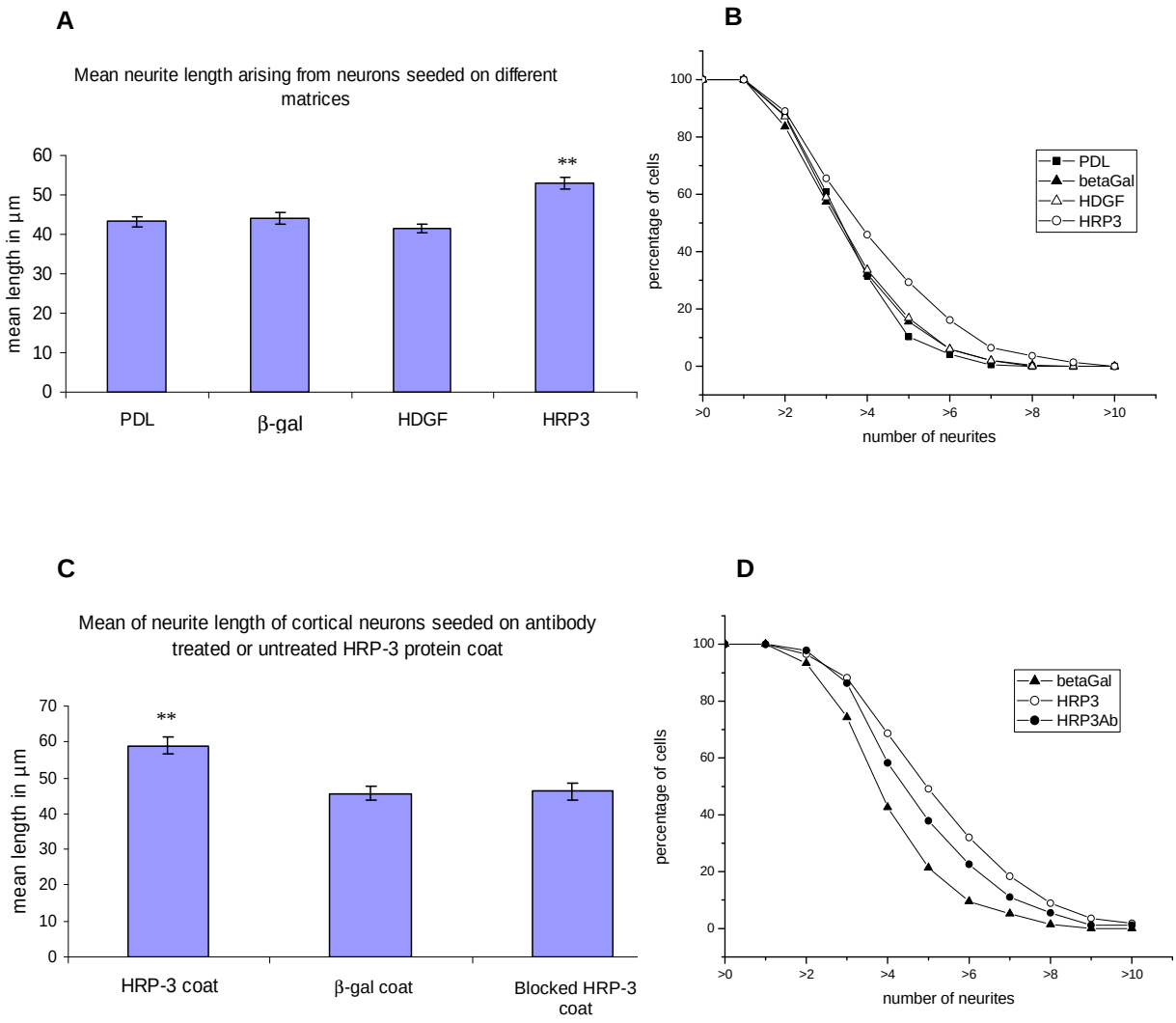


**Figure 42: Surface-immobilized HRP-3 promoted neuritic outgrowth and cell sprouting of primary cortical neurons**. Mouse primary cortical neurons were seeded on PDL-coated glass coverslips coated with His-tagged HRP-3, His-tagged HDGF, His-tagged β-gal. After 48 hours neurons were fixed and immunostained against a neuronal marker (β-III-tubulin). Random pictures were taken for each condition under a fluorescence microscope. The mean neurite length (A) and number of neurites arising from β-III-tubulin positive neurons (B) were analyzed independently. HRP-3 as a coat increased the mean neurite length as well as the number of neurites arising from neurons when compared to other substrates. Pre-incubating the HRP-3 coated coverslip with specific antiHRP-3 antibodies before seeding neurons on them was able to block the positive effects of this protein regarding the previously mentioned morphological characters (C + D). Number of cells examined per condition ≈200; **$p<0.0001$

Although the amount of HDGF adhered to glass was significantly higher than the amount of adhered HRP-3, the neurite outgrowth on the latter protein coat was

significantly higher. This indicated that the neurite outgrowth promoting effect of HRP-3 was a specific effect for this protein when used as an extracellular matrix and could not be related to an improved adhesion to the substrate. This effect was a specific reproducible effect (see supplementary data S 6) not achieved even by the closely related family member HDGF.

As a further control for the specificity of this effect, HRP-3 coated coverslips were blocked with a specific antiHRP-3 antibody before using them as a substrate for seeding cortical neurons. Comparing the mean neurite length produced by these neurons with the values obtained from neurons seeded on unblocked HRP-3 coat as well as β-gal coat demonstrated that the antibody blocking of the protein was able to completely inhibit the positive effect of HRP-3 on neuritogenesis (Figure 42C & D).

# 5. Discussion

## 5.1 HRP-3 expression in vivo and in vitro

The family of Hepatoma-Derived Growth Factor related proteins comprises six members: HDGF, HDGF related protein -1 to 4 and lens epithelial-derived growth factor (LEDGF) all of which show homology in the N-terminal 98 amino acids (Nakamura, et al., 1994; Izumoto, et al., 1997; Ikegame, et al., 1999; Ge, et al., 1998). Whereas HDGF is expressed in a wide variety of tissues, the expression of HRP-3 is restricted to the nervous tissue. Previous data indicated that both HDGF and HRP-3 are expressed by differentiated neurons with different expression patterns (Abouzied, et al., 2005). Western blot analysis of protein extracts of different brain regions demonstrated a rather ubiquitous expression of HDGF family members in different brain regions. HDGF is almost evenly distributed (Abouzied, et al., 2005; Zhou, et al., 2004) whereas HRP-3 expression level varies between the different brain regions (El-Tahir, et al., 2006). On the cellular level within the rodent brain, HRP-3 showed a more restricted expression when compared to HDGF. Purkinje cells in the cerebellum and neurons within the subiculum and cornu ammonis of the hippocampus were strongly HRP-3 positive whereas cerebellar granular cells appeared to be HRP-3 negative. The term granular cell is used to describe major cell populations of tiny neurons found in the cerebral cortex, olfactory bulb, granular layer of the cerebellum and the dentate gyrus. These cells are similar in being born late during development and expressing at least one common molecular marker, termed RU49. This has led to the suggestion that these diverse kinds of granule cells are of a common developmental origin (Yang, et al., 1996). Interestingly, granular cells having these common origin and characteristics show a weak expression signal of HRP-3 in the dentate gyrus and a lack of its expression in the cerebellum. Beside the correlation between HRP-3 expression and neuronal origin, the expression pattern of this protein in cerebellar neuron subtypes correlates also with the transmitter phenotype of these cells. Whereas granule cells are mostly glutamatergic (excitatory), almost all the other neurons in this brain structure use gamma amino butyric acid (GABA, inhibitory) as a neurotransmitter. In a similar way, Ptf1a, which was reported to be a lineage determinator in the cerebellum, is also exclusively

expressed by GABAergic neurons of the cerebellum (Hoshino, et al., 2005; Sellick, et al., 2004). At least in the cerebellum, HRP-3 might be a marker distinguishing between excitatory and inhibitory neuronal subpopulations. Except for neurons, very low amounts of HRP-3 could be detected in oligodendrocytes located in the brain stem and in glial cells. On the other hand, white matter tracts of the cerebellum contained no HRP-3 expressing cells. Studies on the place and time of birth of oligodendrocytes have demonstrated heterogeneity inside this cell population. It is possible that HRP-3 expression in oligodendrocytes is also dependent on their time of birth similar to the observations for granule neurons. Unlike oligodendrocytes which contained limited amounts of the protein, astrocytes in vivo could not be detected as HRP-3 positive cells. In contrast to the restricted expression of HRP-3, HDGF was found in neurons, astrocytes and oligodendroglia, in meningeal fibroblasts and ependymal cells. Immunostainings presented in this work indicate that both proteins, HDGF and HRP-3, were expressed in the majority of neurons in adult mouse brain. The overlapping expression pattern of HDGF and HRP-3 in neuronal cell nuclei in vivo and in vitro suggests different functions for both proteins that may include proliferation, differentiation as well as cell survival in addition to other unknown functions. On the other hand, the almost neuron-specific expression pattern of HRP-3 points to special function(s) for this protein that may include cell polarization and/or maintaining of the newly produced cell processes.

HRP-3 expression during mouse embryogenesis showed that its expression is not only restricted to the developing brain but rather expressed in the whole nervous tissue. Interesting in its embryonic expression was the early detected signal within both the central and the peripheral nervous system. Directly after the three germ layers: ectoderm, mesoderm and endoderm have taken their positions within the embryo (gastrulation phase), neurulation begins and the neural tube is developed from the ectoderm. The stimulation of ectoderm to form the neural tube is mediated by some morphogenic factors released by the notochord, like e.g. sonic hedgehog (SHH) which regulates organogenesis and signals for the development of motor neurons (Echelard, et al., 1993). The rostral (apical) part of the formed

neural tube will form the brain with its divisions and the caudal (lower) part will form the spinal cord.

HRP-3 was expressed in the whole neural tube which will form the nervous tissue early after its closure. However, HRP-3 expression levels varied strongly within the different parts of the neural tube. Looking from a transverse view, HRP-3 showed an intense signal in the oval bundle and motor neurons and a weaker signal in rest structures. These discriminate expression levels within the different structures of the neural tube point to possibly different roles or a variable degree of importance of the protein in the different cell types. Both sympathetic and dorsal root ganglia which originate from the migrating neural crest cells and are parts of the peripheral nervous system were expressing HRP-3 as well. Dorsal root ganglia consist of neuronal cells of different subtypes. The strongest HRP-3 signal in embryonic DRG neurons was detected in the cytoplasm as well as in the single processes arising from some neurons having a unipolar outline. In a differently looking neuronal cell population, only a weak nuclear signal for HRP-3 was detected. The strong signal for HRP-3 detected in E10.5 dorsal root ganglia remained through out all the later embryonic time points as developmental neurogenesis was still going on. Looking at the embryo from a sagittal view, it was detected that HRP-3 was expressed also within the whole embryonic brain.

Brain neocortex is composed mainly of neurons named the cortical neurons. These neurons are generated by the asymmetric division of progenitor cells within the ventricular zone next to the lateral ventricles. At first, progenitor cells divide asymmetrically, producing glial cells and neuronal cells (Noctor, et al., 2001). The fibres of the glial cells produced in the first divisions of the progenitor cells become radially oriented, spanning the thickness of the cortex from the ventricular zone to the outer pial surface. Some other progenitor cells begin to divide asymmetrically producing a postmitotic cell (a cortical neuron) and a daughter progenitor cell (Rakic, 1988). The radially oriented fibres of the glial cells function as a scaffold for the produced postmitotic neurons migrating outwards from the ventricular zone. The layered structure of the mature cerebral cortex is formed in an inside out manner as the newly born cells always migrate through the older layers during development (Brazel, et al., 2003; Jessell and Sanes, 2000) as shown in figure 43.

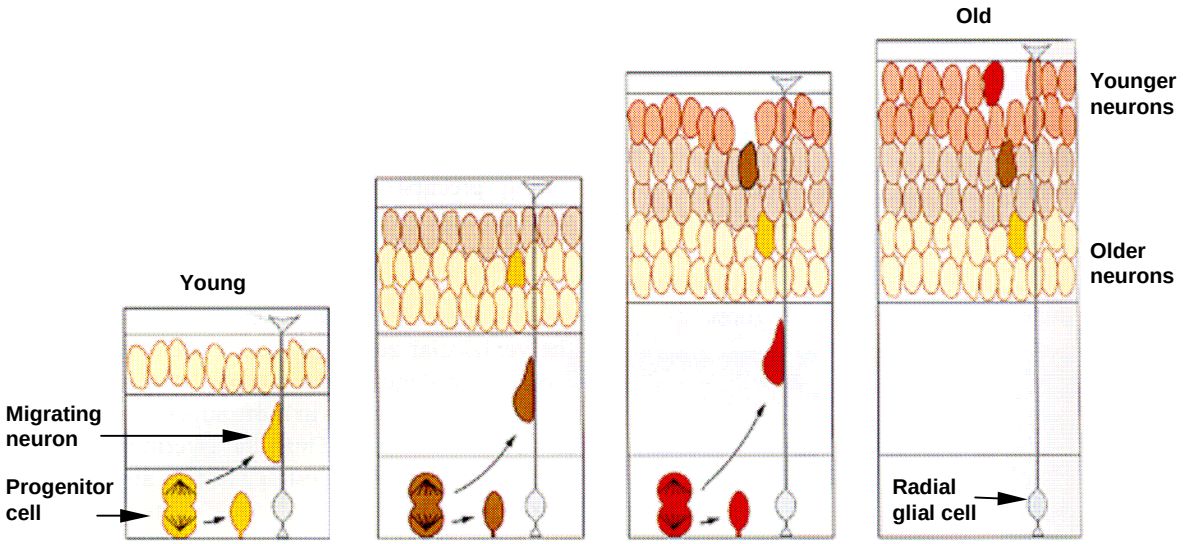


**Figure 43: Generation and migration of neurons in the mammalian cerebral cortex.** Cortical neurons are generated in an inside-first, outside-last order. Neurons born within the ventricular zone at early stages migrate to the deepest layers of the cortical plate. Neurons generated at later stages migrate past the earlier-generated neurons to form the more superficial layers of the cortex.

HRP-3 showed a widespread and early expression in the murine developing cerebral cortex cells which implies a possible role for this protein in developmental patterning and neurogenesis. From embryonic stages to the adulthood, HRP-3 showed dynamic variations in the subcellular localization as well as the number of cells expressing the protein. During the prenatal development of the mouse brain cortex, a huge number of homogenously distributed neurons expressed HRP-3. During this time, cortex was still developing and neurons were migrating along their way to their final destinies so that it is difficult to recognize the layered structure of the neocortex. On the other hand, postnatal and adult mouse brain neocortex showed a well-defined, layered structure. Directly after birth, the number of cells expressing HRP-3 in the neocortex seemed to be down regulated. In addition to that, these HRP-3 positive neurons were not homogenously distributed all over the neocortex like in embryonic stages, rather they were enriched in certain cortical layers. For example, layers I, IV and V showed the lowest number of HRP-3 positive neurons whereas layers II, III and VI were rich in HRP-3 positive neurons (according to the layers numbers mentioned in the introduction and results).

Another major difference between the developing and mature mouse brain was the subcellular localization of the protein within neurons. Whereas in the

embryonic brain mainly an extranuclear signal was detected in the developing cells, this signal gradually disappeared leaving almost only a nuclear signal in the well differentiated adult cortical neurons.

There are some proteins that are expressed, similar to HRP-3, in the early embryonic stage like fibroblast growth factors (FGFs) and heparin binding growth associated molecule (HB-GAM). Both FGFs and HB-GAM share some characters with the closely related family member HDGF, as they are heparin-binding proteins that exert mitogenic effect on many cell types and are also actively secreted proteins (Asahina et al., 2002; Burgess and Maciag, 1989). FGFs participate in many developmental, plasticity and repair processes including neurogenesis, cell survival, axonal growth, neuroprotection, learning and memory and are expressed in early embryonic stages (Reuss and von Bohlen und Halbach, 2003). In a similar way, HB-GAM is a protein that is strongly and widely expressed during embryonic and early postnatal stages and fades in adult rat brain (Rauvala, et al., 1994; Rauvala, et al., 1989).

The localization change of HRP-3 signal observed in tissue could also be detected in cultured primary neurons. In vitro, cultured mouse embryonic DRG (sensory) neurons showed an extranuclear expression signal for HRP-3 in young neurons which decreased by aging making place for the increasing nuclear HRP-3 signal in the mature sensory neurons. However both HRP-3 and HDGF were expressed in cortical neurons nuclei, only HRP-3 showed an additional and prominent expression signal in neurites of in vitro cultured mouse cortical neurons which was similar to that observed for cultured rat cortical neurons (Abouzied, et al., 2004). As the expression pattern of HDGF in mouse cortical neurons remained unchanged over time, HRP-3 showed a dynamic change regarding its expression pattern. Similar to the change in its localization observed in DRG neurons, young immature cortical neurons were showing a predominating cytoplasmic signal that was fading out by getting older. In the same time, a predominating nuclear signal was observed in older mature neurons. This developmental, stage-dependent change in localization was not only observed in primary neurons, but also in an inducible cell model, B35 neuroblastoma cells. These cells were expressing no HRP-3 during their proliferating stages but shortly after being induced to

differentiate, B35 cells showed a cytoplasmic HRP-3 expression signal. Interestingly, mature differentiated B35 cells were showing a strong expression signal for HRP-3 within their nuclei. Such a switch between cytoplasmic and nuclear pattern of expression may be explained by a possible need for a high level of HRP-3 in the cytoplasm of immature neuronal cells to promote differentiation and consequently reaching structural maturity. As soon as the neuronal cell has acquired its final mature structure and the neurite network is already established, there should be -according to this postulation- no need for HRP-3 in the cytoplasm. Thus, it can be speculated that the presence of HRP-3 within the cell nucleus could be a character of structural maturity in neurons expressing it. These findings regarding the dynamic change of the localization of HRP-3 between developing and mature cortical and sensory neurons in vivo as well as in vitro spot more light on the importance of this protein during the maturation steps in a neuron's life. This developmentally regulated expression pattern was also reported for another family member, LEDGF. LEDGF is expressed in the eye as a nuclear protein in the well-differentiated cells of ciliary body, iris and the photoreceptor cells of retina. On the other hand, it is expressed as a cytosolic protein in differentiating lens fibre cells and superficial corneal epithelial cells. In other words, the differentiation of lens epithelial cells is associated with a progressive change towards a nuclear LEDGF signal (Kubo, et al., 2003).

This hypothesis regarding the connection between the developmental stage and the cellular localization of HRP-3 signal can also be utilized to explain the extranuclear HRP-3 expression signal noticed in some areas of adult mouse brain. HRP-3 was detected as a cytosolic protein in areas like hippocampus, a region that is important for learning and memory (Van Praag, et al., 2002; Altman & Das, 1965; Kaplan & Hinds, 1977; Kuhn, et al., 1996; Kornack & Rakic, 1999; Eriksson, et al., 1998). Also in cerebral cortex, Purkinje cell layer and the ventral horns of the adult mouse spinal cord HRP-3 was detected as a cytosolic protein. These mentioned areas in addition to the lateral subventricular and subgranular zones of the dentate gyrus (hippocampus), optic nerve, olfactory bulb, caudate nucleus, spinal cord and many brain stem and forebrain structures have been shown to contain mitotic cells undergoing adult neurogenesis (Altman & Das, 1965; Altman & Das, 1966; Altman, 1969a & 1969b; Abrous, et al., 2005; Luzzati, et al., 2006;

Gage, 2007). To date, the function of this cell genesis in the normal intact adult brain and spinal cord is not known but researchers suggest that some of the new cells can become neuronal or glial cells (Horner, et al., 2000). Some others suggest that the newly born, young neurons provide a greater degree of plasticity to the mature brain (Biebel, et al., 2000) or function to replace dying neurons as a latent mechanism for brain repair (Mitchell, et al., 2004). Detecting an extranuclear HRP-3 signal which refers mostly to a differentiating neuron within the areas where adult neurogenesis is expected makes it reasonable to conclude a possible function(s) for this protein during cell maturation or in cell regeneration and repair processes. On the other hand its expression in the adult PNS axons (adult mouse sciatic nerve) may suggest a role for HRP-3 in impulse conduction or in maintaining axonal integrity.

## 5.2 Intracellular roles of HRP-3

As mentioned before, HRP-3 was expressed in primary cortical neurons early after seeding. An important finding was that the expression pattern of HRP-3 at this time point reflected an uneven, polarized distribution within the cytoplasm where its expression showed a local increase at the point where neuritogenesis would begin. At the areas of beginning neuritogenesis, tubulin units polymerize to form a strong core of microtubules. This polymerization regulates the events of cellular polarity and initiation of differentiation through sets of microtubules stabilizing and destabilizing proteins (Dehmelt & Halpain, 2004). Microtubules together with neurofilaments and actin constitute the elements of a neuron cytoskeleton (Hughes, 1953; Nakai, 1956). The local (polarized) increase in HRP-3 expression at the point where a process starts to elongate within the cytoplasm of very young neurons may point to the involvement of HRP-3 in neuron polarization process and a possible interaction with cytoskeleton element(s).

Both actin filaments and microtubules are necessary for axon extension. Actin filament polymerization drives the forward-extension of both filopodia and lamellipodia. Additionally, actin network of the cell cortex tends to resist gross shape changes. Consequently, actin-destabilizing drugs facilitate neurite outgrowth (Edson, et al., 1993; Knowles, et al., 1994; Bradke and Dotti, 1999). On the other hand, microtubule polymerization and transport of organelles mediate the

engorgement process and provide the core for a growing cell process. Microtubules must be dynamically unstable to allow growth cone formation. Therefore, both microtubule-stabilizing and -destabilizing poisons (drugs) can inhibit neurite outgrowth (Baas and Ahmad, 1993; Rochlin, et al., 1996; Liao, et al., 1995; Tanaka, et al., 1995; Jordan and Wilson, 1998; Kaverina, et al., 1998; Waterman-Storer and Salmon, 1999; Goode, et al., 2000; Kabir, et al., 2001).
The facts of stabilization and destabilization of the cytoskeleton elements could be successfully employed to explain the inability of cultured primary neurons to extend neurites, and fibroblasts and trophoblasts to loose their stress fibres when the expression of palladin or synapsin II was attenuated (Boukhelifa, et al., 2001; Ferreira, et al., 1994; Parast and Otey, 2000). Both proteins were identified as cytoskeleton-associated proteins. Whereas palladin was shown to play a possible role in establishing the polarized neuronal morphology and to maintain the integrity of organized cytoskeleton (Boukhelifa, et al., 2001; Parast and Otey, 2000), synapsin II regulates neurotransmitter release and plays a role in the formation of nerve terminals (Chilcote, et al., 1994).

An important finding was the close and direct relation between the cellular expression level of HRP-3 and neurite length. A reduction in the endogenous HRP-3 level within cortical neurons resulted in a significant reduction in the length of the produced neurite whereas increasing cellular level of HRP-3 resulted in a significant increase in neurite length.
Wild type HRP-3 transfected into cells was shown before to localize to cell nuclei (Ikegame, et al., 1999). It was also found that this nuclear translocation of wild type HRP-3 after transfection was related to the nuclear localising signals, NLSs and more precisely to NLS2 rather than NLS1 in a similar way to HDGF (Nakamura, et al., 1994; Ikegame, et al., 1999; El-Tahir, et al., 2009). The basic lysine residues of the nuclear localizing signal included in the carboxyl terminal (NLS2) were identified, for both HDGF and HRP-3, as a prerequisite for directing the protein into the nucleus.

Although excluding HRP-3 from the nucleus did not hinder its neurite outgrowth promoting effect on the cells, excluding HDGF from cell nucleus was enough to block its effect as a mitogen for Vascular Smooth Muscle cells (VSM, Everett, et

al., 2001). In other words, the nuclear localizing signal in the amino terminus (NLS1) is the one involved in promoting the neuritogenesis however not important for nuclear localization. This can be explained by the fact that HRP-3 interacts with the microtubules through its HATH region (where NLS1 is located) not through its C-terminus (where NLS2 is located, El-tahir, et al., 2009).

In brief, the direct relation between the cellular expression level of HRP-3 and neurite length in addition to the redistribution of HRP-3 from the cytoplasm to the nucleus during the maturation process strongly suggests a role for this protein during neuritogenesis. Recently, it has been reported that these neuritogenetic effects of HRP-3 are mediated through its interaction with tubulin dimers and assembled microtubules and its ability to promote the bundling of microtubules (El-tahir, et al., 2009).

## 5.3 Extracellular roles of HRP-3

Other than the tissue expression pattern and the subcellular localization in the adult mouse brain (Abouzied, et al., 2004; El-Tahir, et al., 2006), not much data regarding the functions and importance of HRP-3, were known up to now. In this study it was possible to uncover some of its extracellular roles in primary mouse cortical neurons. Primary rodent cortical neurons were shown before to have a high expression level of HRP-3 (Abouzied, et al., 2004; El-Tahir, et al., 2009). They have been long ago utilized as a tool for studying the effect of different proteins and growth factors like neurotrophins, HB-GAM, and also HDGF (Yuen, et al., 1996; Raulo, et al., 1992; Kinnunen, et al., 1996; Zhou, et al., 2004) as they are very sensitive to the absence of nutrients and growth factors. They may show survival difficulties in the absence of many proliferating and/or differentiating factors that affect their survival (Oppenheim, 1996; deLapeyrier, 1997; Giehl, 2001). Many proteins were shown to exert a neurotrophic effect on neurons like HMG1 (Zhou, et al., 2004), CNTF (Sendtner, et al., 1992 & 1994) and HB-GAM (Raulo, et al., 1992 & 1994). Among HDGF family members, LEDGF exerts survival and neuroprotective effects in addition to its established proliferative effects (Inomata, et al., 2003; Matsui, et al., 2001; Singh, et al., 1999 & 2000; Nakamura, et al., 2000). Marubuchi and Zhou and their co-workers have detected the release of HDGF in the cultured neurons supernatants and proved its

importance for neuronal cell survival as a neurotrophic factor (Marubuchi, et al., 2006; Zhou, et al., 2004). Interestingly, HRP-3 was found to be released in the supernatants of cultured mouse primary cortical neuron although it lacks a signal peptide-like hydrophobic region within its amino acid sequence. It was previously concluded that HDGF and CNTF as well as acidic and basic FGFs which all lack a signal peptide-like hydrophobic region (Burgess and Maciag, 1989) are secreted via non classical secretory pathways (Zhou, et al., 2004; Marubuchi, et al., 2006). Although the secretion mechanism is still to be investigated, HRP-3 may be secreted also via non classical secretory pathway(s) that is similar to or different from HDGF's pathway. Interestingly, HRP-3, either released by the neurons themselves or exogenously-applied as a supplement to the culture medium, specifically functioned as a survival-promoting and a neurotrophic factor for cortical neurons. However, the mechanisms behind the effects of soluble HRP-3 on cortical neurons remain to be elucidated. Neurotrophic, survival-promoting, and neurite outgrowth promoting effects of some proteins like HDGF, CNTF and BDNF on rodents hippocampal or motor neurons were also achievable by the exogenously-applied, affinity-purified recombinant proteins (Zhou, et al., 2004; Marubuchi, et al., 2006; Arakawa, et al., 1990; Sendtner, et al., 1990 & 1992; Oppenheim, et al., 1991 & 1992; Yan, et al., 1992; Henderson, et al., 1993; Koliatsos, et al., 1993; Mitsumoto, et al., 1994). Recent lines of evidence indicate that some neurotrophic factors are involved in synaptic modification, neurotransmitter release, and long term potentiation (Black, 1999; Lu and Chow, 1999; Chao, 2000; Poo, 2001; Yamada, et al., 2002). In addition, some neurotrophic factors like BDNF have been reported to modulate hippocampal plasticity and memory in cell and animal models (Jankowsky and Patterson, 1999; Thoenen, 2000; Egan, et al., 2003). Furthermore, literature on the subject of neurotrophic factors and their roles in neurodegenerative diseases, including Alzheimer's and Parkinson's diseases, is expanding prodigiously (Siegel and Chauhan, 2000). Hence HRP-3 is presented here as a novel neurotrophic factor, it is not impossible to find in the near future a role for HRP-3 in healing, delaying or preventing at least one of the neurodegenerative diseases.

On the other hand, HRP-3 used as an extracellular matrix for cell growth provided a proper substrate for neuronal cell adhesion as well as differentiation. In its

substrate bound form, HRP-3 was able specifically and significantly to promote neurite outgrowth and to induce the production of multiple neurites per cell. Using other proteins including HDGF as substrates allowed only cell adhesion but not any further effects on length or number of neurites. The decreased neurite length of neurons seeded on blocked HRP-3 coats provided an additional confirmation for the specificity of substrate-bound HRP-3 effects. Since the adhesiveness of neurons to surface structure is a necessary but not a sufficient condition for neurite outgrowth, these effects of HRP-3 on neurite outgrowth and cell sprouting can not be regarded only to improved adherence of neurons to the protein coated culture matrix.

Neurite outgrowth promoting effect of substrate bound proteins was previously reported for some proteins like HB-GAM, amphoterin, fibronectin and Chondroitin/Dermatan sulphate when they were used as substrates for neuronal cell growth (Raulo, et al., 1992; Hori, et al., 1995; Li, et al., 2007). For these proteins also, it was not the improved adhesiveness of cells to the substrate that caused neurite outgrowth. It was shown before that highly adhesive surfaces may fail to promote neurite outgrowth. This was proved by Rauvala who showed that both fibronectin and concanavalin A had nearly the same adhesiveness properties but only cells on fibronectin were able to sprout and differentiate (Rauvala, 1984).
Another protein that enhances neurite outgrowth is amphoterin which belongs to the high mobility group proteins (Parkkinen, et al., 1993). This protein exerts extracellular functions in the developing nervous and hematopoietic systems (Rauvala and Pihlaskari, 1987; Rauvala, et al., 1988; Merenmies, et al., 1991; Parkkinen, et al., 1993; Daston and Ratner, 1991; Daston and Ratner, 1994). Hori and co-workers showed that RAGE (receptor of advanced glycation end product) binds amphoterin and mediates neurite extension on amphoterin-coated substrates (Hori, et al., 1995). In fact, HRP-3 sequence lacks the HMG box that is conserved among HMG family proteins and is essential for the interaction with RAGE. This makes HRP-3 more likely to interact with a different receptor(s) to promote neurites outgrowth when used as an extracellular substrate.

These in vitro findings suggest that for cortical neurons, HRP-3 plays many important roles: first, HRP-3 either secreted by neurons into their supernatant or

exogenously-applied to supplement their supernatant is of great importance for cell survival and integrity of neurites network and acts as a novel neurotrophic factor. Second, HRP-3 in its substrate-bound form promotes neurite outgrowth as well as sprouting of cortical neurons. These mentioned effects result in helping the neuronal cell to make connections to more cells both by keeping the integrity of the existing neurites network as well as by increasing the number and length of their cell-to-cell communication organs (neurites). All these functions reflect how important HRP-3 is during the life time of a neuron. Its role starts early in the young cells by promoting its differentiation and neuritogenesis. Later, when the neuronal cell matures and shows an established neurite network, HRP-3 remains as a very important factor in keeping the integrity of this established network of connections and hence, cell survival.

## 5.4 HRP-3 expression in pathological conditions

As HRP-3 was shown to be expressed in PNS (sciatic nerve) under normal conditions, it was interesting to find a correlation between the nerve damage and a modification in the level and distribution of HRP-3 signal. When a peripheral nerve is exposed to damage, the axonal end that is closer to the brain does not die but it undergoes a *wallerian degeneration*. After some time, the axon begins to heal and grow down the intact empty insulation cover (Mark and Greenberg, 1994). Because of the intrinsic reactive capacity of peripheral axons and the permissive environment provided by Schwann cells and the extracellular matrix, adult mammalian peripheral nerves are capable of regenerating and regaining gradual functional restoration (Fawcett and Keynes, 1990). Some growth factors like FGFs were reported to be up regulated in most DRG neurons as well as Schwann cells, satellite cells and macrophages following axotomy (Grothe, et al., 2001). Neuronal cells in the ganglion attached to a damaged nerve also react to nerve injury by a chromatolytic reaction. They show swelling of cell bodies, an eccentric nucleus position and dissolution of Nissl substance in addition to massive protein synthesis necessary for the regeneration steps (Lieberman, 1971). These morphological changes were observed in the damaged-nerve model (crushed sciatic nerve) and were accompanied by a dramatic change in the expression pattern of HRP-3.

Under damage conditions, the pre-existing nuclear HRP-3 signal was almost lost and only a structured cytoplasmic signal could be detected in ganglionic neurons. These observed changes in HRP-3 expression while the nerve goes through the healing phase led to the conclusion that an extranuclear expression of HRP-3 in stressed neurons may be a part of the nerve repair mechanism. In other words redistribution of HRP-3 in the cytoplasm may be related to the tendency of the cells to regain their ability to differentiate and compensate for the damaged fibres. As a result, they loose one of their maturity characters, namely the nuclear HRP-3 signal.

In another pathological condition, but in the CNS, HRP-3 expression was studied. In this case, medulloblastoma as a CNS tumour was examined for HRP-3 expression. Medulloblastoma is one of the highly malignant primary brain tumours. This tumour originates in the cerebellum or brain stem possibly from cells of the external granular layer (Allen and Epstein, 1982). Under physiological conditions, this granular cell layer showed a very weak expression signal for HRP-3. Where the tumour developed within the cerebellar granular cell layer no increase in HRP-3 expression level was detected. In vitro experiments using a cell line derived from this tumour type supported the in vivo data, as it showed that HRP-3 over expression within these cells was not sufficient to increase cell proliferation rate compared to the control.

## 5.5 Perspectives

In the next stages it will be of great importance to detect the receptor(s) responsible for the different roles identified for HRP-3 until now. Detecting such receptor(s) will possibly help in detecting more undiscovered roles for this protein. An additional line to investigate further roles for HRP-3 would be achieved if its gene could be successfully knocked out. By knocking out HRP-3 it would be possible to know how important HRP-3 is for the development of the nervous system and the whole animal. Also investigating the ability of HRP-3 supplements to rescue or protect susceptible neurons within animal models of neurodegenerative diseases would be an important and interesting step to confirm its neurotrophic effects *in vivo*.

# 6. Summary

In this work, HRP-3 is presented as a hepatoma-derived growth factor family member that exhibits a unique expression pattern. In the first part of this work, HRP-3 expression is shown to be restricted to the nervous system from the very early stages in the embryonic life until the adulthood. Interestingly, HRP-3 is restricted to neurons and shows a developmental stage-dependent expression pattern in cortical and sensory neurons both in vivo and in primary culture models prepared from both cell types in vitro. HRP-3 is expressed in the extranuclear compartment in embryonic nervous tissue and almost restricted to the nuclear compartment in the adult mouse nervous tissue.

The second part of this work focused on the possible intracellular and extracellular roles of HRP-3. It was possible to prove that the intracellular level of HRP-3 plays an important role in promoting neurite outgrowth and neuronal cell sprouting. Reducing the intracellular level of HRP-3 in one of the primary cell culture models using synthetic siRNAs against HRP-3 resulted in negative effects on neuronal cell differentiation. This effect was reversed by over-expressing HRP-3 within an inducible neuronal cell model. The nuclear localising signal located in the carboxy terminus (NLS2) of HRP-3 is the one responsible for its nuclear localisation while the nuclear localising signal located in its amino terminus (NLS1) is the one responsible for its neurite outgrowth promoting effect. These effects of HRP-3 are mediated through its interaction with microtubules as shown in studies based partially on this work.

The results also show that extracellular HRP-3 has a positive effect on the differentiation of primary cortical neurons. It is also released by cortical neurons themselves to promote their own survival and differentiation and can protect primary cortical neurons cultured in stressful, supplement-free conditions.

Together, the results of this work point to interesting roles of HRP-3 during the development of the nervous system. This work can be the basis for further interesting studies that may include an explanation of the molecular mechanisms through which it exerts its roles like detecting the receptor through which HRP-3 signals and the signalling transduction pathways that result in these effects.

# 7. Zusammenfassung

Die vorgestellte Arbeit befasst sich mit HRP-3 einem Mitglied der Hepatoma-derived growth factor Proteinfamilie (HDGF, LEDGF und HRP1-4). Im ersten Teil wird die differentielle Regulation der HRP-3-Expression in der Maus als Modellorganismus näher beschrieben. Dabei zeigt sich, dass die HRP-3-Expression weitestgehend auf Neurone beschränkt ist. Dabei sind interessanterweise bestimmte Neuronenpopulationen – Körnerzellen des Kleinhirns und Hypothalamus – von der Expression ausgenommen. Darüber hinaus wird in der Arbeit eine interessante Veränderung in der intrazellulären Lokalisation von HRP-3 von einer extranukleären Lokalisation im embryonalen Nervensystem zu einer nahezu vollständig nukleären in der adulten Maus beschrieben. In zwei Zellkulturmodellen von primären Neuronen kann diese Veränderung der HRP-3-Lokalisation *in Vitro* nachvollzogen werden.

Der zweite Teil der Arbeit ist auf mögliche Funktionen von HRP-3 fokussiert. Da die Mitglieder der HDGF-Proteinfamilie auch sezerniert werden, wird dabei zunächst zwischen Funktionen von intrazellulärem und extrazellulärem HRP-3 unterschieden. Durch die Reduktion der HRP-3-Menge mit Hilfe von kleinen synthetischen RNAs konnte in einem der primären Neuronenmodelle eine Beteiligung von HRP-3 an der Differenzierung der Nervenzellen in Kultur nachgewiesen werden. Eine Überexpression in einem induzierbaren neuronalen Differenzierungsmodell bestätigte diese Beobachtung. In Studien, die teilweise über diese Arbeit hinausgehen, konnte gezeigt werden, dass die Interaktion von HRP-3 mit Komponenten des Zytoskeletts wichtig für diese Funktion von intrazellulärem HRP-3 ist.

Weiterhin zeigen die Ergebnisse dieser Arbeit, dass extrazelluläres HRP-3 ebenfalls einen positiven Einfluss auf die Differenzierung von Neuronen hat. Darüber hinaus hat das Protein eine starke protektive Wirkung auf diese Zellen unter Kulturbedingungen die suboptimal sind und daher eine Art neuronale Stressbedingung darstellen.

Insgesamt deuten die Ergebnisse dieser Arbeit auf eine interessante Rolle von HRP-3 während der Entwicklung des Nervensystems hin und bilden die Grundlage für weitere Studien, die die Aufklärung der genauen Mechanismen dieser Wirkungen, wie zum Beispiel mögliche HRP-3-Rezeptoren und Signal-transduktionswege, zum Ziel haben werden.

# 7. References


1 Aaronson, S. A., Rubin, J. S., Finch, P. W., Wong, J., Marchese, C., Falco, J., Taylor, W. G. and Kraus, M. H. (1990) Growth factor-regulated pathways in epithelial cell proliferation. Am Rev Respir Dis **142**, S7-10

2 Abouzied, M. M., Baader, S. L., Dietz, F., Kappler, J., Gieselmann, V. and Franken, S. (2004) Expression patterns and different subcellular localization of the growth factors HDGF (hepatoma-derived growth factor) and HRP-3 (HDGF-related protein-3) suggest functions in addition to their mitogenic activity. Biochem J **378**, 169-176

3 Abouzied, M. M., El-Tahir, H. M., Prenner, L., Haberlein, H., Gieselmann, V. and Franken, S. (2005) Hepatoma-derived growth factor. Significance of amino acid residues 81-100 in cell surface interaction and proliferative activity. J Biol Chem **280**, 10945-10954

4 Abrous, D. N., Koehl, M. and Le Moal, M. (2005) Adult neurogenesis: from precursors to network and physiology. Physiol Rev **85**, 523-569

5 Ahmed, S., Reynolds, B. A. and Weiss, S. (1995) BDNF enhances the differentiation but not the survival of CNS stem cell-derived neuronal precursors. J Neurosci **15**, 5765-5778

6 Allen, J. C. and Epstein, F. (1982) Medulloblastoma and other primary malignant neuroectodermal tumors of the CNS. The effect of patients' age and extent of disease on prognosis. J Neurosurg **57**, 446-451

7 Altman, J. (1969a) Autoradiographic and histological studies of postnatal neurogenesis. 3. Dating the time of production and onset of differentiation of cerebellar microneurons in rats. J Comp Neurol **136**, 269-293

8 Altman, J. (1969b) Autoradiographic and histological studies of postnatal neurogenesis. IV. Cell proliferation and migration in the anterior forebrain, with special reference to persisting neurogenesis in the olfactory bulb. J Comp Neurol **137**, 433-457

9 Altman, J. and Das, G. D. (1965) Autoradiographic and histological evidence of postnatal hippocampal neurogenesis in rats. J Comp Neurol **124**, 319-335

10 Altman, J. and Das, G. D. (1966) Autoradiographic and histological studies of postnatal neurogenesis. I. A longitudinal investigation of the kinetics, migration and transformation of cells incorporating tritiated thymidine in neonate rats, with special reference to postnatal neurogenesis in some brain regions. J Comp Neurol **126**, 337-389

11 Altman, J. and Das, G. D. (1965) Post-natal origin of microneurones in the rat brain. Nature **207**, 953-956

12 Amaral, D. and Lavenex, P. (2006) The Hippocampus Book "Ch 3. Hippocampal Neuroanatomy", in Andersen P, Morris R, Amaral D, Bliss T, O'Keefe J. Oxford University Press

13 Amaral, D. G. (1978) A Golgi study of cell types in the hilar region of the hippocampus in the rat. J Comp Neurol **182**, 851-914

14 Anderson P, Bliss TV, Skrede KK. (1971) Lamellar organization of hippocampal pathways. Exp Brain Res **13**(2):222-38

15 Arakawa, Y., Sendtner, M. and Thoenen, H. (1990) Survival effect of ciliary neurotrophic factor (CNTF) on chick embryonic motoneurons in culture: comparison with other neurotrophic factors and cytokines. J Neurosci **10**, 3507-3515

16 Arsenijevic, Y. and Weiss, S. (1998) Insulin-like growth factor-I is a differentiation factor for postmitotic CNS stem cell-derived neuronal precursors: distinct actions from those of brain-derived neurotrophic factor. J Neurosci **18**, 2118-2128

17 Asahina, K., Sato, H., Yamasaki, C., Kataoka, M., Shiokawa, M., Katayama, S., Tateno, C. and Yoshizato, K. (2002) Pleiotrophin/heparin-binding growth-associated molecule as a mitogen of rat hepatocytes and its role in regeneration and development of liver. Am J Pathol **160**, 2191-2205

18 Ashwell, K. W., Waite, P. M. and Marotte, L. (1996) Ontogeny of the projection tracts and commissural fibres in the forebrain of the tammar wallaby (Macropus eugenii): timing in comparison with other mammals. Brain Behav Evol **47**, 8-22

19 Attiah, D. G., Kopher, R. A. and Desai, T. A. (2003) Characterization of PC12 cell proliferation and differentiation-stimulated by ECM adhesion proteins and neurotrophic factors. J Mater Sci Mater Med **14**, 1005-1009

20 Baas, P. W. and Ahmad, F. J. (1993) The transport properties of axonal microtubules establish their polarity orientation. J Cell Biol **120**, 1427-1437

21 Barde, Y. A. (1990) The nerve growth factor family. Prog Growth Factor Res **2**, 237-248

22 Bayer, S. A. and Altman, J. (1991) Bayer SA, Altman J (1991) Neocortical development. New York: Raven Press

23 Bernard, K., Litman, E., Fitzpatrick, J. L., Shellman, Y. G., Argast, G., Polvinen, K., Everett, A. D., Fukasawa, K., Norris, D. A., Ahn, N. G. and Resing, K. A. (2003) Functional proteomic analysis of melanoma progression. Cancer Res **63**, 6716-6725

24 Bernfield, M., Kokenyesi, R., Kato, M., Hinkes, M. T., Spring, J., Gallo, R. L. and Lose, E. J. (1992) Biology of the syndecans: a family of transmembrane heparan sulfate proteoglycans. Annu Rev Cell Biol **8**, 365-393

25 Biebl, M., Cooper, C. M., Winkler, J. and Kuhn, H. G. (2000) Analysis of neurogenesis and programmed cell death reveals a self-renewing capacity in the adult rat brain. Neurosci Lett **291**, 17-20

26 Birren, S. J., Lo, L. and Anderson, D. J. (1993) Sympathetic neuroblasts undergo a developmental switch in trophic dependence. Development **119**, 597-610

27 Black, I. B. (1999) Trophic regulation of synaptic plasticity. J Neurobiol **41**, 108-118

28 Bothwell, M. (1995) Functional interactions of neurotrophins and neurotrophin receptors. Annu Rev Neurosci **18**, 223-253

29 Bottenstein, J. E. and Sato, G. H. (1979) Growth of a rat neuroblastoma cell line in serum-free supplemented medium. Proc Natl Acad Sci U S A **76**, 514-517

30 Boukhelifa, M., Parast, M. M., Valtschanoff, J. G., LaMantia, A. S., Meeker, R. B. and Otey, C. A. (2001) A role for the cytoskeleton-associated protein palladin in neurite outgrowth. Mol Biol Cell 12, 2721-2729

31 Bradke, F. and Dotti, C. G. (1999) The role of local actin instability in axon formation. Science **283**, 1931-1934

32 Bradshaw, R. A., Blundell, T. L., Lapatto, R., McDonald, N. Q. and Murray-Rust, J. (1993) Nerve growth factor revisited. Trends Biochem Sci **18**, 48-52

33 Brazel, C. Y., Romanko, M. J., Rothstein, R. P. and Levison, S. W. (2003) Roles of the mammalian subventricular zone in brain development. Prog Neurobiol **69**, 49-69

34 Brewer, G.J. (1995) Serum-free B27/neurobasal medium supports differentiated growth of neurons from the striatum, substantia nigra, septum, cerebral cortex, cerebellum, and dentate gyrus. J Neurosci Res. **42**(5):674-83

35 Brewster, W. J., Fernyhough, P., Diemel, L. T., Mohiuddin, L. and Tomlinson, D. R. (1994) Diabetic neuropathy, nerve growth factor and other neurotrophic factors. Trends Neurosci **17**, 321-325

36 Brodmann, K (1909) Vergleichende Lokalisationslehre der Grosshirnrinde in ihren Prinzipien dargestellt auf Grund des Zellenbaues, Johann Ambrosius Barth Verlag, Leipzig

37 Bronner-Fraser, M. (1988) Distribution and function of tenascin during cranial neural crest development in the chick. J Neurosci Res **21**, 135-147

38 Burgess, W. H. and Maciag, T. (1989) The heparin-binding (fibroblast) growth factor family of proteins. Annu Rev Biochem **58**, 575-606

39 Cai, D., Shen, Y., De Bellard, M., Tang, S. and Filbin, M. T. (1999) Prior exposure to neurotrophins blocks inhibition of axonal regeneration by MAG and myelin via a cAMP-dependent mechanism. Neuron **22**, 89-101

40 Calof, A. L. (1995) Intrinsic and extrinsic factors regulating vertebrate neurogenesis. Curr Opin Neurobiol **5**, 19-27

41 Cameron, H. A. and McKay, R. D. (2001) Adult neurogenesis produces a large pool of new granule cells in the dentate gyrus. J Comp Neurol **435**, 406-417

42 Cattaneo, E. and McKay, R. (1990) Proliferation and differentiation of neuronal stem cells regulated by nerve growth factor. Nature **347**, 762-765

43 Caviness, V. S., Jr. (1982) Neocortical histogenesis in normal and reeler mice: a developmental study based upon [3H]thymidine autoradiography. Brain Res **256**, 293-302

44 Caviness, V. S., Jr., Takahashi, T. and Nowakowski, R. S. (1995) Numbers, time and neocortical neuronogenesis: a general developmental and evolutionary model. Trends Neurosci **18**, 379-383

45 Chao, M. V. (2000) Trophic factors: An evolutionary cul-de-sac or door into higher neuronal function? J Neurosci Res **59**, 353-355

46 Chen, M., Zhang, L., Zhang, H. Y., Xiong, X., Wang, B., Du, Q., Lu, B., Wahlestedt, C. and Liang, Z. (2005) A universal plasmid library encoding all permutations of small interfering RNA. Proc Natl Acad Sci U S A **102**, 2356-2361

47 Cherepanov, P., Devroe, E., Silver, P. A. and Engelman, A. (2004) Identification of an evolutionarily conserved domain in human lens epithelium-derived growth factor/transcriptional co-activator p75 (LEDGF/p75) that binds HIV-1 integrase. J Biol Chem **279**, 48883-48892

48 Cherepanov, P., Maertens, G., Proost, P., Devreese, B., Van Beeumen, J., Engelborghs, Y., De Clercq, E. and Debyser, Z. (2003) HIV-1 integrase forms stable tetramers and associates with LEDGF/p75 protein in human cells. J Biol Chem **278**, 372-381

49 Chilcote, T. J., Siow, Y. L., Schaeffer, E., Greengard, P. and Thiel, G. (1994) Synapsin IIa bundles actin filaments. J Neurochem **63**, 1568-1571

50 Choi, B. H. (1988) Prenatal gliogenesis in the developing cerebrum of the mouse. Glia **1**, 308-316

51 Cilley, R. E., Zgleszewski, S. E. and Chinoy, M. R. (2000) Fetal lung development: airway pressure enhances the expression of developmental genes. J Pediatr Surg **35**, 113-118; discussion 119

52 Clegg, C. H., Linkhart, T. A., Olwin, B. B. and Hauschka, S. D. (1987) Growth factor control of skeletal muscle differentiation: commitment to

terminal differentiation occurs in G1 phase and is repressed by fibroblast growth factor. J Cell Biol **105**, 949-956

53 Cohen, J., Burne, J. F., Winter, J. and Bartlett, P. (1986) Retinal ganglion cells lose response to laminin with maturation. Nature **322**, 465-467

54 Cory, A. H., Owen, T. C., Barltrop, J. A. and Cory, J. G. (1991) Use of an aqueous soluble tetrazolium/formazan assay for cell growth assays in culture. Cancer Commun **3**, 207-212

55 D'Arcangelo, G., Miao, G. G., Chen, S. C., Soares, H. D., Morgan, J. I. and Curran, T. (1995) A protein related to extracellular matrix proteins deleted in the mouse mutant reeler. Nature **374**, 719-723

54 Daston, M. M. and Ratner, N. (1994) Amphoterin (P30, HMG-1) and RIP are early markers of oligodendrocytes in the developing rat spinal cord. J Neurocytol **23**, 323-332

55 Daston, M. M. and Ratner, N. (1991) Expression of P30, a protein with adhesive properties, in Schwann cells and neurons of the developing and regenerating peripheral nerve. J Cell Biol **112**, 1229-1239

56 Date, I., Shingo, T., Ohmoto, T. and Emerich, D. F. (1997) Long-term enhanced chromaffin cell survival and behavioral recovery in hemiparkinsonian rats with co-grafted polymer-encapsulated human NGF-secreting cells. Exp Neurol **147**, 10-17

57 DeHamer, M. K., Guevara, J. L., Hannon, K., Olwin, B. B. and Calof, A. L. (1994) Genesis of olfactory receptor neurons in vitro: regulation of progenitor cell divisions by fibroblast growth factors. Neuron **13**, 1083-1097

58 Dehmelt, L. and Halpain, S. (2004) Actin and microtubules in neurite initiation: are MAPs the missing link? J Neurobiol **58**, 18-33

59 deLapeyriere, O. and Henderson, C. E. (1997) Motoneuron differentiation, survival and synaptogenesis. Curr Opin Genet Dev **7**, 642-650

60 DiCicco-Bloom, E., Friedman, W. J. and Black, I. B. (1993) NT-3 stimulates sympathetic neuroblast proliferation by promoting precursor survival. Neuron **11**, 1101-1111

61 Dietz, F., Franken, S., Yoshida, K., Nakamura, H., Kappler, J. and Gieselmann, V. (2002) The family of hepatoma-derived growth factor proteins: characterization of a new member HRP-4 and classification of its subfamilies. Biochem J **366**, 491-500

62 Doetsch, F., Caille, I., Lim, D. A., Garcia-Verdugo, J. M. and Alvarez-Buylla, A. (1999) Subventricular zone astrocytes are neural stem cells in the adult mammalian brain. Cell **97**, 703-716

63 Doherty, P. and Walsh, F. S. (1991) The contrasting roles of N-CAM and N-cadherin as neurite outgrowth-promoting molecules. J Cell Sci Suppl **15**, 13-21

64 Dotti, C. G., Sullivan, C. A. and Banker, G. A. (1988) The establishment of polarity by hippocampal neurons in culture. J Neurosci **8**, 1454-1468

65 Dunlop, S. A., Tee, L. B., Lund, R. D. and Beazley, L. D. (1997) Development of primary visual projections occurs entirely postnatally in the fat-tailed dunnart, a marsupial mouse, Sminthopsis crassicaudata. J Comp Neurol **384**, 26-40

66 Dziadek, M. and Timpl, R. (1985) Expression of nidogen and laminin in basement membranes during mouse embryogenesis and in teratocarcinoma cells. Dev Biol **111**, 372-382

67 Echelard, Y., Epstein, D. J., St-Jacques, B., Shen, L., Mohler, J., McMahon, J. A. and McMahon, A. P. (1993) Sonic hedgehog, a member of a family of putative signaling molecules, is implicated in the regulation of CNS polarity. Cell **75,** 1417-1430

68 Edson, K., Weisshaar, B. and Matus, A. (1993) Actin depolymerisation induces process formation on MAP2-transfected non-neuronal cells. Development **117**, 689-700

69 Egan, M. F., Kojima, M., Callicott, J. H., Goldberg, T. E., Kolachana, B. S., Bertolino, A., Zaitsev, E., Gold, B., Goldman, D., Dean, M., Lu, B. and Weinberger, D. R. (2003) The BDNF val66met polymorphism affects activity-dependent secretion of BDNF and human memory and hippocampal function. Cell **112**, 257-269

70 Elbashir, S. M., Harborth, J., Lendeckel, W., Yalcin, A., Weber, K. and Tuschl, T. (2001) Duplexes of 21-nucleotide RNAs mediate RNA interference in cultured mammalian cells. Nature **411**, 494-498

71 El-Tahir, H. M., Abouzied, M. M., Gallitzendoerfer, R., Gieselmann, V. and Franken, S. (2009) Hepatoma-derived growth factor-related protein-3 interacts with microtubules and promotes neurite outgrowth in mouse cortical neurons. J Biol Chem **284**, 11637-11651

72 El-Tahir, H. M., Dietz, F., Dringen, R., Schwabe, K., Strenge, K., Kelm, S., Abouzied, M. M., Gieselmann, V. and Franken, S. (2006) Expression of hepatoma-derived growth factor family members in the adult central nervous system. BMC Neurosci **7**, 6

73 Enomoto, H., Yoshida, K., Kishima, Y., Kinoshita, T., Yamamoto, M., Everett, A. D., Miyajima, A. and Nakamura, H. (2002) Hepatoma-derived growth factor is highly expressed in developing liver and promotes fetal hepatocyte proliferation. Hepatology **36**, 1519-1527

74 Enomoto, H., Yoshida, K., Kishima, Y., Okuda, Y. and Nakamura, H. (2002) Participation of hepatoma-derived growth factor in the regulation of fetal hepatocyte proliferation. J Gastroenterol **37** Suppl 14, 158-161

75 Eriksson, P. S., Perfilieva, E., Bjork-Eriksson, T., Alborn, A. M., Nordborg, C., Peterson, D. A. and Gage, F. H. (1998) Neurogenesis in the adult human hippocampus. Nat Med **4**, 1313-1317

76 Everett, A. D. (2001) Identification, cloning, and developmental expression of hepatoma-derived growth factor in the developing rat heart. Dev Dyn **222**, 450-458

77 Everett, A. D., Lobe, D. R., Matsumura, M. E., Nakamura, H. and McNamara, C. A. (2000) Hepatoma-derived growth factor stimulates smooth muscle cell growth and is expressed in vascular development. J Clin Invest **105**, 567-575

78 Everett, A. D., Narron, J. V., Stoops, T., Nakamura, H. and Tucker, A. (2004) Hepatoma-derived growth factor is a pulmonary endothelial cell-expressed angiogenic factor. Am J Physiol Lung Cell Mol Physiol **286**, L1194-1201

79 Fawcett, J. W. and Keynes, R. J. (1990) Peripheral nerve regeneration. Annu Rev Neurosci **13**, 43-60

80 Ferreira, A., Kosik, K. S., Greengard, P. and Han, H. Q. (1994) Aberrant neurites and synaptic vesicle protein deficiency in synapsin II-depleted neurons. Science **264**, 977-979

81 Fine, E. J., Ionita, C. C. and Lohr, L. (2002) The history of the development of the cerebellar examination. Semin Neurol **22**, 375-384

82 Finlay, B. L. and Darlington, R. B. (1995) Linked regularities in the development and evolution of mammalian brains. Science **268**, 1578-1584

83 Fire, A., Xu, S., Montgomery, M., Kostas, S., Driver, S. and Mello, C. (1998) Potent and specific genetic interference by double-stranded RNA in *Caenorhabditis elegans*. Nature **391**, 806–811

84 Friedman, W. J., Ernfors, P. and Persson, H. (1991) Transient and persistent expression of NT-3/HDNF mRNA in the rat brain during postnatal development. J Neurosci **11**, 1577-1584

85 Fujioka, T., Fujioka, A. and Duman, R. S. (2004) Activation of cAMP signaling facilitates the morphological maturation of newborn neurons in adult hippocampus. J Neurosci **24**, 319-328

86 Gage, F. H., Coates, P. W., Palmer, T. D., Kuhn, H. G., Fisher, L. J., Suhonen, J. O., Peterson, D. A., Suhr, S. T. and Ray, J. (1995) Survival and differentiation of adult neuronal progenitor cells transplanted to the adult brain. Proc Natl Acad Sci U S A **92**, 11879-11883

87 Gage, F. H., Kempermann, G. and Song, H. (2007) Adult Neurogenesis eds. Cold Spring Harbor Laboratory Press, Cold Spring Harbor, NY.

88 Gao, W. Q., Dybdal, N., Shinsky, N., Murnane, A., Schmelzer, C., Siegel, M., Keller, G., Hefti, F., Phillips, H. S. and Winslow, J. W. (1995) Neurotrophin-3 reverses experimental cisplatin-induced peripheral sensory neuropathy. Ann Neurol **38**, 30-37

89 Ge, H., Si, Y. and Roeder, R. G. (1998) Isolation of cDNAs encoding novel transcription coactivators p52 and p75 reveals an alternate regulatory mechanism of transcriptional activation. Embo J **17**, 6723-6729

90 Gensburger, C., Labourdette, G. and Sensenbrenner, M. (1987) Brain basic fibroblast growth factor stimulates the proliferation of rat neuronal precursor cells in vitro. FEBS Lett **217**, 1-5

91 Giehl, K. M. (2001) Trophic dependencies of rodent corticospinal neurons. Rev Neurosci **12**, 79-94

92 Goffinet, A. M. (1984) Events governing organization of postmigratory neurons: studies on brain development in normal and reeler mice. Brain Res **319**, 261-296

93 Goode, B. L., Drubin, D. G. and Barnes, G. (2000) Functional cooperation between the microtubule and actin cytoskeletons. Curr Opin Cell Biol **12**, 63-71

94 Goodlett, C. R. and Horn, K. H. (2001) Mechanisms of alcohol-induced damage to the developing nervous system. Alcohol Res Health **25**, 175-184

95 Gospodarowicz, D., Ferrara, N., Schweigerer, L. and Neufeld, G. (1987) Structural characterization and biological functions of fibroblast growth factor. Endocr Rev **8**, 95-114

96 Gospodarowicz, D., Neufeld, G. and Schweigerer, L. (1987) Fibroblast growth factor: structural and biological properties. J Cell Physiol Suppl Suppl **5**, 15-26

97 Gotz, B., Scholze, A., Clement, A., Joester, A., Schutte, K., Wigger, F., Frank, R., Spiess, E., Ekblom, P. and Faissner, A. (1996) Tenascin-C contains distinct adhesive, anti-adhesive, and neurite outgrowth promoting sites for neurons. J Cell Biol **132**, 681-699

98 Grothe, C., Meisinger, C. and Claus, P. (2001) In vivo expression and localization of the fibroblast growth factor system in the intact and lesioned rat peripheral nerve and spinal ganglia. J Comp Neurol **434**, 342-357

99 Gueneau, G., Privat, A., Drouet, J. and Court, L. (1982) Subgranular zone of the dentate gyrus of young rabbits as a secondary matrix. A high-resolution autoradiographic study. Dev Neurosci **5**, 345-358

100 Halfter, W., Chiquet-Ehrismann, R. and Tucker, R. P. (1989) The effect of tenascin and embryonic basal lamina on the behavior and morphology of neural crest cells in vitro. Dev Biol **132**, 14-25

101 Hamilton, A. J. and Baulcombe, D. C. (1999) A species of small antisense RNA in posttranscriptional gene silencing in plants. Science **286**, 950-952

102 Hannon, G. J. (2002) RNA interference. Nature **418**, 244-251

103 Hanson, M. G., Jr., Shen, S., Wiemelt, A. P., McMorris, F. A. and Barres, B. A. (1998) Cyclic AMP Elevation Is Sufficient to Promote the Survival of Spinal Motor Neurons In Vitro. J. Neurosci. **18**, 7361-7371

104 Haque, N. S. and Isacson, O. (2000) Neurotrophic factors NGF and FGF-2 alter levels of huntingtin (IT15) in striatal neuronal cell cultures. Cell Transplant **9**, 623-627

105 He, H. T., Finne, J. and Goridis, C. (1987) Biosynthesis, membrane association, and release of N-CAM-120, a phosphatidylinositol-linked form of the neural cell adhesion molecule. J Cell Biol **105**, 2489-2500

106 Henderson, C. E., Camu, W., Mettling, C., Gouin, A., Poulsen, K., Karihaloo, M., Rullamas, J., Evans, T., McMahon, S. B., Armanini, M. P. and et al. (1993) Neurotrophins promote motor neuron survival and are present in embryonic limb bud. Nature **363**, 266-270

107 Hida, H., Jung, C. G., Wu, C. Z., Kim, H. J., Kodama, Y., Masuda, T. and Nishino, H. (2003) Pleiotrophin exhibits a trophic effect on survival of dopaminergic neurons in vitro. Eur J Neurosci **17**, 2127-2134

108 Hori, O., Brett, J., Slattery, T., Cao, R., Zhang, J., Chen, J. X., Nagashima, M., Lundh, E. R., Vijay, S., Nitecki, D. and et al. (1995) The receptor for advanced glycation end products (RAGE) is a cellular binding site for amphoterin. Mediation of neurite outgrowth and co-expression of rage and amphoterin in the developing nervous system. J Biol Chem **270**, 25752-25761

109 Horner, P. J., Power, A. E., Kempermann, G., Kuhn, H. G., Palmer, T. D., Winkler, J., Thal, L. J. and Gage, F. H. (2000) Proliferation and differentiation of progenitor cells throughout the intact adult rat spinal cord. J Neurosci **20**, 2218-2228

110 Hoshino, M., Nakamura, S., Mori, K., Kawauchi, T., Terao, M., Nishimura, Y. V., Fukuda, A., Fuse, T., Matsuo, N., Sone, M., Watanabe, M., Bito, H., Terashima, T., Wright, C. V., Kawaguchi, Y., Nakao, K. and Nabeshima, Y. (2005) Ptf1a, a bHLH transcriptional gene, defines GABAergic neuronal fates in cerebellum. Neuron **47**, 201-213

111 Hu, T. H., Huang, C. C., Liu, L. F., Lin, P. R., Liu, S. Y., Chang, H. W., Changchien, C. S., Lee, C. M., Chuang, J. H. and Tai, M. H. (2003) Expression of hepatoma-derived growth factor in hepatocellular carcinoma. Cancer **98**, 1444-1456

112 Huang, J. S., Chao, C. C., Su, T. L., Yeh, S. H., Chen, D. S., Chen, C. T., Chen, P. J. and Jou, Y. S. (2004) Diverse cellular transformation capability of overexpressed genes in human hepatocellular carcinoma. Biochem Biophys Res Commun **315**, 950-958

113 Hughes, A. (1953) The growth of embryonic neurites; a study of cultures of chick neural tissues. J Anat **87**, 150-162

114 Hunter, C., Harrison, F. R., Hutton, D. R., Troup, G. J. and Wilson, G. L. (1989) Free radicals in stouts and ales. Med J Aust **151**, 417-418

115 Hunter, C. N., van Grondelle, R. and Olsen, J. D. (1989) Photosynthetic antenna proteins: 100 ps before photochemistry starts. Trends Biochem Sci **14**, 72-76

116 Hunter, C. P. (1999) Genetics: a touch of elegance with RNAi. Curr Biol **9**, R440-442

117 Husmann, K., Faissner, A. and Schachner, M. (1992) Tenascin promotes cerebellar granule cell migration and neurite outgrowth by different domains in the fibronectin type III repeats. J Cell Biol **116**, 1475-1486

118 Ikegame, K., Yamamoto, M., Kishima, Y., Enomoto, H., Yoshida, K., Suemura, M., Kishimoto, T. and Nakamura, H. (1999) A new member of a hepatoma-derived growth factor gene family can translocate to the nucleus. Biochem Biophys Res Commun **266**, 81-87

119 Inomata, Y., Hirata, A., Koga, T., Kimura, A., Singh, D. P., Shinohara, T. and Tanihara, H. (2003) Lens epithelium-derived growth factor: neuroprotection on rat retinal damage induced by N-methyl-D-aspartate. Brain Res **991**, 163-170

120 Izumoto, Y., Kuroda, T., Harada, H., Kishimoto, T. and Nakamura, H. (1997) Hepatoma-derived growth factor belongs to a gene family in mice showing significant homology in the amino terminus. Biochem Biophys Res Commun **238**, 26-32

121 Jalkanen, M., Elenius, K. and Rapraeger, A. S. (1993) Syndecan: Regulator of cell morphology and growth factor action at the cell-matrix interface. Trends Glycosci Glycotechnol **5**, 107-120

122 Jana, S., Chakraborty, C. and Nandi, S. (2004) Mechanisms and roles of the RNA-based gene silencing. Electronic Journal of Biotechnology 7(3), 15

123 Jankowsky, J. L. and Patterson, P. H. (1999) Cytokine and growth factor involvement in long-term potentiation. Mol Cell Neurosci **14**, 273-286

124 Jessell and Sanes. (2000) Principles of Neuroscience. E. Kandel, editor

125 Joester, A. and Faissner, A. (2001) The structure and function of tenascins in the nervous system. Matrix Biol **20**, 13-22

126 Johansson, C. B., Momma, S., Clarke, D. L., Risling, M., Lendahl, U. and Frisen, J. (1999) Identification of a neural stem cell in the adult mammalian central nervous system. Cell **96**, 25-34

127 Jordan, M. A. and Wilson, L. (1998) Use of drugs to study role of microtubule assembly dynamics in living cells. Methods Enzymol **298**, 252-276

128 Kabir, N., Schaefer, A. W., Nakhost, A., Sossin, W. S. and Forscher, P. (2001) Protein kinase C activation promotes microtubule advance in neuronal growth cones by increasing average microtubule growth lifetimes. J Cell Biol **152**, 1033-1044

129 Kandel, E. R., Schwartz, J. H. and Jessell, T. M. (2000) Principles of Neural Science. McGraw-Hill, New York

130 Kaplan, M. S. and Hinds, J. W. (1977) Neurogenesis in the adult rat: electron microscopic analysis of light radioautographs. Science **197**, 1092-1094

131 Kasschau, K. D., Xie, Z., Allen, E., Llave, C., Chapman, E. J., Krizan, K. A. and Carrington, J. C. (2003) P1/HC-Pro, a viral suppressor of RNA silencing, interferes with Arabidopsis development and miRNA unction. Dev Cell **4**, 205-217

132 Kaverina, I., Rottner, K. and Small, J. V. (1998) Targeting, capture, and stabilization of microtubules at early focal adhesions. J Cell Biol **142**, 181-190

133 Kempermann, G., Kuhn, H. G. and Gage, F. H. (1997) Genetic influence on neurogenesis in the dentate gyrus of adult mice. Proc Natl Acad Sci U S A **94**, 10409-10414

134 Kilpatrick, T. J. and Bartlett, P. F. (1995) Cloned multipotential precursors from the mouse cerebrum require FGF-2, whereas glial restricted precursors are stimulated with either FGF-2 or EGF. J Neurosci **15**, 3653-3661

135 Kinnunen, T., Raulo, E., Nolo, R., Maccarana, M., Lindahl, U. and Rauvala, H. (1996) Neurite outgrowth in brain neurons induced by heparin-binding growth-associated molecule (HB-GAM) depends on the specific interaction of HB-GAM with heparan sulfate at the cell surface. J Biol Chem **271**, 2243-2248

136 Kishima, Y., Yoshida, K., Enomoto, H., Yamamoto, M., Kuroda, T., Okuda, Y., Uyama, H. and Nakamura, H. (2002) Antisense oligonucleotides of hepatoma-derived growth factor (HDGF) suppress the proliferation of hepatoma cells. Hepatogastroenterology **49**, 1639-1644

137 Klar, A., Baldassare, M. and Jessell, T. M. (1992) F-spondin: a gene expressed at high levels in the floor plate encodes a secreted protein that promotes neural cell adhesion and neurite extension. Cell **69**, 95-110

138 Knowles, R., LeClerc, N. and Kosik, K. S. (1994) Organization of actin and microtubules during process formation in tau-expressing Sf9 cells. Cell Motil Cytoskeleton **28**, 256-264

139 Koliatsos, V. E., Clatterbuck, R. E., Winslow, J. W., Cayouette, M. H. and Price, D. L. (1993) Evidence that brain-derived neurotrophic factor is a trophic factor for motor neurons in vivo. Neuron **10**, 359-367

140 König, N., Valet, J. and Fulcrand, J. M., R. (1977) The time of origin of cajal-retzius cells in the rat temporal cortex, an autoradiographic study. Neurosci. Lett. **4**, 21-26

141 Kornack, D. R. and Rakic, P. (1999) Continuation of neurogenesis in the hippocampus of the adult macaque monkey. Proc Natl Acad Sci U S A **96**, 5768-5773

142 Korsching, S. (1993) The neurotrophic factor concept: a reexamination. J Neurosci **13**, 2739-2748

143 Kubo, E., Singh, D. P., Fatma, N., Shinohara, T., Zelenka, P., Reddy, V. N. and Chylack, L. T. (2003) Cellular distribution of lens epithelium-derived growth factor (LEDGF) in the rat eye: loss of LEDGF from nuclei of differentiating cells. Histochem Cell Biol **119**, 289-299

144 Kuhn, H. G., Dickinson-Anson, H. and Gage, F. H. (1996) Neurogenesis in the dentate gyrus of the adult rat: age-related decrease of neuronal progenitor proliferation. J Neurosci **16**, 2027-2033

145 Kumar, Abbas, Fausto, *Robbins* and *Cotra.* (2004) Pathologic Basis of Disease. Elsevier

146 Kuo, M. D., Oda, Y., Huang, J. S. and Huang, S. S. (1990) Amino acid sequence and characterization of a heparin-binding neurite-promoting factor (p18) from bovine brain. J Biol Chem **265**, 18749-18752

147 Kuroda, T., Tanaka, H., Nakamura, H., Nishimune, Y. and Kishimoto, T. (1999) Hepatoma-derived growth factor-related protein (HRP)-1 gene in spermatogenesis in mice. Biochem Biophys Res Commun **262**, 433-437

148 Laaroubi, K., Delbe, J., Vacherot, F., Desgranges, P., Tardieu, M., Jaye, M., Barritault, D. and Courty, J. (1994) Mitogenic and in vitro angiogenic activity of human recombinant heparin affin regulatory peptide. Growth Factors **10**, 89-98

149 Lander, A. D. (1993) Proteoglycans in the nervous system. Curr Opin Neurobiol **3**, 716-723

150 Lathia, J. D., Patton, B., Eckley, D. M., Magnus, T., Mughal, M. R., Sasaki, T., Caldwell, M. A., Rao, M. S., Mattson, M. P. and ffrench-Constant, C. (2007) Patterns of laminins and integrins in the embryonic ventricular zone of the CNS. J Comp Neurol **505**, 630-643

151 Letourneau, P. C., Condic, M. L. and Snow, D. M. (1994) Interactions of developing neurons with the extracellular matrix. J Neurosci **14**, 915-928

152 Li, F., Shetty, A. K. and Sugahara, K. (2007) Neuritogenic activity of chondroitin/dermatan sulfate hybrid chains of embryonic pig brain and their mimicry from shark liver. Involvement of the pleiotrophin and hepatocyte growth factor signaling pathways. J Biol Chem **282**, 2956-2966

153 Li, Y. S., Milner, P. G., Chauhan, A. K., Watson, M. A., Hoffman, R. M., Kodner, C. M., Milbrandt, J. and Deuel, T. F. (1990) Cloning and expression of a developmentally regulated protein that induces mitogenic and neurite outgrowth activity. Science **250**, 1690-1694

154 Liao, G., Nagasaki, T. and Gundersen, G. G. (1995) Low concentrations of nocodazole interfere with fibroblast locomotion without significantly affecting microtubule level: implications for the role of dynamic microtubules in cell locomotion. J Cell Sci **108** (Pt 11), 3473-3483

155 Lieberman, A. R. (1971) The axon reaction: a review of the principal features of perikaryal responses to axon injury. Int Rev Neurobiol **14**, 49-124

156 Lillien, L. and Cepko, C. (1992) Control of proliferation in the retina: temporal changes in responsiveness to FGF and TGF alpha. Development **115**, 253-266

157 Lindahl, U., Lidholt, K., Spillmann, D. and Kjellen, L. (1994) More to "heparin" than anticoagulation. Thromb Res **75**, 1-32

158 Llano, M., Vanegas, M., Fregoso, O., Saenz, D., Chung, S., Peretz, M. and Poeschla, E. M. (2004) LEDGF/p75 determines cellular trafficking of diverse lentiviral but not murine oncoretroviral integrase proteins and is a component of functional lentiviral preintegration complexes. J Virol **78**, 9524-9537

159 Llave, C., Xie, Z., Kasschau, K. D. and Carrington, J. C. (2002) Cleavage of Scarecrow-like mRNA targets directed by a class of Arabidopsis miRNA. Science **297**, 2053-2056

160 Lochter, A., Vaughan, L., Kaplony, A., Prochiantz, A., Schachner, M. and Faissner, A. (1991) J1/tenascin in substrate-bound and soluble form displays contrary effects on neurite outgrowth. J Cell Biol **113**, 1159-1171

161 Logan, A. (1990) Intracrine regulation at the nucleus--a further mechanism of growth factor activity? J Endocrinol **125**, 339-343

162 Lois, C. and Alvarez-Buylla, A. (1993) Proliferating subventricular zone cells in the adult mammalian forebrain can differentiate into neurons and glia. Proc Natl Acad Sci U S A **90**, 2074-2077

163 Longo, F. M., Holtzman, D. M., Grimes, M. L. and Mobley, W. C. (1993) Nerve growth factor: actions in the peripheral and central nervous systems. In: Neurotrophic Factors. Fallon J, Loughlin S, eds, New York, Academic Press

164 Lu, B. and Chow, A. (1999) Neurotrophins and hippocampal synaptic transmission and plasticity. J Neurosci Res **58**, 76-87

165 Lu, B. and Figurov, A. (1997) Role of neurotrophins in synapse development and plasticity. Rev Neurosci **8**, 1-12

166 Luskin, M. B. and Shatz, C. J. (1985) Neurogenesis of the cat's primary visual cortex. J Comp Neurol **242**, 611-631

167 Luzzati, F., De Marchis, S., Fasolo, A. and Peretto, P. (2006) Neurogenesis in the caudate nucleus of the adult rabbit. J Neurosci **26**, 609-621

168 Mackie, E. J., Tucker, R. P., Halfter, W., Chiquet-Ehrismann, R. and Epperlein, H. H. (1988) The distribution of tenascin coincides with pathways of neural crest cell migration. Development **102**, 237-250

169 Maertens, G., Cherepanov, P., Pluymers, W., Busschots, K., De Clercq, E., Debyser, Z. and Engelborghs, Y. (2003) LEDGF/p75 is essential for nuclear and chromosomal targeting of HIV-1 integrase in human cells. J Biol Chem **278**, 33528-33539

170 Maisonpierre, P. C., Belluscio, L., Friedman, B., Alderson, R. F., Wiegand, S. J., Furth, M. E., Lindsay, R. M. and Yancopoulos, G. D. (1990) NT-3, BDNF, and NGF in the developing rat nervous system: parallel as well as reciprocal patterns of expression. Neuron **5**, 501-509

171 Marchionni, M. A., Goodearl, A. D., Chen, M. S., Bermingham-McDonogh, O., Kirk, C., Hendricks, M., Danehy, F., Misumi, D., Sudhalter, J., Kobayashi, K. and et al. (1993) Glial growth factors are alternatively spliced erbB2 ligands expressed in the nervous system. Nature **362**, 312-318

172 Marin-Padilla, M. (1998) Cajal-Retzius cells and the development of the neocortex. Trends Neurosci **21**, 64-71

173 Marin-Padilla, M. (1971) Early prenatal ontogenesis of the cerebral cortex (neocortex) of the cat (Felis domestica). A Golgi study. I. The primordial neocortical organization. Z Anat Entwicklungsgesch **134**, 117-145

174 Mark, S. and Greenberg, M. D. (1994) " Injury Classification System "; in Handbook of Neurosurgery

175 Marubuchi, S., Okuda, T., Tagawa, K., Enokido, Y., Horiuchi, D., Shimokawa, R., Tamura, T., Qi, M. L., Eishi, Y., Watabe, K., Shibata, M., Nakagawa, M. and Okazawa, H. (2006) Hepatoma-derived growth factor, a new trophic factor for motor neurons, is up-regulated in the spinal cord of PQBP-1 transgenic mice before onset of degeneration. J Neurochem **99**, 70-83

176 Matsui, H., Lin, L. R., Singh, D. P., Shinohara, T. and Reddy, V. N. (2001) Lens epithelium-derived growth factor: increased survival and decreased DNA breakage of human RPE cells induced by oxidative stress. Invest Ophthalmol Vis Sci **42**, 2935-2941

177 McKay, I. and Leigh, I. (1993) Growth factors, a practical approach. Oxford university press

178 Meister, G. and Tuschl, T. (2004) Mechanisms of gene silencing by double-stranded RNA. Nature **431**, 343-349

179 Merenmies, J., Pihlaskari, R., Laitinen, J., Wartiovaara, J. and Rauvala, H. (1991) 30-kDa heparin-binding protein of brain (amphoterin) involved in neurite outgrowth. Amino acid sequence and localization in the filopodia of the advancing plasma membrane. J Biol Chem **266**, 16722-16729

180 Meyer, G. and Goffinet, A. M. (1998) Prenatal development of reelin-immunoreactive neurons in the human neocortex. J Comp Neurol **397**, 29-40

181 Meyer, R. B., Jr. and Miller, J. P. (1974) Analogs of cyclic AMP and cyclic GMP: general methods of synthesis and the relationship of structure to enzymic activity. Life Sci **14**, 1019-1040

182 Meyer-Franke, A., Wilkinson, G. A., Kruttgen, A., Hu, M., Munro, E., Hanson, M. G., Jr., Reichardt, L. F. and Barres, B. A. (1998) Depolarization and cAMP elevation rapidly recruit TrkB to the plasma membrane of CNS neurons. Neuron **21**, 681-693

183 Mitchell, B. D., Emsley, J. G., Magavi, S. S., Arlotta, P. and Macklis, J. D. (2004) Constitutive and induced neurogenesis in the adult mammalian brain: manipulation of endogenous precursors toward CNS repair. Dev Neurosci **26**, 101-117

184 Mitsiadis, T. A., Muramatsu, T., Muramatsu, H. and Thesleff, I. (1995) Midkine (MK), a heparin-binding growth/differentiation factor, is regulated by retinoic acid and epithelial-mesenchymal interactions in the developing mouse tooth, and affects cell proliferation and morphogenesis. J Cell Biol **129**, 267-281

185 Mitsumoto, H., Ikeda, K., Klinkosz, B., Cedarbaum, J. M., Wong, V. and Lindsay, R. M. (1994) Arrest of motor neuron disease in wobbler mice cotreated with CNTF and BDNF. Science **265**, 1107-1110

186 Muller, F. and O'Rahilly, R. (1990) The human brain at stages 21-23, with particular reference to the cerebral cortical plate and to the development of the cerebellum. Anat Embryol (Berl) **182**, 375-400

187 Murphy, M., Drago, J. and Bartlett, P. F. (1990) Fibroblast growth factor stimulates the proliferation and differentiation of neural precursor cells in vitro. J Neurosci Res **25**, 463-475

188 Nakai, J. (1956) Dissociated dorsal root ganglia in tissue culture. Am J Anat **99**, 81-129

189 Nakamura, H., Izumoto, Y., Kambe, H., Kuroda, T., Mori, T., Kawamura, K., Yamamoto, H. and Kishimoto, T. (1994) Molecular cloning of complementary DNA for a novel human hepatoma-derived growth factor. Its homology with high mobility group-1 protein. J Biol Chem **269**, 25143-25149

190 Nakamura, H., Kambe, H., Egawa, T., Kimura, Y., Ito, H., Hayashi, E., Yamamoto, H., Sato, J. and Kishimoto, S. (1989) Partial purification and characterization of human hepatoma-derived growth factor. Clin Chim Acta **183**, 273-284

191 Nakamura, M., Singh, D. P., Kubo, E., Chylack, L. T., Jr. and Shinohara, T. (2000) LEDGF: survival of embryonic chick retinal photoreceptor cells. Invest Ophthalmol Vis Sci **41**, 1168-1175

192 Neumann, S., Bradke, F., Tessier-Lavigne, M. and Basbaum, A. I. (2002) Regeneration of sensory axons within the injured spinal cord induced by intraganglionic cAMP elevation. Neuron **34**, 885-893

193 Noctor, S. C., Flint, A. C., Weissman, T. A., Dammerman, R. S. and Kriegstein, A. R. (2001) Neurons derived from radial glial cells establish radial units in neocortex. Nature **409**, 714-720

194 Nolte, J. (2002) The Human Brain, An Introduction to Its Functional Anatomy. Mosby, Inc. St. Louis, Missouri

195 Okuda, Y., Nakamura, H., Yoshida, K., Enomoto, H., Uyama, H., Hirotani, T., Funamoto, M., Ito, H., Everett, A. D., Hada, T. and Kawase, I. (2003) Hepatoma-derived growth factor induces tumorigenesis in vivo through both direct angiogenic activity and induction of vascular endothelial growth factor. Cancer Sci **94**, 1034-1041

196 Oliver, J. A. and Al-Awqati, Q. (1998) An endothelial growth factor involved in rat renal development. J Clin Invest **102**, 1208-1219

197 O'Neill, P. (2001) First rat HIV model. Trends in Molecular Medicine **7**, 434

198 Oppenheim, R. W. (1996) Neurotrophic survival molecules for motoneurons: an embarrassment of riches. Neuron **17**, 195-197

199 Oppenheim, R. W., Prevette, D., Yin, Q. W., Collins, F. and MacDonald, J. (1991) Control of embryonic motoneuron survival in vivo by ciliary neurotrophic factor. Science **251**, 1616-1618

200 Oppenheim, R. W., Yin, Q. W., Prevette, D. and Yan, Q. (1992) Brain-derived neurotrophic factor rescues developing avian motoneurons from cell death. Nature **360**, 755-757

201 Palmer, T. D., Takahashi, J. and Gage, F. H. (1997) The adult rat hippocampus contains primordial neural stem cells. Mol Cell Neurosci **8**, 389-404

202 Parast, M. M. and Otey, C. A. (2000) Characterization of palladin, a novel protein localized to stress fibers and cell adhesions. J Cell Biol **150**, 643-656

203 Parkkinen, J., Raulo, E., Merenmies, J., Nolo, R., Kajander, E. O., Baumann, M. and Rauvala, H. (1993) Amphoterin, the 30-kDa protein in a family of HMG1-type polypeptides. Enhanced expression in transformed cells, leading edge localization, and interactions with plasminogen activation. J Biol Chem **268**, 19726-19738

204 Plasterk, R. H. (2002) RNA silencing: the genome's immune system. Science **296**, 1263-1265

205 Poo, M. M. (2001) Neurotrophins as synaptic modulators. Nat Rev Neurosci **2**, 24-32

206 Rakic, P. (1978) Neuronal migration and contact guidance in the primate telencephalon. Postgrad Med J **54** Suppl 1, 25-40

207 Rakic, P. (1988) Specification of cerebral cortical areas. Science 241, 170-176

208 Raulo, E., Chernousov, M. A., Carey, D. J., Nolo, R. and Rauvala, H. (1994) Isolation of a neuronal cell surface receptor of heparin binding growth-associated molecule (HB-GAM). Identification as N-syndecan (syndecan-3). J Biol Chem **269**, 12999-13004

209 Raulo, E., Julkunen, I., Merenmies, J., Pihlaskari, R. and Rauvala, H. (1992) Secretion and biological activities of heparin-binding growth-associated molecule. Neurite outgrowth-promoting and mitogenic actions of the recombinant and tissue-derived protein. J Biol Chem **267**, 11408-11416

210 Raulo, E., Tumova, S., Pavlov, I., Pekkanen, M., Hienola, A., Klankki, E., Kalkkinen, N., Taira, T., Kilpelainen, I. and Rauvala, H. (2005) The two thrombospondin type I repeat domains of the heparin-binding growth-associated molecule bind to heparin/heparan sulfate and regulate neurite extension and plasticity in hippocampal neurons. J Biol Chem **280**, 41576-41583

211 Rauvala, H. (1989) An 18-kd heparin-binding protein of developing brain that is distinct from fibroblast growth factors. Embo J **8**, 2933-2941

212 Rauvala, H. (1984) Neurite outgrowth of neuroblastoma cells: dependence on adhesion surface--cell surface interactions. J Cell Biol **98**, 1010-1016

213 Rauvala, H., Merenmies, J., Pihlaskari, R., Korkolainen, M., Huhtala, M. L. and Panula, P. (1988) The adhesive and neurite-promoting molecule p30: analysis of the amino-terminal sequence and production of antipeptide antibodies that detect p30 at the surface of neuroblastoma cells and of brain neurons. J Cell Biol **107**, 2293-2305

214 Rauvala, H. and Pihlaskari, R. (1987) Isolation and some characteristics of an adhesive factor of brain that enhances neurite outgrowth in central neurons. J Biol Chem **262**, 16625-16635

215 Rauvala, H., Vanhala, A., Castren, E., Nolo, R., Raulo, E., Merenmies, J. and Panula, P. (1994) Expression of HB-GAM (heparin-binding growth-associated molecules) in the pathways of developing axonal processes in vivo and neurite outgrowth in vitro induced by HB-GAM. Brain Res Dev Brain Res **79**, 157-176

216 Ray, J., Peterson, D. A., Schinstine, M. and Gage, F. H. (1993) Proliferation, differentiation, and long-term culture of primary hippocampal neurons. Proc Natl Acad Sci U S A **90**, 3602-3606

217 Reichardt, L. F. and Tomaselli, K. J. (1991) Extracellular matrix molecules and their receptors: functions in neural development. Annu Rev Neurosci **14**, 531-570

218 Reist, N. E., Magill, C. and McMahan, U. J. (1987) Agrin-like molecules at synaptic sites in normal, denervated, and damaged skeletal muscles. J Cell Biol **105**, 2457-2469

219 Reuss, B. and von Bohlen und Halbach, O. (2003) Fibroblast growth factors and their receptors in the central nervous system. Cell Tissue Res **313**, 139-157

220 Reynolds, B. A. and Weiss, S. (1992) Generation of neurons and astrocytes from isolated cells of the adult mammalian central nervous system. Science **255**, 1707-1710

221 Rice, D. S. and Curran, T. (2001) Role of the reelin signaling pathway in central nervous system development. Annu Rev Neurosci **24**, 1005-1039

222 Richards, L. J., Kilpatrick, T. J. and Bartlett, P. F. (1992) De novo generation of neuronal cells from the adult mouse brain. Proc Natl Acad Sci U S A **89**, 8591-8595

223 Rickmann, M., Chronwall, B. M. and Wolff, J. R. (1977) On the development of non-pyramidal neurons and axons outside the cortical plate: the early marginal zone as a pallial anlage. Anat Embryol (Berl) **151**, 285-307

224 Robinson, S. R. and Dreher, B. (1990) The visual pathways of eutherian mammals and marsupials develop according to a common timetable. Brain Behav Evol **36**, 177-195

225 Rochlin, M. W., Wickline, K. M. and Bridgman, P. C. (1996) Microtubule stability decreases axon elongation but not axoplasm production. J Neurosci **16**, 3236-3246

226 Ross, A., Sobue, G., Hotta, H. and Reddy, U. (1991) current topics in microbiology and immunology. Springer verlag. New york

227 Ruoslahti, E. and Yamaguchi, Y. (1991) Proteoglycans as modulators of growth factor activities. Cell **64**, 867-869

*228* Sambrook, J., Fritsch, E. F. and Maniatis, T. (1989) Molecular Cloning: A Laboratory Manual, 2nd ed. Cold Spring Harbor Laboratory, *Cold Spring Harbor*

229 Schubert, D., Heinemann, S., Carlisle, W., Tarikas, H., Kimes, B., Patrick, J., Steinbach, J. H., Culp, W. and Brandt, B. L. (1974) Clonal cell lines from the rat central nervous system. Nature **249**, 224-227

230 Sellick, G. S., Barker, K. T., Stolte-Dijkstra, I., Fleischmann, C., Coleman, R. J., Garrett, C., Gloyn, A. L., Edghill, E. L., Hattersley, A. T., Wellauer, P. K., Goodwin, G. and Houlston, R. S. (2004) Mutations in PTF1A cause pancreatic and cerebellar agenesis. Nat Genet **36**, 1301-1305

231 Sendtner, M., Carroll, P., Holtmann, B., Hughes, R. A. and Thoenen, H. (1994) Ciliary neurotrophic factor. J Neurobiol **25**, 1436-1453

232 Sendtner, M., Holtmann, B., Kolbeck, R., Thoenen, H. and Barde, Y. A. (1992b) Brain-derived neurotrophic factor prevents the death of motoneurons in newborn rats after nerve section. Nature **360**, 757-759

233 Sendtner, M., Kreutzberg, G. W. and Thoenen, H. (1990) Ciliary neurotrophic factor prevents the degeneration of motor neurons after axotomy. Nature **345**, 440-441

234 Sendtner, M., Schmalbruch, H., Stockli, K. A., Carroll, P., Kreutzberg, G. W. and Thoenen, H. (1992a) Ciliary neurotrophic factor prevents degeneration of motor neurons in mouse mutant progressive motor neuronopathy. Nature **358**, 502-504

235 Shah, N. M., Marchionni, M. A., Isaacs, I., Stroobant, P. and Anderson, D. J. (1994) Glial growth factor restricts mammalian neural crest stem cells to a glial fate. Cell **77**, 349-360

236 Sheppard, A. M., and A. L. Pearlman. (1997) Abnormal organization of preplate neurons and their associated extracellular matrix: an early manifestation of altered neocortical development in the reeler mutant mouse. J. Comp. Neurol **378**, 173-179

237 Shim, C., Kwon, H. B. and Kim, K. (1996) Differential expression of laminin chain-specific mRNA transcripts during mouse preimplantation embryo development. Mol Reprod Dev **44**, 44-55

238 Siegel, G. J. and Chauhan, N. B. (2000) Neurotrophic factors in Alzheimer's and Parkinson's disease brain. Brain Res Brain Res Rev **33**, 199-227

239 Singh, D. P., Ohguro, N., Chylack, L. T., Jr. and Shinohara, T. (1999) Lens epithelium-derived growth factor: increased resistance to thermal and oxidative stresses. Invest Ophthalmol Vis Sci **40**, 1444-1451

240 Singh, D. P., Ohguro, N., Kikuchi, T., Sueno, T., Reddy, V. N., Yuge, K., Chylack, L. T., Jr. and Shinohara, T. (2000) Lens epithelium-derived growth factor: effects on growth and survival of lens epithelial cells, keratinocytes, and fibroblasts. Biochem Biophys Res Commun **267**, 373-381

241 Smyth, N., Vatansever, H. S., Murray, P., Meyer, M., Frie, C., Paulsson, M. and Edgar, D. (1999) Absence of basement membranes after targeting the LAMC1 gene results in embryonic lethality due to failure of endoderm differentiation. J Cell Biol **144**, 151-160

242 Sonderegger, P. and Rathjen, F. G. (1992) Regulation of axonal growth in the vertebrate nervous system by interactions between glycoproteins belonging to two subgroups of the immunoglobulin superfamily. J Cell Biol **119**, 1387-1394

243 Song, H. J., Ming, G. L. and Poo, M. M. (1997) cAMP-induced switching in turning direction of nerve growth cones. Nature **388**, 275-279

244 Sporn, M. B. and Todaro, G. J. (1980) Autocrine secretion and malignant transformation of cells. N Engl J Med **303**, 878-880

245 Stern, C. D., Norris, W. E., Bronner-Fraser, M., Carlson, G. J., Faissner, A., Keynes, R. J. and Schachner, M. (1989) J1/tenascin-related molecules are not responsible for the segmented pattern of neural crest cells or motor axons in the chick embryo. Development **107**, 309-319

246 Super, H., Soriano, E. and Uylings, H. B. (1998) The functions of the preplate in development and evolution of the neocortex and hippocampus. Brain Res Brain Res Rev **27**, 40-64

247 Tan, S. S., Crossin, K. L., Hoffman, S. and Edelman, G. M. (1987) Asymmetric expression in somites of cytotactin and its proteoglycan ligand is correlated with neural crest cell distribution. Proc Natl Acad Sci U S A **84**, 7977-7981

248 Tanaka, E., Ho, T. and Kirschner, M. W. (1995) The role of microtubule dynamics in growth cone motility and axonal growth. J Cell Biol **128**, 139-155

249 Thoenen, H. (2000) Neurotrophins and activity-dependent plasticity. Prog Brain Res **128**, 183-191

250 Thoenen, H. (1995) Neurotrophins and neuronal plasticity. Science **270**, 593-598

251 Thorsteinsdottir, S. (1992) Basement membrane and fibronectin matrix are distinct entities in the developing mouse blastocyst. Anat Rec **232**, 141-149

252 Timmusk, T., Belluardo, N., Metsis, M. and Persson, H. (1993) Widespread and developmentally regulated expression of neurotrophin-4 mRNA in rat brain and peripheral tissues. Eur J Neurosci **5**, 605-613

253 Timpl, R. and Brown, J. C. (1996) Supramolecular assembly of basement membranes. Bioessays **18**, 123-132

254 Uylings HBM, Van Eden CG, Parnavelas JG and Kalsbeek, A. (1990) The prenatal and postnatal development of rat cerebral cortex. In: The cerebral cortex of the rat. Kolb E, Tees RC, eds, Cambridge, MA: MIT Press. pp. 35-76

255 van Praag, H., Schinder, A. F., Christie, B. R., Toni, N., Palmer, T. D. and Gage, F. H. (2002) Functional neurogenesis in the adult hippocampus. Nature **415**, 1030-1034

256 Vescovi, A. L., Reynolds, B. A., Fraser, D. D. and Weiss, S. (1993) bFGF regulates the proliferative fate of unipotent (neuronal) and bipotent (neuronal/astroglial) EGF-generated CNS progenitor cells. Neuron **11**, 951-966

257 Voinnet, O. (2002) RNA silencing: small RNAs as ubiquitous regulators of gene expression. Curr Opin Plant Biol **5**, 444-451

258 Waterman-Storer, C. M. and Salmon, E. (1999) Positive feedback interactions between microtubule and actin dynamics during cell motility. Curr Opin Cell Biol **11**, 61-67

259 Wehrle, B. and Chiquet, M. (1990) Tenascin is accumulated along developing peripheral nerves and allows neurite outgrowth in vitro. Development **110**, 401-415

260 Wu, T. C., Wan, Y. J., Chung, A. E. and Damjanov, I. (1983) Immunohistochemical localization of entactin and laminin in mouse embryos and fetuses. Dev Biol **100**, 496-505

261 Wyss, J. M. and Sripanidkulchai, B. (1985) The development of Ammon's horn and the fascia dentata in the cat: a [3H]thymidine analysis. Brain Res **350**, 185-198

262 Yah, Q., Matheson, C., Lopez, O.T. and Miller, J.A. (1994) The biological responses of axotomized adult motoneurons to brain-derived neurotrophic factor, J. Neurosci. **14**, 5281-5291

263 Yamada, K., Mizuno, M. and Nabeshima, T. (2002) Role for brain-derived neurotrophic factor in learning and memory. Life Sci **70**, 735-744

264 Yan, Q., Elliott, J. and Snider, W. D. (1992) Brain-derived neurotrophic factor rescues spinal motor neurons from axotomy-induced cell death. Nature **360**, 753-755

265 Yanagishita, M. and Hascall, V. C. (1992) Cell surface heparan sulfate proteoglycans. J Biol Chem **267**, 9451-9454

266 Yang, D., Bierman, J., Tarumi, Y. S., Zhong, Y. P., Rangwala, R., Proctor, T. M., Miyagoe-Suzuki, Y., Takeda, S., Miner, J. H., Sherman, L. S., Gold, B. G. and Patton, B. L. (2005) Coordinate control of axon defasciculation and myelination by laminin-2 and -8. J Cell Biol **168**, 655-666

267 Yang, X. W., Zhong, R. and Heintz, N. (1996) Granule cell specification in the developing mouse brain as defined by expression of the zinc finger transcription factor RU49. Development **122**, 555-566

268 Yu, W. M., Chen, Z. L., North, A. J. and Strickland, S. (2009) Laminin is required for Schwann cell morphogenesis. J Cell Sci **122**, 929-936

269 Yu, W. M., Feltri, M. L., Wrabetz, L., Strickland, S. and Chen, Z. L. (2005) Schwann cell-specific ablation of laminin gamma1 causes apoptosis and prevents proliferation. J Neurosci **25**, 4463-4472

270 Yuen, E. C., Howe, C. L., Li, Y., Holtzman, D. M. and Mobley, W. C. (1996) Nerve growth factor and the neurotrophic factor hypothesis. Brain Dev **18**, 362-368

271 Yuen, E. C., Li, Y., Mischel, R. E., Howe, C. L., Holtzman. and Mobley, W. C. (1996) Neurotrophins and the Neurotrophic Factor Hypothesis. Neural Notes **1**(4), 3-7

272 Yuen, E. C. and Mobley, W. C. (1995) Therapeutic applications of neurotrophic factors in disorders of motor neurons and peripheral nerves. Mol Med Today **1**, 278-286

273 Yurchenco, P. D. (1994) Assembly of laminin and type IV collagen into basement membrane networks. Extracellular matrix assembly and structure. New York: Academic Press. p 351-388

274 Yurchenco, P. D. and O'Rear, J. J. (1994) Basement membrane assembly. Methods Enzymol **245**, 489-518

275 Zamore, P. D. (2002) Ancient pathways programmed by small RNAs. Science **296**, 1265-1269

276 Zhou, Z., Yamamoto, Y., Sugai, F., Yoshida, K., Kishima, Y., Sumi, H., Nakamura, H. and Sakoda, S. (2004) Hepatoma-derived growth factor is a neurotrophic factor harbored in the nucleus. J Biol Chem **279**, 27320-27326

# 9. Appendix

## 9.1 Supplementary data

### 9.1.1 HRP-3 expression in mouse E13.5 neural tube

**Figure S 1: HRP-3 expression in E 13.5 neural tube visualized by a fluorescently labelled secondary antibody**. Coronal floating sections showing the neural tube were prepared from PFA-fixed E13.5 embryo immersed in ice cold PBS using Leica vibratome. Section was stained against HRP-3 using a fluorescently labelled secondary antibody. The whole staining steps were performed in perforated-bottom small cups placed in the wells of a tissue culture 24-well plate. The stained section was examined under confocal laser scan microscope and the strongest signal was detected in the oval bundles (OB), in the area of motor neuron cell bodies (MNC), the floor plate (FP) and the ependymal cell layer (EL) surrounding the central canal (CC). A weaker signal was detected in the spinal ganglia (SG), anterior and posterior nerve roots (ANR and PNR respectively) and the remaining parts of the neural tube. Roof plate (RP), in contrast to the floor plate did not show a significant HRP-3 expression signal. This pattern is similar to that obtained by the avidin-biotin complex method displayed in the results but it does not include the sympathetic ganglia and spinal nerves showing only the neural tube. Red dotted line represents the central canal outline. Bar is 50 µm.

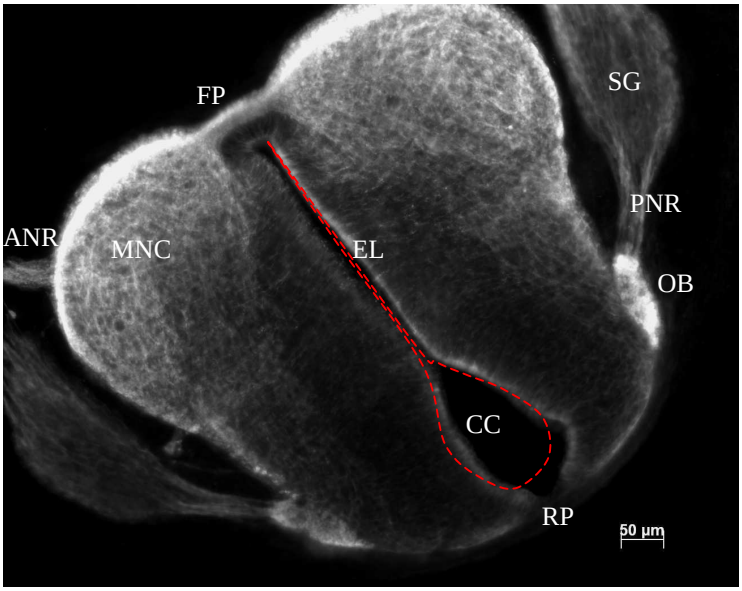

### 9.1.2 Vector-based HRP-3siRNA reduced endogenous level of HRP-3 in primary cortical neurons

**Figure S2: Vector-based HRP-3siRNAs reduced HRP-3 level in primary cortical neurons**. One day old primary cortical neurons were transfected with vector based HRP-3siRNA or control vector (pSilencer) together with GFPC3 (in 10:1 ratio) using MaTRa magnetic beads. Two days after transfection cells were fixed and immunostained against HRP-3 (red channel), GFP (green channel) and β-III-tubulin (blue channel). A remarkable reduction of HRP-3 level in HRP-3siRNA targeted neurons was observed (arrows in C-H) compared to the adjacent untargeted or the control siRNA targeted neurons (arrows in I-K). Bars are 20 µm.

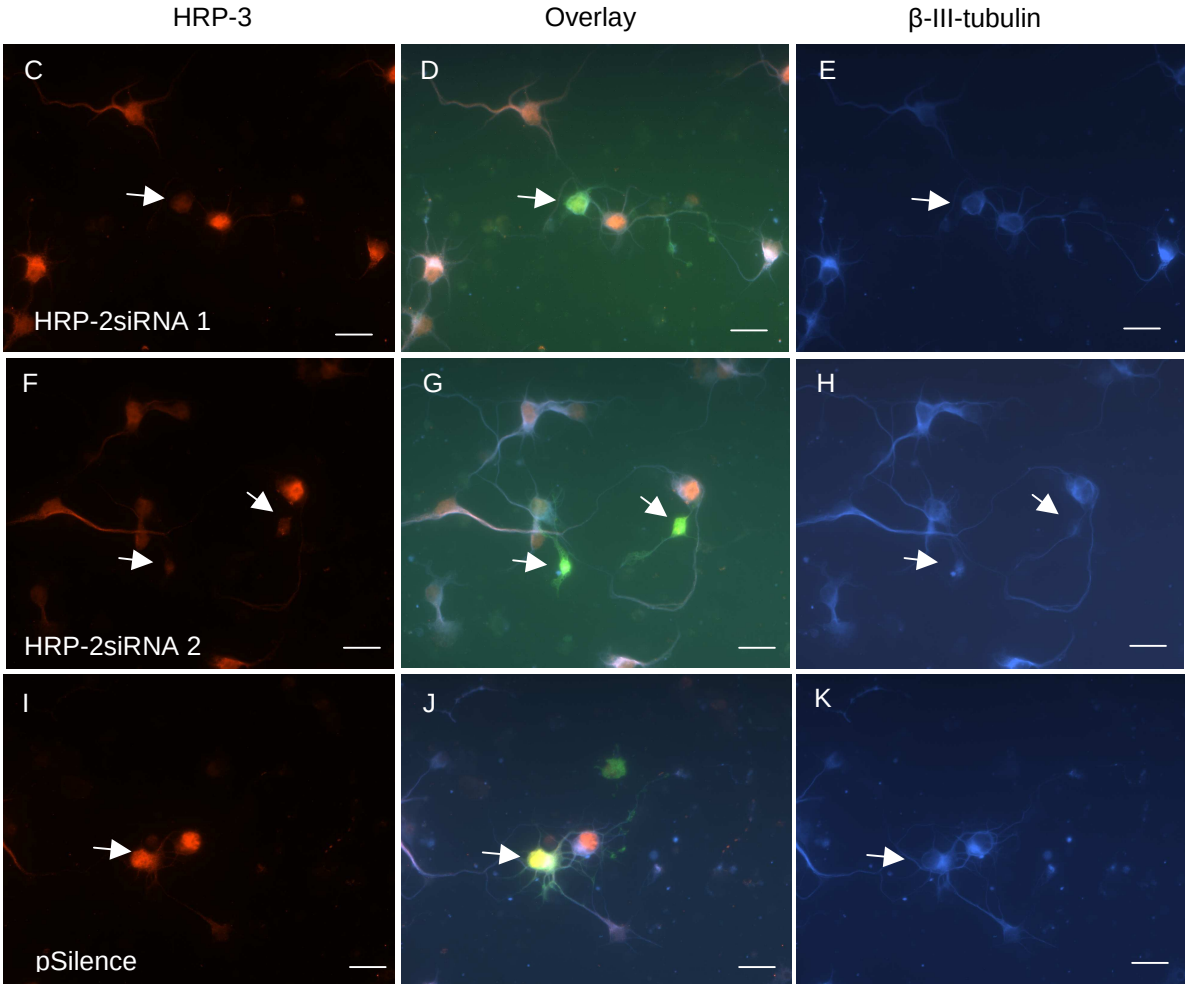

### 9.1.3 The effect of reducing the endogenous HRP-3 level on neuritogenesis

**Figure S 3: Reducing endogenous HRP-3 level resulted in shorter neurites and less cell sprouting.** Primary cortical neurons were transfected with different HRP-3siRNAs directly before seeding using Lipofectamin 2000 as mentioned under methods. A scramble (ctrl siRNA) was used as a negative control. In the first experiment (A1 & B1) the control was Cy3 labelled siRNA and in the second and third experiments (A2, A3 & B2) it was unlabelled. Two days after transfection cells were fixed and immunostained against HRP-3 and β-III-tubulin to verify the identity of the transfected cells. More than 200 randomly chosen neurons were analysed from each condition in a blind way. Data analysis showed a reproducible and highly significant reduction in both the mean neurite length as well as the number of neurites arising from the cell body of HRP-3siRNA transfected neurons compared to control transfected neurons. The extent of reduction in neurite length was more obvious when only targeted neurons (detected by the Cy3 signal) were analysed as seen in A1 in which only neurons with a reduced endogenous HRP-3 level were taken in consideration. In both cases, with labelled or unlabelled targeted cells, the experiments resulted in similar results every time. Bars represent the standard error and asterisks indicate a significant mean neurite length over HRP-3siRNA transfected neurons.

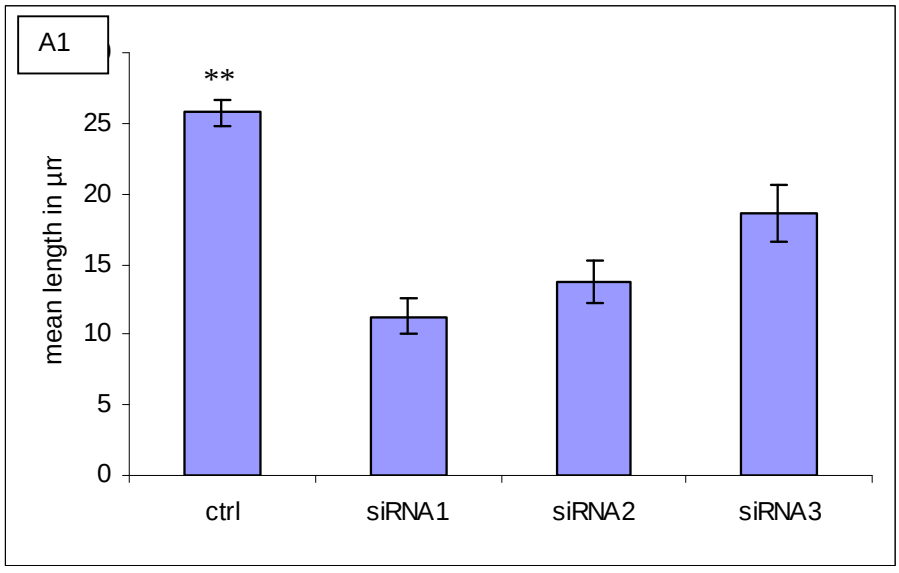

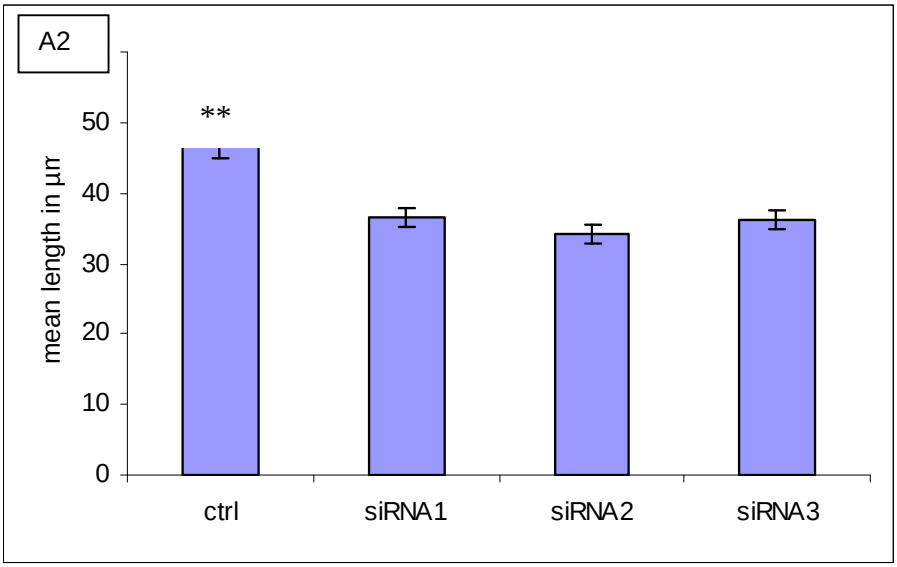
A2
**
mean length in µm
50
40
30
20
10
0
ctrl
siRNA1
siRNA2
siRNA3

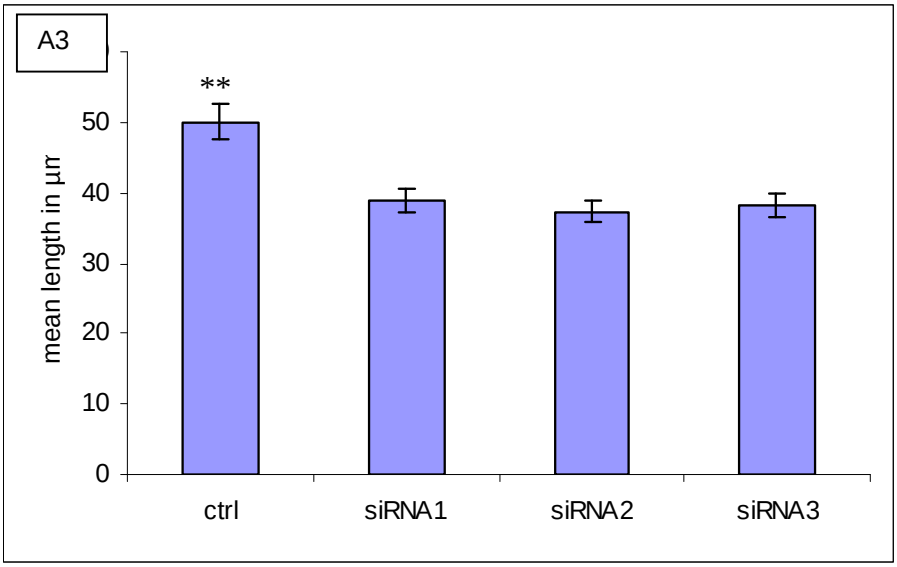
A3
**
mean length in µm
50
40
30
20
10
0
ctrl
siRNA1
siRNA2
siRNA3

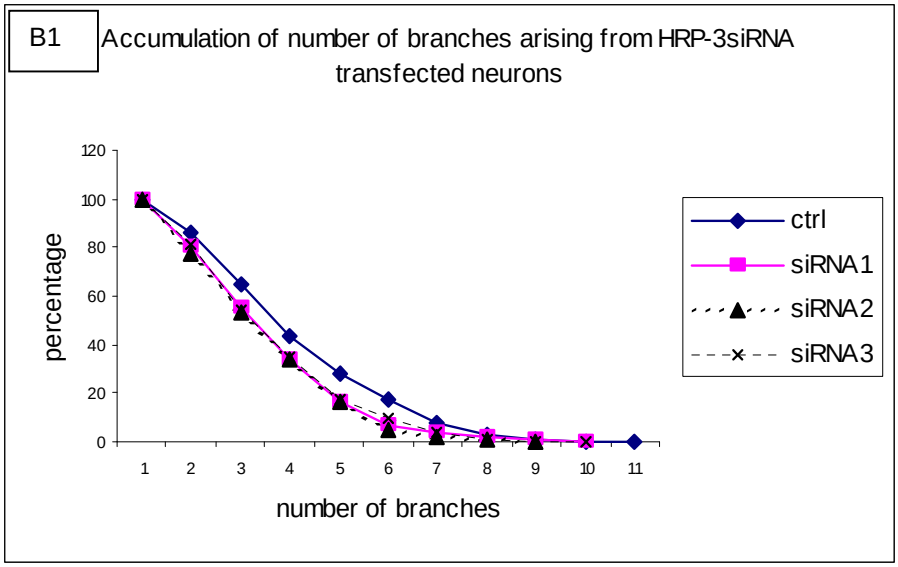
B1
Accumulation of number of branches arising from HRP-3siRNA transfected neurons
percentage
120
100
80
60
40
20
0
1
2
3
4
5
6
7
8
9
10
11
number of branches
ctrl
siRNA1
siRNA2
siRNA3

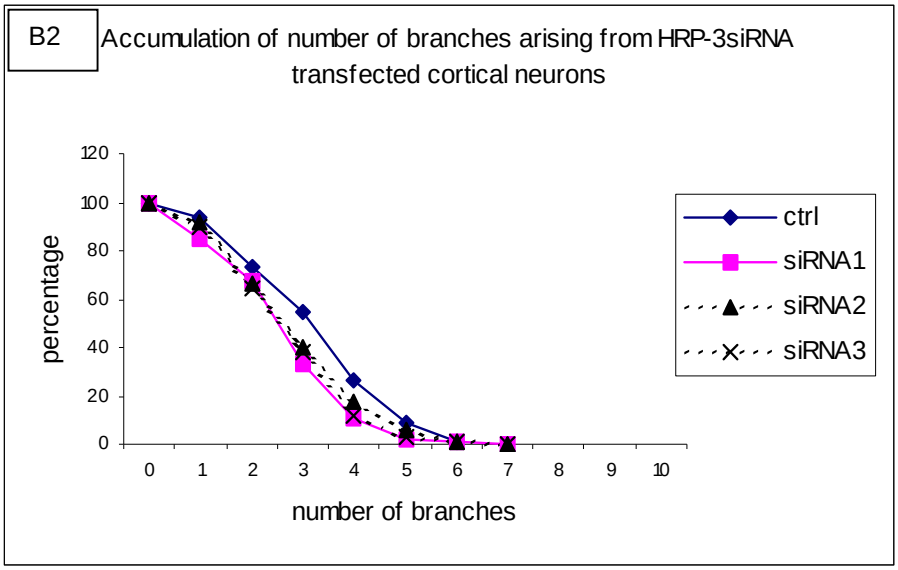
B2
Accumulation of number of branches arising from HRP-3siRNA transfected cortical neurons
120
100
80
60
40
20
0
percentage
0
1
2
3
4
5
6
7
8
9
10
number of branches
ctrl
siRNA1
siRNA2
siRNA3

### 9.1.4 Role of nuclear localization signals 1 & 2 in the neuritogenetic effect of HRP-3

**Figure S 4: NLS1 is responsible for the neurite outgrowth promoting effect of HRP-3 tested in B35 cells.** B35 neuroblastoma cells were transfected with different NLS mutant constructs, wild type HRP-3 or the empty vector together with GFPC3 in a DNA ratio of 10 to 1 to detect the positively transfected cells under fluorescence microscope. Twenty four hours after transfection, differentiation was induced with 1 mM dBcAMP and cells were fixed and stained three days later. The length of the longest neurite arising from randomly chosen positively transfected cells in two independent experiments was estimated in a blinded assay. Performing the experiments under the same conditions resulted in the same tendency. In the first graph bars represent the standard error and asterisks indicate a significant mean over the control.

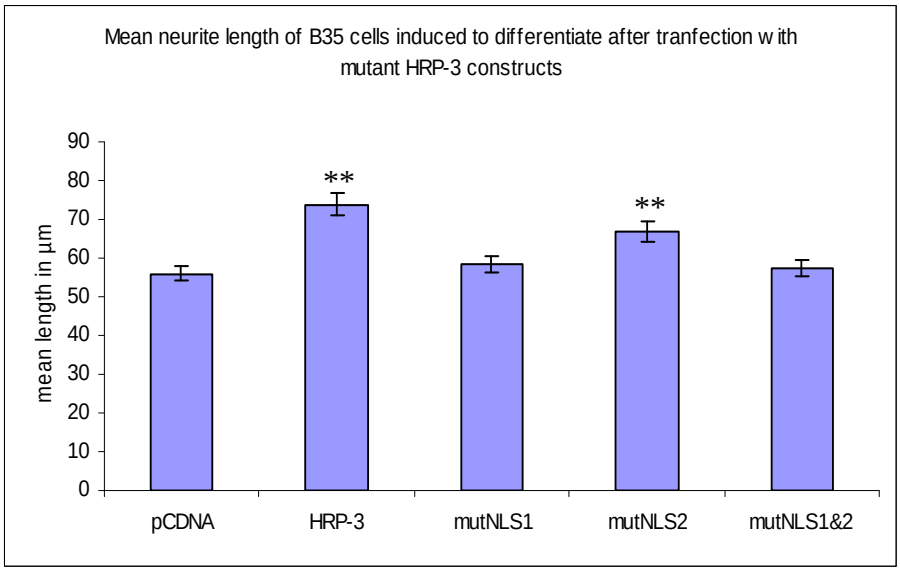

### 9.1.5 Neuron rescue by soluble HRP-3

**figure S 5: Soluble HRP-3 rescued mouse primary cortical neurons cultured under supplement-free conditions.** Primary mouse cortical neurons were seeded into PDL-coated 48-well tissue culture plate in complete NBM. One day after seeding, neurons were thoroughly washed and incubated in supplement-free DMEM or DMEM supplemented with 100 ng/ml HRP-3, 100 ng/ml β-gal or 5 % FCS. Three days later, alamar blue was added to the culture medium according to manufacturer's instructions and fluorescence was measured at 535 nm excitation wave length and 595 emission wave length. The experiments showed similar results every time with minor differences related to culture conditions.

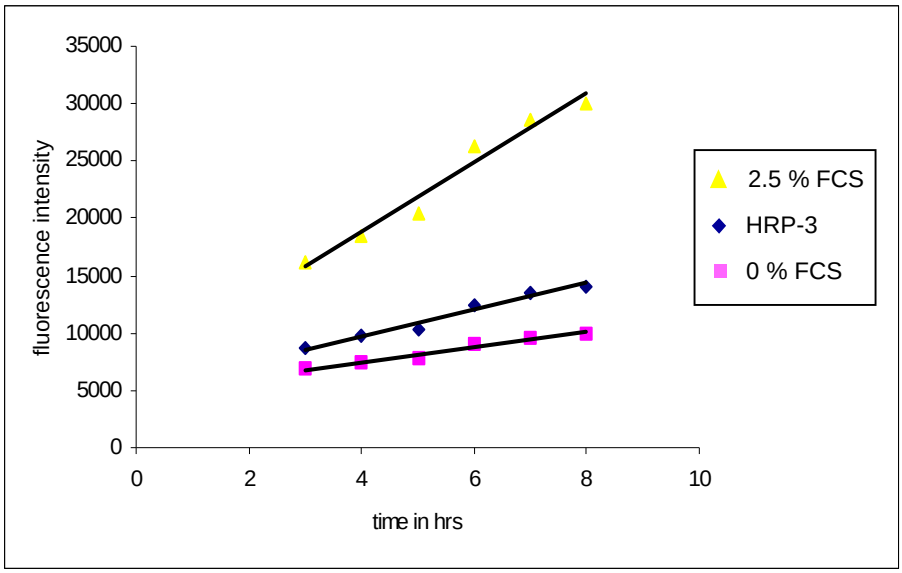


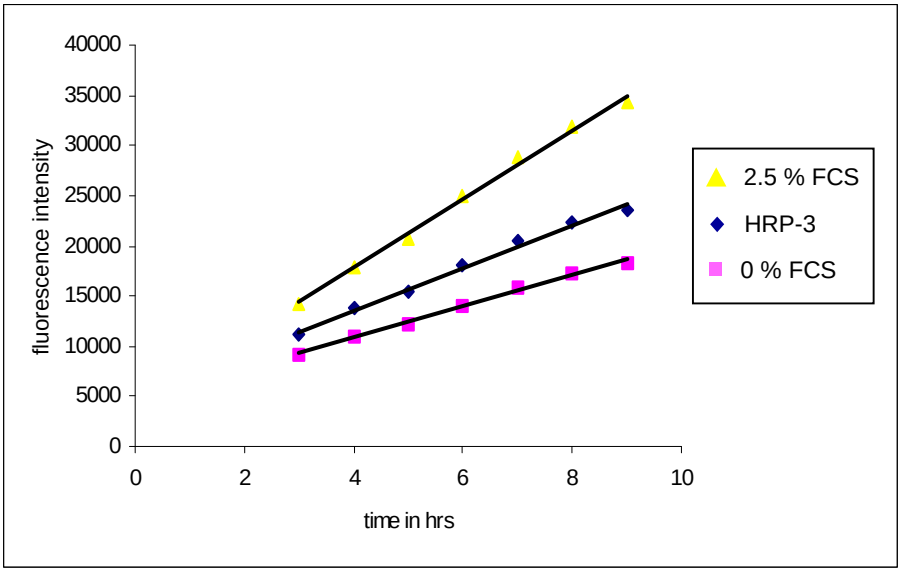

### 9.1.6 Determination of protein amount bound to glass surface

**Figure S 6: His-tagged HDGF bound PDL-coated glass coverslips more efficiently than his-tagged HRP-3 did but HRP-3 coat promoted neurite outgrowth stronger than HDGF coat.** Different proteins (his-tagged HRP-3, his-tagged HDGF, his-tagged β-gal or BSA) were used to coat PDL coated glass coverslips for 1 hr at 37℃. A colorimetric enzymat ic assay was used to estimate the amounts of bound protein in each case. The absorbance values showed that the amount of bound protein in case of HDGF was higher than the other tested proteins including HRP-3. However it did not exert any significant effects over the control concerning neurite outgrowth promoting. HRP-3 coat showed a medium absorbance value but its effects regarding neurite outgrowth promoting were extremely significant.

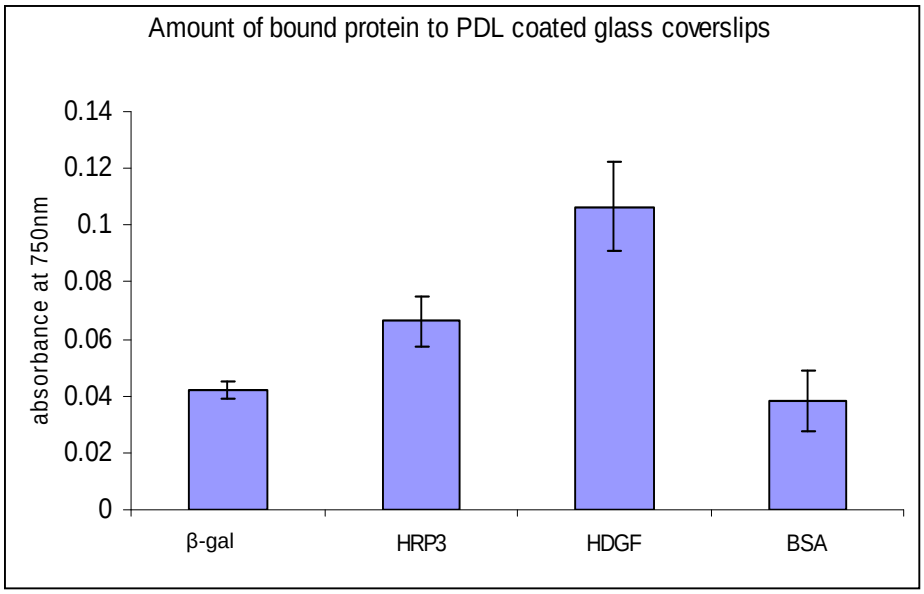

### 9.1.7 Effect of substrate bound HRP-3 on neuritogenesis

**Figure S 7: HRP-3 as an extracellular matrix promoted neurite outgrowth and branching of primary cortical neurons.** Mouse primary cortical neurons were seeded on PDL-coated glass coverslips coated with histagged HRP-3, histagged HDGF, histagged β-gal as mentioned under methods. After 48 hours neurons were fixed and immunostained against a neuronal marker (β-III-tubulin). Random pictures from two different independent experiments were taken for each condition under a fluorescence microscope. The mean of neurite length (A1 & A2) and number of neurites arising from β-III-tubulin positive neurons (B) were analyzed independently. HRP-3 as a coat significantly increased the mean neurite length as well as the number of neurites arising from neurons in a reproducible manner when compared to the other substrates.

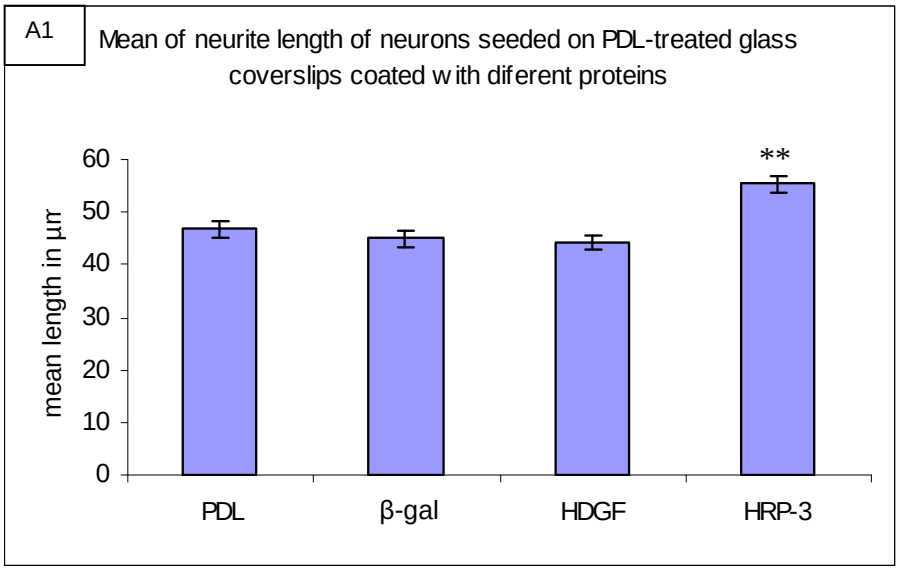

A2

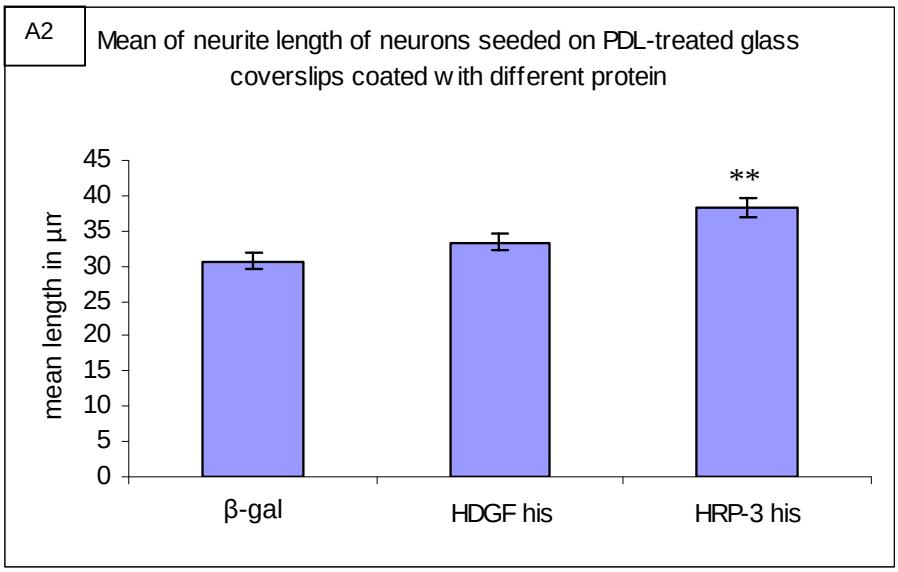
Mean of neurite length of neurons seeded on PDL-treated glass coverslips coated with different protein
mean length in µm
45
40
35
30
25
20
15
10
5
0
**
β-gal
HDGF his
HRP-3 his

B

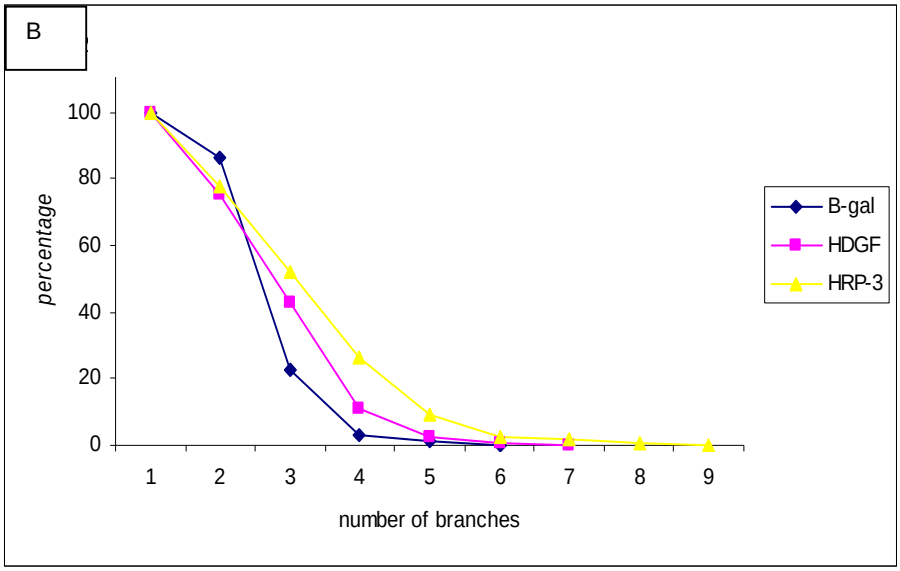
percentage
100
80
60
40
20
0
1
2
3
4
5
6
7
8
9
number of branches
B-gal
HDGF
HRP-3

## 9.2 Vector maps

### 9.2.1 pCDNA3

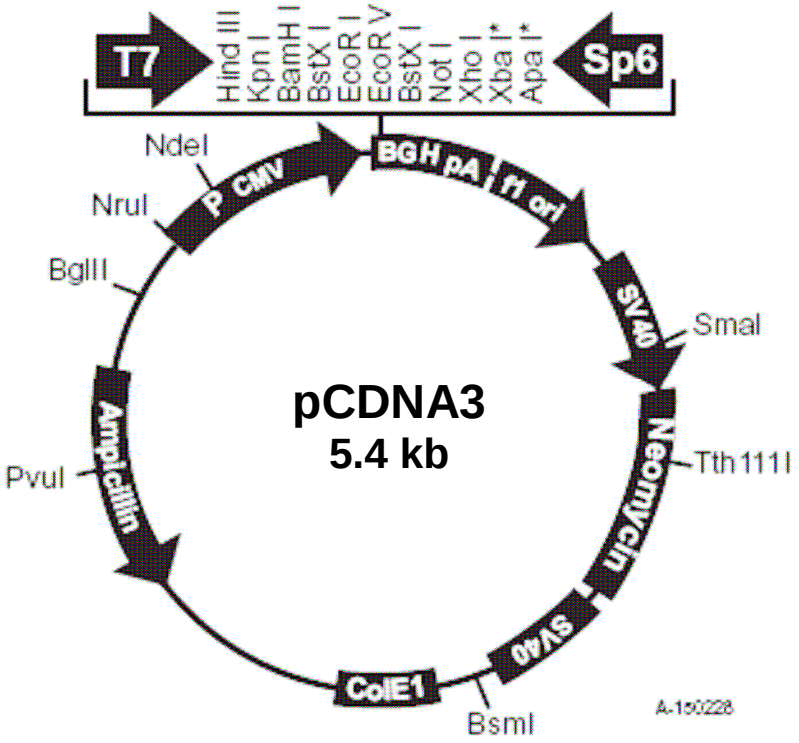


### 9.2.3 pEGFP-C3

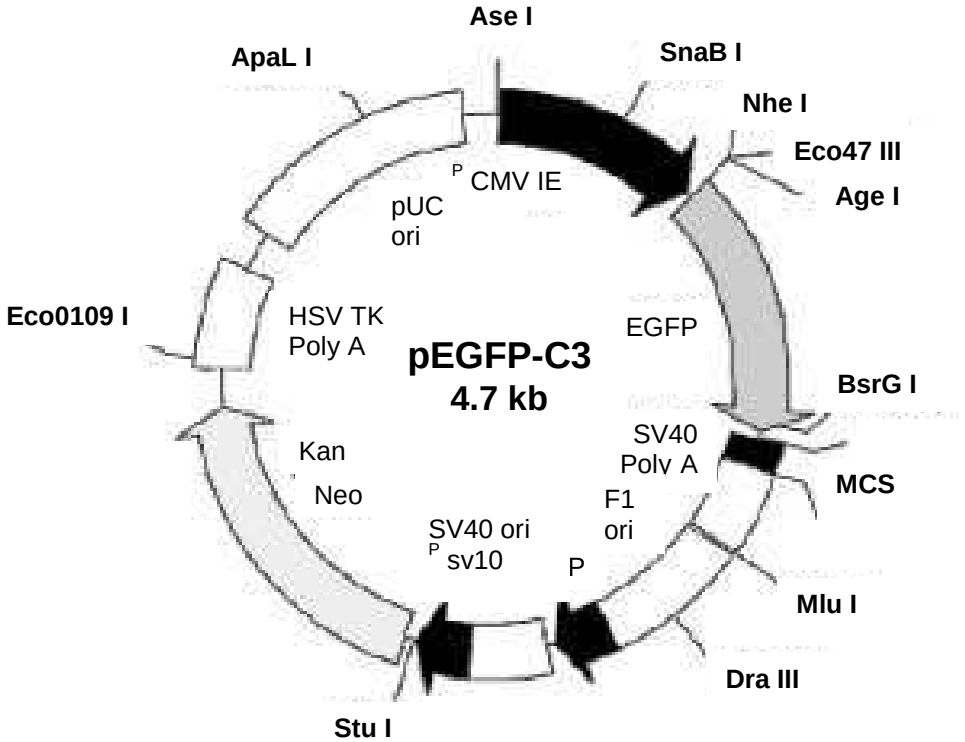

### 9.2.3 pBluescript

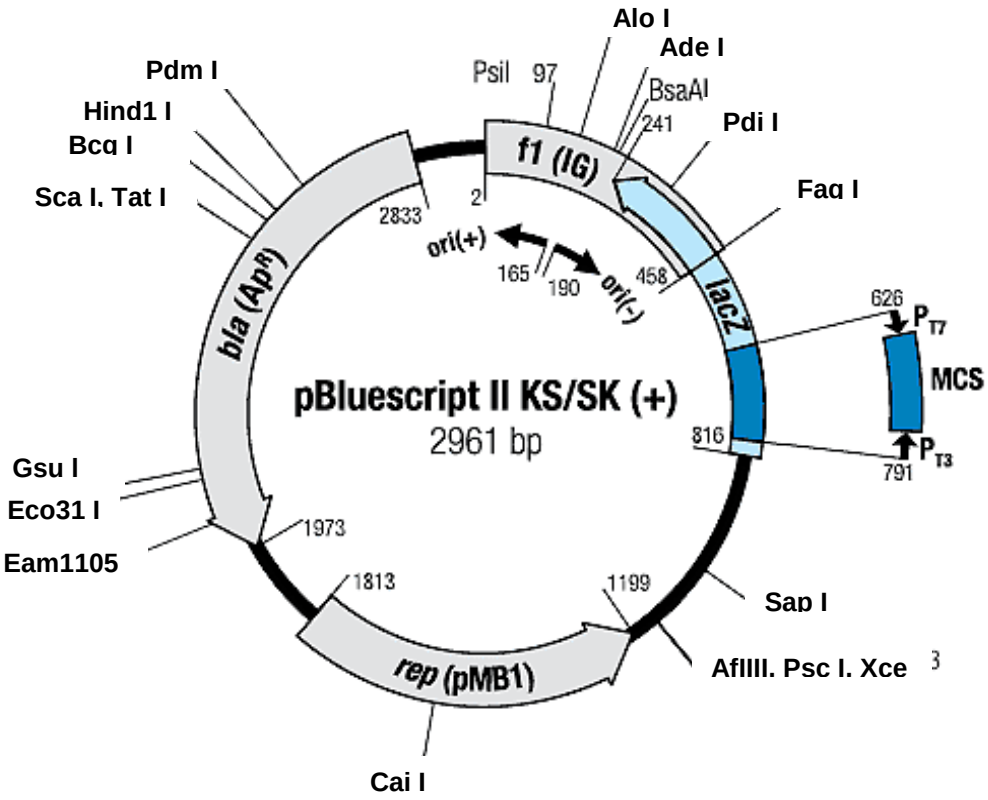


### 9.2.4 pSilencer 3.0 H1